भारतीय ग्रहीय विज्ञान सम्मेलन

Indian Planetary Science Conference

आयोजक

भारतीय ग्रहीय विज्ञान संघ

Organised by

Indian Planetary Science Association

IPSC 2023

मार्च 22 - 24, 2023 March

भौतिक अनुसंधान प्रयोगशाला

Physical Research Laboratory

अहमदाबाद Ahmedabad 380009

Volume of Abstracts

Sponsors:

Abstract Title	**Page No.**

Streaming Plasma Instability in Lunar Ionosphere

Vipin K. Yadav[1], Mehul Chakraborty[2] and Rajneesh Kumar[2]

[1]Space Physics Laboratory (SPL), Vikram Sarabhai Space Centre (VSSC), Thumba, Thiruvananthapuram 695022, Kerala

[2]Department of Physics, Banaras Hindu University (BHU), Varanasi 221005, Uttar Pradesh

*Corresponding Author E-mail: vkyadavcsp@gmail.com

Plasma instabilities are the non-linear processes occurring in plasmas when excess energy gets accumulated in a plasma system. When the plasma system becomes incapable of holding this excess energy, it releases it thereby triggering plasma instabilities. These instabilities are often observed in space plasma systems such as the Sun, planetary ionospheres, etc. Earth's natural satellite Moon has a very thin atmosphere and hence a feeble plasma ionosphere. However, this tenuous lunar plasma environment is a place of several non-linear plasma phenomena. The solar wind, which strikes the lunar surface unhindered due to the absence of global lunar magnetic field, is capable of triggering plasma instability in the lunar exosphere.

In the lunar plasma environment, two-stream instability (TSI) generation is studied analytically which comes into existence due to the interaction of solar wind with the lunar electron plasma near the exosphere. Subsequently, the conditions for the TSI to come into existence are obtained and the growth of this instability with time the passage of time is estimated as shown in Figure 1.

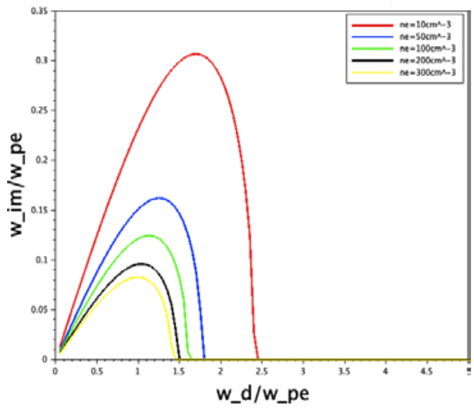

Figure 1: The TSI growth factor with *k* for different n_e.

The TSI growth factor is found to be a function of lunar electron number density, solar wind electron number density and the solar wind electron thermal velocity. The lunar TSI can explain the observation and presence of high electron density in lunar ionosphere as it leads to the bunching of solar wind electrons which increases the electron number density of the lunar ionosphere.

Particle-In-Cell (PIC) simulations are also carried out for the visual depiction of this plasma TSI evolution with time in phase space [1].

References:

[1] Mehul Chakraborty, Vipin K. Yadav, and Rajneesh Kumar (2023), *ASR, 71, doi:10.1016/j.asr.2022.11.050*

A comparison of the impacts of CMEs and CIRs on the Martian dayside and nightside ionospheric species

L. Ram[1,*], D. Rout[2], R. Rathi[1] and S. Sarkhel[1]

[1]Department of Physics, Indian Institute of Technology Roorkee, Roorkee – 247667, Uttarakhand, India

[2]GFZ German Research Centre for Geosciences, Potsdam, Germany

*l_ram@ph.iitr.ac.in

The space weather events like coronal mass ejections (CMEs) and corotating interaction regions (CIRs) pose significant effects on the ionosphere of Mars. The previous studies have demonstrated the depletion and energization of the Martian ionosphere during these solar events. However, there is no comprehensive investigation that shows the relative difference between the impact of CMEs and CIRs on the Martian ionosphere. Hence, it motivates us to study the behavior of the Martian dayside and nightside ionosphere and the potential role of these events in the evolution of planetary atmospheres over time. Measurements from the Mars Atmosphere and Volatile EvolutioN (MAVEN) spacecraft, orbiting Mars are used for investigating the impact of CMEs and CIRs on Martian ionospheric species. We have chosen 15 CME and 15 CIR events at Mars from the existing catalogs and have extensively analyzed the Martian dayside and nightside profiles of ionospheric species during each of the CME and CIR events. We have selected those orbit plasma density profiles which showed significant differences from the mean quiet time profile during each event. The primary focus of this study is to provide a comparative average scenario of the variation of Martian ionospheric species during CME and CIR events between 150-500 km altitudes. A significant difference can be observed in the profiles of the Martian dayside and nightside ionospheric species (O^+, O_2^+, CO_2^+, NO^+, C^+, N^+, & OH^+) during CMEs and CIRs. The difference is more prominent on the nightside in comparison to the dayside ionosphere. We have observed that the plasma densities were lower during CIRs compared to CMEs. During CIRs, the nightside ion density is one order of magnitude less (above 250 km) in comparison to CMEs. The mean peak altitude and density of the lighter ions (O^+, C^+, N^+, & OH^+) were at lower altitudes during the CIRs compared to CMEs. Therefore, this study suggests that the impact of CIRs on the Martian ionospheric species is more prominent compared to CMEs. The detailed results from the study will be presented in the conference.

Design and development of Neutral and Ion Mass Spectrometer (NIMS)

(P. Sharma[1*], A. Verma[1], S.K. Goyal[1], R.R. Mahajan[1], N. Upadhyay[1] and V. Sheel[1])

[1]Physical Research Laboratory, Ahmedabad

[*] E-mail: ***piyush@prl.res.in***

Since the inception of space exploration more than fifty years ago, Mass Spectrometry has proliferated unique chemical and physical insights on the characteristics of other planetary bodies in the Solar System. A variety of Mass Spectrometer types, including Quadrupole, Time-of-flight, and Ion trap, have and will continue to deepen our understanding of the formation and evolution of exploration targets like the surfaces and atmospheres of planets and their moons. An important impetus for the continuing exploration of Moon, Mars, and Venus involves assessing the habitability of solar system bodies and, ultimately, the search for life—a monumental effort that can be advanced by mass spectrometry. Modern flight-capable mass spectrometers, in combination with ionization techniques enable sensitive detection of exospheric ions, Atmospheric gases to Strengthen the traces of Bio-signatures.

Neutral and Ion Mass Spectrometer (NIMS), based on Quadrupole Field technique is being developed at PRL. NIMS consists of four cylindrical rods with applied direct-current (DC) and radio-frequency (RF) electric fields that are used for ion separation. It consists of the detector probe and its processing electronics. The Ionizer, Quadrupole Mass Filter, and Detector sub-assemblies constitute the Detector head. NIMS has an operational mass range of 2-200amu and a peak width (Δm) of 0.5amu. The detector head is enclosed inside a shield tube that also provides a common ground for the instrument. NIMS shall function in two modes: a) The Neutral Mode and b) The Ion Mode. The current development aspects of NIMS are discussed below briefly:

The successful design of NIMS ensures the following:

- Structural topology optimization of components of NIMS without loss in functional performance of the instrument
- Meeting the assembly requirements by providing appropriate physical, geometric and positioning tolerances for the components and addressing the sequencing of sub-assemblies

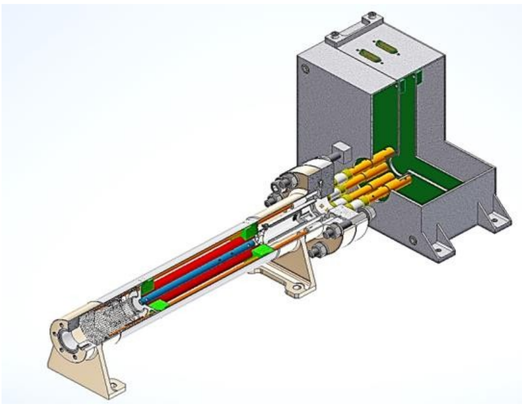

Fig1: 3-D Cross Sectional view of NIMS Package (Mechanical assembly and Electronics unit)

The instrument shall employ a faraday-cup and a CEM as detectors, where CEM needs to be biased at -2.5kV (ranging from 0 to -3kV) to achieve appropriate gain for the detection of targeted species. The bread-board development of the electronics has been carried out Viz.: Electronics for Ionizer Control, RF scanning, HV circuit for CEM biasing, FPGA based processing electronics and LabVIEW based data acquisition. The current status of the development and it`s results will be discussed along with the next course of action.

Characterization of Silicon Photomultiplier (SiPM) detectors for high energy X-ray measurements in future space missions

S. K. Goyal*[1,2], Amisha P. Naik[2], P. Sharma[1]

[1]Physical Research Laboratory, Ahmedabad
[2]Institute of Technology, Nirma University, Ahmedabad
**Email: goyal@prl.res.in*

Silicon Photomultiplier (SiPM) is a semiconductor device, which has very high internal gain (~10^6), Photo Detection Efficiency (PDE) very similar to the Photo Multiplier Tube (PMT) and can be used to detect single photons. Here, Scintillation detector + SiPMs are being planned for various applications such as measurements of high energy X-rays emitted from the planetary surfaces (such as emission from Pb210), Measurements of high – energy charged particles (H^+ and He^{++}) in delta E- E mode in STEPS-ASPEX-Aditya-L1 and for focal plane detector & Compton polarimeter for hard X-ray astronomical observations. Multiple options of the scintillation detectors have been studied and tested such as CsI (Tl), $LaBr_3$ (Ce), BC408, $CeBr_3$ and NaI (Tl). Selection of Scintillation detector for a particular application is based on several parameters like radiation type (X-ray or charged particles), output photons / keV, detector's energy resolution, energy range, and detection efficiency. At present, $CeBr_3$ detector in rectangular configuration is being planned for high energy X-ray measurements (20 – 400 keV) and plastic scintillator (BC408) in rectangular configuration is planned for high-energy charged particle detection for delta E – E detector for energy >5 MeV.

Here, we report the work carried out for the characterization of SiPM and its response in the hardened environments. The understanding of SiPM noise is required to specify the operating parameters such as pulse shaping time of the electronic circuits. The shaping time in the front-end electronics (FEE) needs to be selected to a value such that all the output photons of scintillation are collected in that period and at the same time there is a minimum contribution from the SiPM dark counts. Dark count rates are dependent on the pixel sizes and total active area of SiPM. Dark count rate increases with the increase in the pixel sizes / active area.

In this work, some of the useful parameters of SiPMs such as quenching resistor, breakdown voltage are derived with their dependences on the ambient temperature. The $CeBr_3$ with SiPM is also characterized with various operating temperatures. In this paper, the salient features of SiPM detector, characterization results from both 1) SiPM as standalone detector and 2) $CeBr_3$+SiPM detector module will be presented.

Supra-thermal & Energetic Particle Spectrometer (STEPS), subsystem of Aditya Solarwind & Particle Experiment (ASPEX) onboard Aditya-L1

S. K. Goyal[1*], A. R. Patel[1], Neeraj K. Tiwari[1], P. Sharma[1], J. Sebastian[1], A. Sarda[1], B. Dalal[1], T. Ladiya[1], S. V. Vadawale[1], M. Shanmugam[1], D. Chakrabarty[1], A. Sarkar[1], N. Singh[1], S. Kumar[1], D. Painkra[1], P. Kumar[1], B. Bapat[2], P. R. Adhyaru[1], M. S. Shah[1], H. Adalja[1], A. Bhardwaj[1], and P. Janardhan[1]

[1]Physical Research Laboratory, Ahmedabad
[2]Indian Institute of Science Education and Research, Pune

Aditya-L1 is the forthcoming Indian solar mission, going to be placed in a Halo orbit around Sun-Earth Lagrangian – 1 (L1) point. Sun-Earth L1 point is ~1.5 million km from Earth, out of Earth's magnetosphere which provides unhindered view of the Sun. Aditya Solar wind & Particle EXperiment (ASPEX) is one of the seven science payloads onboard the Aditya - L1 satellite. The primary objective of ASPEX is to make in-situ, multi-directional measurements of the solar wind, supra-thermal and high-energy particles in the energy range of 100 eV/n to 5 MeV/n. ASPEX measurements will help in understanding the roles of the solar and interplanetary processes in the acceleration of solar wind particles and generation of supra-thermal and solar energetic particles. In addition to this, multi-directional measurements will further help in understanding the anisotropy in the energy distribution of particles arriving from different directions. The measurement of the particle flux is also planned to be used as space weather forecasting tool for the arrival of Coronal Mass Ejections (CMEs) on Earth.

The ASPEX payload has two independent subsystems *viz.* Solar Wind Ion Spectrometer (SWIS) & Supra Thermal Energetic Particle Spectrometer (STEPS). SWIS is a low energy ion spectrometer consisting of hemispherical electrostatic analyzer and magnetic mass analyzer for the identification of the He^{++} and H^{+} particles in the range of 100 eV to 20 keV. While the STEPS uses customized Si-PIN detectors and plastic scintillators in the delta E-E configuration mode for energy measurement and identification of the species (H^{+} and He^{++}) in the energy range of 20 keV/n to 5 MeV/n.

STEPS has been devised into 3 packages i.e. 1) STEPS-1, 2) STEPS-2A and 3) STEPS-2B which provide H^{+} and He^{++} measurements from six directions that include radial (towards the Sun, called as SR unit), Parker (along the Parker Spiral, called as PS unit), intermediate (between radial and Parker, called as IM unit), Earthward (EP unit) and across the ecliptic plane in both the north (NP) and south (SP) directions. SR, PS and EP units provide species differentiated energy spectrum for every 1 second integration time while IM, NP and SP units are providing integrated species energy spectrum for every 1 second. STEPS data is going to be made available in CDF format in three levels i.e. Level0, Level1 and Level2.

The flight hardware for the STEPS has undergone various calibration activities and qualification tests. The hardware has been delivered to Aditya-L1 project for further integration tests with the spacecraft. In this paper, the overall configuration of the flight model of the STEPS, its salient features and results will be presented.

Compact and Simple Deployment Mechanisms of Solar Panels in CubeSats and RoverDoors in Lunar or Planetary Missions

Aman Sharma*, Amit Nath, Adarsh Kumar Singh, Rintu Prasad Gupta, and Debrup Hui

Ghani Khan Choudhury Institute of Engineering and Technology, Narayanpur, Malda - 732141

*Corresponding Author E-mail: amansharma0828@gmail.com

Abstract: The purpose of this project is to mitigate the impact endured by a CubeSat's solar panels during deployment. A stable and synchronized deployment of essential parts like solar cell panels is critical to the satellite mission. To reduce sudden unbalanced vibrations during deployments, two different noble deployment mechanisms of solar panels have been designed: first, by incorporating a spring hinge mechanism that provides damping, and in the second, by using a stepper motor. We use the commonly utilized nichrome burn wire cutting technique as its basis which provides high loading capability, reliable wire cutting, multi-plane constraints, and handling simplicity during the wire tightening process. A working prototype model of the cubesat-solar panel is constructed and tested under various conditions to demonstrate the design's effectiveness and the mechanism's functionality. When the first technique using spring hinge is a passive system, the second system, using a stepper motor, is an active system which can be used throughout the satellite mission life to maximize the power generation by following the sun-inclination angle. The designs are highly reliable, low power consuming, and highly customizable to suit different mission needs. These techniques can also be reliably used during a lunar or planetary mission to deploy/open any doors/panels of the mother ship including in case of any rover ejections. Along with prototype testing for the structural integrity of the solar panels and the mechanisms, we also carried out thermal and random vibration analysis using industry standard simulation tools.

Association of Geomagnetic Storms during 2014-2019 with Solar Wind andInterplanetary Parameters

O. P. Tripathi[1], Saket Kumar[2], Rashmi Sharma[3], Ashish Dwivedi[3], Pooja Pandey[3]

[1]Department of Physics, AKS University, Satna (M.P.) India

[2]Research Scholar, Department of Physics, APS University, Rewa (M.P.) India

[3]Research Scholar, Department of Physics, AKS University, Satna (M.P.) India

Email: omkar8415@gmail.com

Abstract

From the present study we have identified that, if the material carried out by the solar wind originated from sun reached to earth's surface, its radiation would do severe damage to any life that might exist. When energized particles explosion from solar flares pursuit toward Earth, they reach in only eight minutes. The interplanetary causes of total **65** moderate, intense and severe intensity (*Dst* $\leq$ -50 nT) geomagnetic storms that occurred in decline phase of solar cycle 24 (2014–2019) are identified. All moderate to severe intensity geomagnetic storms were associated with peak value of interplanetary magnetic field (IMF B) and southward interplanetary magnetic fields (IMF Bz), indicating that magnetic reconnection was the main mechanism for solar wind energy transfer to the magnetosphere. From the statistical method we have determined positive correlation with correlation coefficient **0.63** between geomagnetic storms and peak value of average interplanetary magnetic field (IMF B), while **0.74** between geomagnetic storms and peak value of southward interplanetary magnetic fields (IMF Bz). Also, we have determined positive correlation between geomagnetic storms and peak value of solar wind plasma parameters (temperature, velocity and pressure) with correlation coefficient **0.25, 0.15 and 0.23** respectively. Studies of geomagnetic storms are more useful to explore impact in radio communications, satellite communication, radar observations, electrical utilities, long distance pipelines and synchronous spacecraft etc.

Keywords: Geomagnetic Storms, Solar Cycle, **S**olar Wind, Interplanetary Magnetic Fields.

DEVELOPMENT OF PDS4 DATA ARCHIVE FOR CHANDRAYAAN-2 MISSION

Ajay Kumar Prashar*, Amitabh, K Suresh, Kannan V Iyer, Abdullah S and Shweta Verma,
Space Applications Centre ISRO Ahmedabad, India, *(ajay_prashar@sac.isro.gov.in)

Chandrayaan-2 (CH-2), India's second mission to the Moon was launched by GSLV-MK-III in July 2019. TMC2, IIRS and OHRC are the optical payloads hosted on the Orbiter which is presently orbiting moon under 100km x 100 km circular orbit. The data collected from the instruments from the orbiter are being received, processed and archived in as PDS4 compliance products under ISRO Science Data Archive (ISDA) at Indian Space Science DataCenter (ISSDC) for dissemination and use by scientific community in India and abroad. Planetary Data System (PDS4) is the de facto international standard for long term archival of planetary science data. Archiving any planetary data in PDS4 involves technical activity. Data needs to be re-engineered by following well defined archive process model. The processmodel contains well defined sequence of steps that needs to be followed during development of an archive. PDS4 has defined the various phases to be followed for development of PDS4 data archive. For Chandrayaan-2 mission, PDS4 Archive Process Model was adopted and tailored by defining activities under each phase of process model. Summary of activities under each phase is mentioned below.

Archive Planning Phase: PDS4 is next generation archive standard. Lots of efforts are envisaged during planning phase for CH-2 mission. The mission has many payloads and teams are located across different ISRO's centers around the country. In order to bring all the teams (project, mission, payload, Principal Investigators (PIs), data processing and archival, operations team at ISSDC) under one umbrella, CH-2 PDS4 Archive Working Group was formed. PDS4 Archive Process for CH-2 mission was tailored as per ISRO's current and future planetary mission requirements.

Definition & Design Phase: In Definition Phase, archive plan and conventions were defined. The Archive Plan consists of deciding what, when, and how to archive. Archive conventions consist of common attributes defined and should be followed across the teams when generating label products of their instruments. As part of archive plan, PDS4 data products types were identified for CH-2 instruments hosted on the orbiter. In design phase, archive structure was design at various levels like mission level (CH-2) design structure, instruments level design structure and finally data products design structure.

Production Phase: In the production phase, Data Processing and Archival software was designed developed and tested based on the planning and design phase mentioned above at ISSDC.

Distribution & Maintenance Phase: This phase comes once instrument lock-in period is over. In this phase long term archive preparation started by taking active archive as input and other PDS4 components - calibration, document, context, miscellaneous and xml_schema is getting assembled with active archive. Once long term archives are ready for validation and verification, peer review process has been carried out.

All the activities under each archive phase mentioned above got successfully completed. As a final outcome, PDS4 Data Archive for all the orbiter payloads were generated, peer reviewed and finally hosted to the scientific user's community via ISSDC data center located at Bengaluru.

References: [1] Chandrayaan-2 Science data management and Archive plan (Chandryaan-2/DP/SAC/SIPG/HRDPD/TR-06/July 2018), [2] Chandrayaan-2 SAC DP – ISSDC Interface for Archival (Chandrayaan-2/DP/SAC/SIPG/HRDPD/TR-13/Dec. 2018), [3] PDS4 Concepts Data Design Working Group October 1, 2018 version 1.11.0, [4] Planetary Data System Standards Reference Version 1.11.0 October 1, 2018, Jet Propulsion Laboratory, [5] The PDS4 Data Provider's Handbook Guide to Archiving Planetary Data Using the PDS4 Standard Version 1.11.0 October 1, 2018, [6] PDS4 Data Dictionary Abridged – Version 1.11.0.0

The Impact of Solar Radiation and Dust Storms on Martian Thermospheric Temperatures

N. V. Rao[1*], V. Leelavathi[1], Ch. Yaswanth[1], and Anil Bhardwaj[2]

[1]National Atmospheric Research Laboratory, Gadanki, India

[2]Physical Research Laboratory, Ahmedabad, India

*Corresponding Author E-mail: nvrao@narl.gov.in

The Martian thermosphere is a highly variable system that is influenced by external forcings, such as solar radiation, lower atmospheric dust, and dynamics. However, the effects of these forcings have not been properly decoupled in the literature, despite previous attempts that were limited by satellite observational constraints. In recent years, the Mars Atmosphere and Volatile EvolutioN (MAVEN) mission has provided comprehensive measurements of the Martian thermosphere across a range of latitudes, local times, and seasons, under medium to low solar activity and variable lower atmospheric dust conditions. These observations provide an ideal set for quantifying the contributions of various forcings.

This study presents a methodology based on multiple linear regression analysis to quantify the contributions of dominant forcings to temperatures. Results show that a 100 solar flux units (sfu) change in solar activity corresponds to a ~136 K change in thermospheric temperatures. Solar insolation constrains seasonal, latitudinal, and diurnal variations to be interdependent, with diurnal variation dominating solar insolation variability, followed by latitudinal and seasonal variations. Both global and regional dust storms lead to considerable enhancements in temperatures of the Martian thermosphere. Using past data of solar fluxes and dust optical depths, the state of the Martian thermosphere is extrapolated back to Martian year (MY) 24. Global dust storms in MY 25, MY 28, and MY 34 raised thermospheric temperatures by ~22-38 K, while a regional dust storm in MY 34 led to ~15 K warming.

MULTI SENSOR LUNAR DIGITAL ELEVATION MODEL (DEM) CO-REGISTRATION

Abdullah S[1*], Baharul Islam[1], Shweta Verma[1], K Suresh[1], Amitabh[1], [1]Space Applications Centre ISRO Ahmedabad, India, *(abdul@sac.isro.gov.in)

Introduction: Terrain Mapping Camera 2 (TMC2) [1], onboard Chandrayaan 2, is a stereo imaging payload (fore, aft and nadir sensors) for high resolution mapping of moon. The DEM has a resolution of 10m obtained from stereo triplet intersection and matching of TMC2 sensors. It is generally observed that the DEM does not meet specified accuracy requirements due to errors in orbit determination, camera pointing, lunar control points for matching etc.

Scope: The inaccurate measurements of various sensors leads to establishing a co-registration [2] technique to align the TMC2 derived products w.r.t. lunar global elevation reference Lunar Orbiter Laser Altimeter (LOLA) [3] DEM. The co-registered product will be having better positional & vertical accuracy than the existing product. This is required as a long term activity for generating DEM mosaic of lunar surface once TMC2 covers the entire moon.

Methodology: To achieve further improvements in geometric quality of data products an Iterative Closed Points (ICPs) [4] based DEM registration technique is derived and implemented for co-registration of TMC2 DEM with LOLA. Cloud Points are generated from both TMC2 and LOLA rasters and nearest points are obtained by nearest neighbor method. After removing outliers, a rigid transformation is iteratively estimated till a threshold is reached. Finally, the transformed cloud is generated as a raster which is the registered DEM.

Results: We have considered 30 TMC2 orbits for analysis, each full strip DEM (length varies from 15deg. latitude i.e. ~500km to 31deg. latitude range i.e. ~1000km, swath/width is 20km) is first compared with corresponding LOLA DEM. After doing 3D registration, the vertical accuracy is improved from ~200m to ~20m in almost all cases. Hence the registered TMC2 DEM is more useful as features are visually better than LOLA since it is optical DEM and geometric accuracy is also close to the reference LOLA DEM.

Conclusion: The co-registration pipeline implemented shows significant improvement in vertical accuracy of the registered TMC2 DEMs. Using the registered DEM as input for ortho-image generation has shown improvements in positional accuracy of ~ 10 to 20m. Future activity is aimed at improving absolute vertical accuracy by reducing errors due to external factors like orbit determination and generation of a seamless mosaic by registering all the acquired strips using bundle block adjustment.

References:

[1] Chowdhury, Arup Roy, et al. "Terrain mapping camera-2 onboard chandrayaan-2 orbiter." Current Science 118.4 (2020): 566.
[2] Barker, M. K., et al. "A new lunar digital elevation model from the Lunar Orbiter Laser Altimeter and SELENE Terrain Camera." Icarus 273 (2016): 346-355.
[3] Smith, David E., et al. "The lunar orbiter laser altimeter investigation on the lunar reconnaissance orbiter mission." Space science reviews 150 (2010): 209-241.
[4] Low, Kok-Lim. "Linear least-squares optimization for point-to-plane icp surface registration." Chapel Hill, University of North Carolina 4.10 (2004): 1-3.

Reproducing LOLA DEM in High Resolution Context from TMC-2 DEM ofChandrayaan-2 using Deep Generative Models

Abdullah S[1*], Subhajit Paul[1], Amitabh[1]

High Resolution Data Processing Division, Signal and Image Processing Group,

Space Applications Centre (ISRO), Ahmedabad-380058 (India)

*(abdul@sac.isro.gov.in)

Abstract- The exploration of lunar surface has always been of huge interest in scientific and commercial community. For this purpose, recently multiple missions have been sent and are planned to study the lunar environment to substantiate effective crewed and robotic missions in the future. In order to plan safe and successful missions, the importance of high resolution global terrain mapping of lunar surface is growing rapidly. Many global and near global lunar digital elevation models (DEM) are available like Lunar Orbiter Laser Altimeter (LOLA) [1], Selene LOLA DEM [2], WAC Digital Terrain Model [3], TMC2 DEM [4] from Chandrayaan-2 etc. LOLA has full global coverage of lunar surface and has the best topographic accuracy up to ~1m. The major disadvantages of LOLA are its resolution (30m) and feature distortion due to interpolation errors in raster. TMC2 of Chandrayaan-2 is a stereo imaging payload which generates high resolution elevation model at 10m resolution with no feature distortion. But the main disadvantage is its topographic accuracy which is approximately 10m and its coverage which is yet to capture the entire lunar surface.

Hence to generate global high resolution lunar terrain map with high topographic accuracy, in this paper we propose to generate super resolved LOLA DEM from TMC2 DEMusing deep learning based algorithms. Deep learning algorithms have gained popularity in different fields of computer vision problem due to its ease in implementation and robustness. Due to this, many researchers are depending on deep learning to solve planetary science data problems like [5] and [6]. So here we are targeting to utilize generative deep learning models with advanced optimization algorithms to generate high resolution DEM with high vertical accuracy using TMC2 DEM.

References:

[1] Barker, M. K., et al. "A new lunar digital elevation model from the Lunar Orbiter Laser Altimeter and SELENE Terrain Camera." Icarus 273 (2016): 346-355.

[2] Smith, David E., et al. "The lunar orbiter laser altimeter investigation on the lunar reconnaissance orbiter mission." Space science reviews 150 (2010): 209-241.

[3] Scholten, F., Oberst, J., Matz, K. D., Roatsch, T., Wählisch, M., Speyerer, E. J., & Robinson, M. S. (2012). GLD100: The near-global lunar 100 m raster DTM from LROC WAC stereo image data. Journal of Geophysical Research: Planets, 117(E12).

[4] Chowdhury, Arup Roy, et al. "Terrain mapping camera-2 onboard chandrayaan-2 orbiter." Current Science 118.4 (2020): 566.

[5] Delgado-Centeno, Jose Ignacio, et al. "Single Image Super-Resolution with Uncertainty Estimation for Lunar Satellite Images." NeurIPS 2021 Workshop on Deep Generative Models and Downstream Applications.

[6] Tewari, Atal, Chennuri Prateek, and Nitin Khanna. "In-orbit lunar satellite image super resolution for selective data transmission." arXiv preprint arXiv:2110.10109 (2021).

Lunar Crater Feature Detection using Deep Learning

K Suresh*, Hemant Kumar Lalwani and Amitabh

Space Applications Centre-ISRO, Ahmedabad, India
*ksuresh@sac.isro.gov.in

Introduction:

Lunar crater feature detection is an active field of research in computer vision algorithms and produced multiple approaches over period of time for detection of craters. Most of the algorithms are limited to detecting craters of size ranging from km to sub-km level or using DEM for detecting the craters. After LRO mission launch on 2009 with Narrow Angle Camera having spatial resolution 50cm per pixel, given new dimension to lunar explorationin better details and with Chandrayaan-2 launch on 2019 with Orbiter High ResolutionCamera (OHRC) having spatial resolution of 28cm opened a new chapter in lunar explorationin greater details. The already developed crater feature detection algorithms are fail to detect meter level craters on OHRC images and manually identifying them is a herculean task.Meter level crater mapping using OHRC images will be of great benefit to scientific team for their crater distribution study, age determination and about secondary crater formation in details. As the lunar surface is getting imaged by higher and higher resolution, the need of having reliable, fully automatic and accurate crater feature detection methodology is inevitable. The recent development, advancements and access to GPU based computational power even in our desktop, triggered a development of wide range of machine learning algorithms, specifically in the field of patter recognition. Our work is concentrated on detecting small craters (~5pixels) from high resolution optical images using deep learning based convolutional neural network.

Relevance of the Work:

As of now, mapping small craters on high resolution images are done manually, especially in identifying meter level craters and also facing the challenge, when the sun azimuth and elevation angles are changed during data acquisitions. We are attempted to demonstrate in identifying craters from high resolution images with varying illumination conditions and small craters (~5pixels) automatically with least processing time. This work will enable the researchers in concentrating on other aspects of the study like crater morphology, distributions and secondary crater creation without worrying about the crater extractionprocesses. High resolution lunar images also pose the another challenge on handling high volume of datasets for subsequent tasks and this work we have handled the high volume datasets seamlessly for crater identification process.

Results/Conclusion:

The developed deep learning model is trained using OHRC images and are tested using TMC and OHRC images. The best detected smallest crates are with 5pixels and has accuracy rate of 93%. The pre-trained weights are used to successfully process the full strip high volume images of TMC and OHRC for detecting craters.

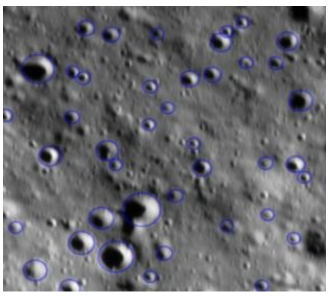

Detected Craters Overlaid on OHRC Images

References:

[1] Haibo Li et al. (2021) *System Science and Control Engineering, 9, 132-140.* [2] Yuqing Mao et al. (2022) *Remote Sens., 14(3), 661.*

Gravity wave driven variability in the Mars ionosphere-thermosphere system

V. Leelavath[1], N. V. Rao[1*], and S. V. B. Rao[2]

[1]National Atmospheric Research Laboratory, Gadanki, India

[2]Sri Venkateswara University, Tirupati, India

*Corresponding author Email: nvrao@narl.gov.in

The majority of the Mars' ionosphere is located within its thermosphere, which means that processes that affect the thermosphere are likely to also affect the ionosphere. The thermosphere-ionosphere system is continuously impacted by several forcings from above and below. The forcings from above include the solar wind, solar flares, coronal massejections, and solar energetic particle events, which have a direct impact on the Martian ionosphere. Forces from below include atmospheric waves such as gravity waves (GWs), thermal tides, and planetary waves, as well as seasonal inflation and contraction of the atmosphere, and circulation changes caused by lower atmospheric dust. In this study, we examine the impact of GWs on the Martian ionosphere-thermosphere system using O_2^+, O^+, and Ar densities measured by the Neutral Gas and Ion Mass spectrometer (NGIMS) instrument on the Mars Atmosphere and Volatile EvolutioN (MAVEN) mission. We extract the amplitudes and (horizontal) wavelengths of the GWs from the density profiles using a seventh-order polynomial fit.

The results of the present study demonstrate that GWs are prevalent in the Martian ionosphere-thermosphere system. We observed that the amplitudes of GWs in ions are approximately two times larger than those in neutrals. While the amplitudes in ions can reach up to 70% of the background densities, the most probable amplitude is 5%. GW amplitudes in ions are more prominent on the nightside compared to the dayside, and are more prevalent during the 2018 global dust storm period than during nominal dust conditions. Furthermore, GW amplitudes in ions increase with decreasing solar activity. All of these results are qualitatively similar to those observed in neutrals. Additionally, the amplitudes of GWs in ions show moderate correlation with those in neutrals, while the wavelengths show a good correlation. We found that the amplitudes of GWs in ions and neutrals exhibit a moderate negative correlation with thermospheric temperatures. These findings suggest that the GWs in ions are a consequence of those in neutrals and that the ion-neutral coupling may be strong in the altitude range studied. However, the correlation between the amplitudes of GWs in ions and neutrals is dependent on local time, with weak correlation on the nightside. Other factors, such as recombination or particle precipitation, may play a role in distorting the wavy nature in ions, and result in weaker correlation with neutral waves on the night side. Additionally, we observed that the correlation between GW amplitudes in ions and neutrals is weaker in strong crustal magnetic field regions, indicating that the magnetic fields influence the motion of the ions and contribute to the distortion of the wavy nature in ions.

Geological Significance for the occurrence of OH/H_2O in the Clavius Crater Region

D. Misra[1,2], M. Bhatt[1], S.A. Sathyan[1] and C. Wöhler[3]
[1]Physical Research Laboratory, Ahmedabad, 380009, India (dibyendu@prl.res.in).
[2] Indian Institute of Technology Gandhinagar, Gandhinagar, 382355, India.
[3] Image Analysis Group, TU Dortmund University, 44227 Dortmund, Germany

The lunar crater Clavius (55º S to 61º S, 9º W to 21º W) is one of the oldest highland craters (~3.85 Ga) [1] with confirmed presence of molecular water based on the results derived from the Stratospheric Observatory for Infrared Astronomy (SOFIA) data. The 6 μm spectral emission feature corresponds to 100-400 $\mu g g^{-1}$ molecular water present in the sunlit crater floor [2]. This study aims at understanding the local geology of the crater Clavius in order to establish small-scale changes that make Clavius a favorable place for accumulating water. Our attempt is to find geological significance for the preservation of bound H_2O, using the Moon Mineralogy Mapper (M^3) data [3] of Chandrayaan-1 [4]. The M^3 data are converted to spectral reflectance using the framework of [5].

We constructed the integrated band depth (IBD) mosaic of the region and also used the elemental maps from [6] for understanding the overall mineralogy of the study region. We found that the dominant mineralogy is Ca^{2+} rich with a great extent of surficial weathering. The reflectance spectra extracted from the specific locations of interest show the presence of the 3 μm absorption feature that occurs due to a stretch of motion in the O-H bond present in OH/H_2O molecule. The Ca-rich region has no prominent spectral signature due to the presence of shocked plagioclase (>25GPa) [7]. The integrated band depth of the 3 μm absorption feature (OHIBD) at different local times of day clearly shows a stable component even at local midday time. The OHIBD images have been prepared using the framework of [5]. Although we observed time-dependent variations in OHIBD, the detected strongly bounded OH/H_2O component confirms SOFIA's findings [2].

Our preliminary understanding of the geology of Clavius suggests that the crater mainly consists of plagioclase, has a hydrous affinity and a relatively high partition coefficient with melt. Due to the framework silicate structure, it has large interstitial spaces for creating preferable sites where OH/H_2O can be implanted through the dangling bond effect [8]. Due to impacts, shocks are propagated, which increases the strain in between the molecular structure of the glass, where the water carried by hydrous micrometeorite can be trapped [9]. In such a lunar high-latitudinal area, also synergistic effects involving impacts of micrometeorites into anhydrous minerals present on the lunar surface implanted by H^+ from the solar wind, may generate the OH/H_2O [10]. We plan to identify craters similar to Clavius from sunlit high-latitude regions in order to understand the general trends of OH/H_2O accumulation in such regions. In future work, we will focus on the use of Imaging Infrared Spectrometer (IIRS) data onboard Chandrayaan-2 [9] for complete characterisation of the 3 μm absorption band and will study its correlation to the SOFIA detected 6 μm emission feature [2].

References: [1] Feoktistova et al. (2021), *LPS LII*, Abstract #2548. [2] Honniball et al. (2021), *Nature Astronomy*, 5(2), 121-127. [3] Pieters et al. (2009), *Current Science*, 500-505. [4] Goswami et al. (2009), *Current Science*, 486-491. [5] Wöhler et al. (2017), *Science advances*, 3(9), e1701286. [6] Bhatt et al. (2019), *Astronomy and Astrophysics*, 627, A155. [7] Cheek et al. (2013), *JGR. Planets*, 118(9), 1805-1820. [8] Chauhan et al. (2021), *Current Science*, 121(3), 391. [9] Daly and Schultz, *Sci. Adv.* (2018);4: eaar2632. [10] Zhu et al. (2019), *PNAS* 116(23), 11165-11170.

Energy-dependent response of the Martian ionospheric electrons to solar forcing

Pavan D Gramapurohit[1], N V Rao[1*], Ch. Yaswanth[1], D S V V D Prasad[2]

1. National Atmospheric Research laboratory, Gadanki, India

2. Department of Physics, Andhra University, Visakhapatnam, India

*Corresponding Author E-mail: nvrao@narl.gov.in

Abstract

The ionosphere of Mars is primarily produced by the ionization of its dominant neutrals, mainly CO_2, through solar extreme ultraviolet (EUV; 10-100 nm) and Soft X-ray (SXR;1-10 nm) radiation. This process results in the production of photoelectrons, which are mostly suprathermal (energy > 1 eV) in nature. Suprathermal electron energy spectra are characterized by He-II photoelectron peaks at 22-27 eV due to solar 30.4 nm radiation and Auger electron peaks at ~500 eV due to <2.3 nm radiation. These suprathermal electrons become thermalized through collisions, resulting in a thermal electron population. Thus, the thermal electrons are primarily sourced from the suprathermal electrons, particularly those produced by the 20-90 nm radiation. To better understand the variability of these electron populations, we studied the response of these electron populations to their respective ionizing radiation. Specifically, we investigated the response of Auger electrons to SXR radiation, He-II photoelectrons to 30.4 nm radiation, and thermal electrons to EUV radiation. We used the suprathermal electron differential energy fluxes measured by the Solar Wind Electron Analyzer and the thermal electron densities measured by Langmuir Probe and Waves instruments on the Mars Atmosphere and Volatile Evolution (MAVEN) mission. We obtained the SXR irradiances from the Extreme Ultraviolet Monitor instrument on MAVEN and the 30.5nm and EUV radiation from Flare Irradiance Spectral Model for Mars. The data used in this study spanned from January 2015 (Martian Year (MY) 32, solar longitude, Ls=263°) to December 2019 (MY 35, Ls=110°), which falls in the declining phase of solar cycle 24.

The results of the present study indicate that the fluxes of suprathermal electrons and densities of thermal electrons are significantly reduced during the solar minimum. Auger electrons exhibit a significant correlation and nearly linear relationship with SXR irradiance, regardless of altitude. However, the response of He-II photoelectrons to 30.5 nm solar irradiance shows a slight deviation from the linear relationship, particularly in the altitude range of 225-350 km and the solar zenith angle (SZA) range of 45°-65°. In these same SZA and altitude ranges, thermal electrons demonstrate a power-law dependence on EUV irradiance. Furthermore, the response of both He-II photoelectrons and thermal electrons to their respective solar irradiances decreases on either side of the altitude and SZA range of maximum response (225-350 km and 45°-65°, respectively). The energy-dependent response of electrons to solar irradiances and their altitude and SZA variation can be explained by considering their dependence on electron temperature and ionization as well as neutral heating efficiencies. Additionally, the responses of He-II photoelectrons and thermal electrons to their respective solar irradiances were found to be decreased near the terminator.

An efficient pulse amplitude measurement technique for radiation or particle detectors

Arpit Patel[1,2,*], Himanshu Mazumdar[2]
[1] Physical Research Laboratory, Ahmedabad 380009,Gujarat,India
[2] Dharmsinh Desai University, Nadiad 387001,Gujarat,India

In radiation detector signal processing, a charge-sensitive preamplifier typically converts the small charge signal from a semiconductor-based detector into voltage form, further amplifies the signal, and measures the energy of the incident radiation. The charge sensitive preamplifier (CSPA) output voltage pulse is amplified using a shaping amplifier that reduces the signal bandwidth. To improve energy resolution, the peak amplitude of the shaping amplifier output must be accurately measured. Recently, it was shown that signals from charge-sensitive preamplifiers can be directly digitized using high-speed analog-to-digital converters (ADCs), followed by further signal processing such as amplification and shaping in field-programmable gate arrays. increase. (FPGA). This method requires a higher sampling analog-to-digital converter (ADC) that consumes more power. For multi-detector systems, these types of methods are very power intensive and difficult to implement in field programmable gate arrays (FPGAs). In this direction, development of technique is started which uses charge-sensitive preamplifiers, shaping amplifiers, low-sampling analog-to-digital converters, and field-programmable gate arrays. LaGrange's interpolation technique is implemented in a field programmable gate array to accurately measure the peak of analog pulses. Results show that the implemented technique provides similar energy resolution compared to pulse processing and standard peak detector-based techniques. The results of same will be discussed in the forum.

A Volumetric Study of Flux Transfer Events at the Dayside Magnetopause and Their Ionospheric Response

Arghyadeep Paul[1*], Bhargav Vaidya[2] and Antoine Strugarek

[1,2] Department of Astronomy Astrophysics and Space Engineering, Indian Institute of Technology Indore, Khandwa Road, Simrol, Indore 453552, India
[3] Département d'Astrophysique/AIM, CEA/IRFU, CNRS/INSU, Université Paris-Saclay, Université de Paris, F-91191, Gif-sur-Yvette, France

*Corresponding Author E-mail: **arghyadeepp@gmail.com**

Localized magnetic reconnection at the dayside magnetopause leads to the production of Flux Transfer Events (FTEs). The magnetic field within the FTEs exhibit complex helical flux-rope topologies. Leveraging the Adaptive Mesh Refinement (AMR) strategy, we perform a 3-dimensional magnetohydrodynamic simulation of the magnetosphere of an Earth-like planet and study the evolution of these FTEs. For the first time, we detect and track the FTE structures in 3D and present a complete volumetric picture of FTE evolution. The temporal evolution of thermodynamic quantities within the FTE volumes confirm that continuous reconnection is indeed the dominant cause of active FTE growth as indicated by the deviation of the P-V curves from an adiabatic profile. An investigation into the magnetic properties of the FTEs show a rapid decrease in the perpendicular currents within the FTE volume exhibiting the tendency of internal currents toward being field aligned. An assessment on the validity of the linear force-free flux rope model for such FTEs show that the structures drift towards a constant-alpha state but continuous reconnection inhibits the attainment of a purely linear force-free configuration. Additionally, the flux enclosed by the selected FTEs are computed to range between 0.3-1.5 MWb. For the selected FTEs, the linear force-free model underestimated the flux content by up to 40% owing to the continuous reconnected flux injection. I shall also highlight the incorporationof a two-way coupled ionospheric model into the global magnetospheric model to probe into the temporal and spatial scales of the ionospheric response associated with these transient events. Ourstudy reveals an intricate coupling between the FTEs and the magnetopause and their ionospheric responses.

References: Arghyadeep Paul, Bhargav Vaidya, & Antoine Strugarek (2022). A Volumetric Study of Flux Transfer Events at the Dayside Magnetopause. The Astrophysical Journal, 938(2), 130.

Morphic Analysis and Mapping of Surface Landforms of Lyot Crater, Mars

Shabana Ebrahim and Nithya Mullassery

Department of PG Studies & Research in Geology, MES Ponnani College (University of Calicut), Ponnani South, Malappuram District, Kerala – 679586.
E-mail: shabnaebrahim@gmail.com; nithyaa.m@gmail.com

Abstract: Being the largest and the deepest impact crater on the northern lowlands, Lyot with a diameter of around 220 km is situated near the hemispheric dichotomy of Mars. The cryosphere would have been penetrated by the impact, revealing the groundwater beneath. Lyot and the outlying areas preserve the effects of ancient, recent groundwater and atmospheric precipitation [1]. Wind-dominated features are ubiquitous on mars and are evolving over time. The key objective of the study is to identify and map major morphological features within the impact crater. The present study utilizes the processed CTX (5-6 m/pixel, 30 km swath) and HRSC DEM, supported by higher resolution HiRISE (25-30 cm/pixel, ~6 km swath). The features identified from the study area include fluvial channels, distal ridges, glacial-like forms, dune forms of various types, etc. The study of aeolian features unravels wind behaviour and current topography, whereas fluvial and glacial-periglacial are crucial in comprehending the history of water on Mars.

Reference: [1] Brooker, L.M. et al. (2015) EPSC2015-810.2015.

Physical and Spectral Characteristics of the Reiner Gamma Swirl

M. Bhatt[1*], C. Wöhler[2], J. Rogall[2], M. Hess[2], Aravind K.[1], S. Ganesh[1], A. Bhardwaj[1]
[1]Physical Research Laboratory, Ahmedabad, 380009, India
[2]Image Analysis Group, TU Dortmund University, Otto-Hahn-Str. 4, 44227 Dortmund, Germany
*megha@prl.res.in

The formation of lunar swirls is still unknown. It can be analyzed by integrating information retrieved from high spatial resolution hyperspectral near-infrared (NIR) and polarimetric datasets. A systematic spectral study in the NIR wavelength region provides a comparison of spectral characteristics of swirls with respect to their surroundings. A spectropolarimetric study at a scale comparable to the hyperspectral NIR data would constrain the physical properties of the swirl regolith, such as the grain size distribution, within the swirl [e.g., 1-2]. We used the Moon Mineralogy Mapper (M³) data of the Chandrayaan-1 mission for understanding the spectral trends of a set of swirls [3] and found that magnetic shielding of the surface from the solar wind alone, a commonly assumed formation mechanism of swirls [e.g., 4-5], cannot explain the observed spectral trends. To further understand the formation of swirls, we conducted systematic imaging polarimetric observations of the Reiner Gamma swirl using PRL's Mount Abu observation facility, covering mainly phase angles around the maximum polarization angle of 100°. Reiner Gamma is the only swirl that can be observed using Earth-based telescopes due to its location on the lunar nearside. It exhibits a rich structure of high-albedo curved lines extending across an area of about 200 km^2.

In this work, we will present results obtained from M³ spectral analysis and from imaging polarimetric observations of Reiner Gamma. The spectral and physical parameters derived from these two independent datasets suggest that the regolith of the Reiner Gamma swirl is compacted and shows variations in compaction within the structure. However, the surface roughness is comparable to the background mare. Our polarimetric observations reveal grain size variations in the range of 40–100 µm within the swirl structure, suggesting the occurrence of surface alteration processes that might have disrupted the regolith microstructure on the swirl. More specifically, the results obtained by the described two independent approaches suggest an external mechanism such as the interaction between the regolith and cometary gas as a formation mechanism of swirls [6, 7], where the magnetic field may have led to a "preservation" of the surficial structures formed by this interaction over geologically long periods of time.

References: [1] Bhatt, M. et al. (2021) 52nd 2430. [2] Dollfus, A. 1998, Icarus , 136, 69. [3] Hess, M. et al. (2020) A&A 639, A12. [4] Hood L. et al. (1979) Science 204, 53-57. [5] Blewett, D. T. et al. (2011) JGR 116, E02002. [6] Shevchenko, V. V. (1993) Astron. Rep. 37(3), 314-319. [7] Pinet, P. et al., (2000) J. Geophys. Res. 105(E4), 9457-9475.

Detailed Geologic Context of Orthopyroxene, Olivine, Spinel (OOS) Exposures on the Moon: Implications for Their Origin

Garima Sodha*, Roshan Adarsh Shukla and Deepak Dhingra

Department of Earth Sciences, Indian Institute of Technology Kanpur, India – 208016

*Corresponding Author Email: garimasd@iitk.ac.in

The occurrence of Orthopyroxene, Olivine, Spinel (OOS) exposures on the Moon is rare with only a few exposures known so far [1, 2, 3]. The discovery of OOS has been a recent addition to the lunar crustal inventory. The understanding of their character, formation mechanism, and role in lunar crustal evolution is still a work in progress. Their exploration is a bit challenging given the limited exposures of OOS. In this work, we have evaluated the detailed geologic context of OOS exposures at Moscoviense basin (27ºN, 148ºE; diameter: ~ 650 km) and Ingenii-Thomson region (32ºS, 163ºE; diameter ~ 282 km) and explored their relevance in drawing information about the origin of these occurrences.

We have analyzed the regional and local scale geologic settings of OOS components using multi-resolution imaging and topography datasets including Lunar Reconnaissance Orbiter Wide Angle Camera (LRO WAC), Narrow Angle Camera (NAC), SELENE Terrain Camera (TC) and digital elevation model (DEM) derived from SELENE TC and Lunar Orbiter Laser Altimeter (LOLA) [4, 5]. Broad scale geologic context illustrated the link of various OOS components with the Moscoviense basin inner ring. These occurrences are associated with undisturbed as well as fresh surfaces [1, 2]. The geological association of mafic lithologies with the basin inner ring has been used by earlier workers to propose that OOS represents the remnants of layered plutons excavated during the basin impact [1]. In contrast, our reported occurrences of OOS at Ingenii-Thomson region are associated with Ingenii basin floor and are potentially related to the ejecta of Thomson crater [3, 6]. These two geological settings of OOS exposures at Moscoviense basin and in the Ingenii-Thomson region are quite different despite both representing deep-seated material exposed at the surface. We have been carrying our detailed characterization of these different geologic settings of OOS to evaluate the layered pluton hypothesis and explore potential alternative explanations for their origin.

References: [1] Pieters et al. (2011) JGR, vol 116, E00G08. [2] Bhatt et al. (2018) Icarus, 303, 149-165. [3] Sodha G. and Dhingra D. (2022), 52nd LPSC, abs #2894. [4] Barker et al. (2016) Icarus, 273, 346-355. [5] Haruyama et al. EPS, 60, 4. [6] Sodha G. and Dhingra D. (2022) GSA Connects, 54, 5, https://doi.org/10.1130/abs/2022AM-382246.

Complex Potential Structures Around Sunlit Moon

Trinesh Sana[1,2], S. K. Mishra[1]

[1]Physical Research Laboratory, Ahmedabad, 380009, India
[2]Indian Institute of Technology, Gandhinagar, 382355, India

*Corresponding Author E-mail: trineshsana@prl.res.in

Being an airless planetary body, the lunar surface undergoes electrostatic charging due to the dynamic interaction between energetic UV radiation and solar wind/ambient plasma. The UV-induced photoelectrons and ambient plasma populations create a space-charge region near the sunlit lunar surface called the photoelectron sheath which is an integral part of the lunar plasma environment [1]. Charged dust particles within the sheath can float in the vicinity of the surface due to electrostatic Coulomb repulsion [2]. The signatures of the lunar plasma environment were indirectly observed as a form of a horizontal glow during the Surveyors and Apollo era [3-4]. Since plasma is key in generating the electrical environment, determining the complex electric potential/ field structures and plasma dynamics within the sheath is of technological interest to efficient instrument operation on lunar modules. Electron distributions measurement of Lunar Prospector (LP) above the dayside lunar surface indirectly implied the existence of a non-monotonic electric potential structure near the lunar surface [5].

This presentation gives an analytical formulation of complex potential structures around the sunlit Moon. The justified solar spectrum, solar wind flux, and Fermi Dirac distribution of the photoelectrons have been taken in the formulation. The photoelectron sheath has been found to be a significant function of solar radiation flux and spectrum, solar wind plasma, surface temperature, surface material characteristics, and angle of solar inclination [6]. In the region of marginal/zero photoemission near the terminator, a traditional Debye sheath forms. While moving towards the equator, the photoelectron contribution increases, yielding monotonic and non-monotonic sheath solutions over a sunlit locations. For the normal solar wind plasma, our calculations demonstrate that non-monotonic potential structures are more stable towards the terminator region, although both potential structures are equally probable near the equator region. For nominal solar wind plasma parameters near the equator, vertical sheath extensions of 60 m and 12 m, corresponding to non-monotonic and monotonic sheaths, have been observed [7]. The Moon briefly passes through the Earth's magnetosphere tail lobe and plasmasheet during each lunar orbit. According to our model, a sufficiently strong negative charge (kV) development is observed near the terminator due to high plasma electron temperature. The surface potential near the equator also acquires a high negative potential. This significant negative potential development over the lunar surface may be harmful to long-term efficient instrument functioning over the Moon, particularly in the terminator region when the Moon passes through Earth's magnetospheric plasma [7]. This study might be valuable in developing test procedures for future lunar exploration missions.

[1] Sodha M. S. and Mishra S. K. (2014) *Phys. Plasmas, 21(9), 093704.* [2] Colwell J. E. et al. (2007) *Rev. of Geophys., 45(2).* [3] Rennilson J. J. and Criswell D. R. (1974) *Moon, 10(2), 121-142.* [4] Zook H. A. and McCoy J. E. (1991) *GRL, 18(11), 2117-2120.* [5] Halekaset al. (2012) EPS, 64, 73-82. [6] Mishra S. K. and Bhardwaj A. (2019) APJ, 884(1), 5. [7] SanaT. and Mishra S. K. (2023) MNRAS, 520(1), 233-246.

Lipidomics as an emerging tool in Astrobiology

Gaurav Yadav[1], Dr. Roohi[1,*]

[1]Protein Research Laboratory, Department of Bioengineering, Integral University, Lucknow

[*]Corresponding Author: Dr. Roohi, Email address: roohi0607@gmail.com

Abstract: Finding the tenability of life in other planetary bodies requires profound information on versatility and limits on Earth. Astrobiology zips in the quest for life on self-reproducing microorganisms equipped to follow Darwinian evolution in liquid water. All recognized living things on Earth are dependent on the organic matter. It incorporates fossils, their biominerals, compounds and metabolites [1]. Concerning astrobiology, omics approach has improved the understandings of the perseverance capabilities of extremophilic microorganisms on Earth. Extremophiles terms organisms that occupy environmental niches regarded as extreme by the standards of most living organisms [2]. The encapsulating membranes in extremophiles are amphiphilic molecules like lipids and fatty acids and their unusual properties play a key role in adaptation to extreme conditions [3]. Metabolomics technique offers quick recognition of minute particles inside carbon-based biological settings and is an interdisciplinary field [4]. Lipidomics, a subfield of metabolomics, has progressed with high precision and specificity that can resolve the essential lipidome. Lipidomics of extremophiles offers to study the lipid composition of contemporary microbes under a variety of stress conditions. Molecular lipid fossils are the geological retention lipids of extremophiles from an early earth record which has gone alterations due to catagenesis and diagenesis [5]. Lipids of contemporary extremophiles are a precursors of molecular lipid fossils and is a good candidate for lipid biosignature to search for past and present life on extra-terrestrial planets [6].

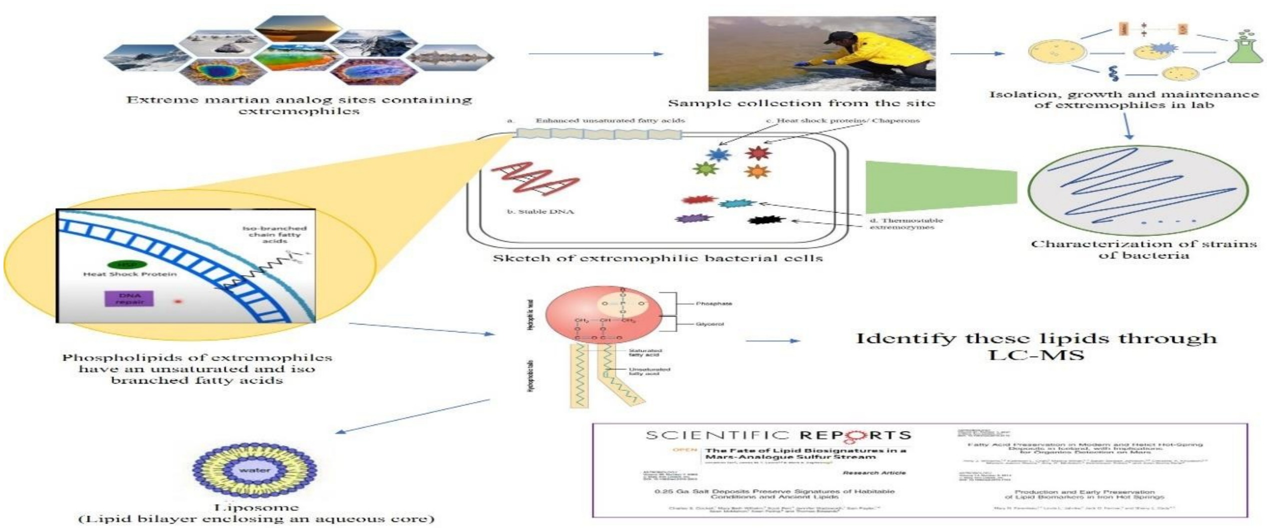

Sample of extremophiles present at martian analogue site are collected for isolation and maintenance. Lipids of extremophiles plays an important role in the adaptation of extremophiles in extreme environment and can be isolated and identified through lipidomics.

References:

1. Shukla AD, Ray D and Bhattacharya S (2017) Sulphate Mineral from Hot Springs in Cold Desert (Ladakh, India): Analogue to Martian Sulphate Deposit? Lunar and Planetary Science (XLVIII) Conference, March 2017, Houston, TX, USA.
2. Irwin JA. Overview of extremophiles and their food and medical applications. InPhysiological and Biotechnological Aspects of Extremophiles 2020 Jan 1 (pp. 65-87). Academic Press.
3. Tan, J., Lewis, J.M.T., and Sephton, M.A. (2018) The fate of lipid biosignatures in a mars analogue sulfur stream. Sci Rep 8:7586.
4. Seyler L, Kujawinski EB, Azua-Bustos A, Lee MD, Marlow J, Perl SM, Cleaves Ii HJ. Metabolomics as an emerging tool in the search for astrobiologically relevant biomarkers. Astrobiology. 2020 Oct 1;20(10):1251-61.
5. Summons, R.E., Albrecht, P., McDonald, G., and Moldowan, J.M. (2008) Molecular biosignatures. Space Sci Rev 135: 133–159.
6. Georgiou CD, Deamer DW. Lipids as universal biomarkers of extraterrestrial life. Astrobiology. 2014 Jun 1;14(6):541-9

Martian cold spot regions and associated properties during the 2018 global dust storm using MRO/MCS observations

Anirban Mandal, Jagabandhu Panda*, Nirvan Abhilash

Department of Earth and Atmospheric Sciences, National Institute of Technology Rourkela, Sector-1, Rourkela, Odisha 769008, India

*Corresponding Author E-mail: jagabandhu@gmail.com ; pandaj@nitrkl.ac.in

The weather and climate on Mars depend heavily on the characteristics of dusts and aerosols. Dust, CO_2, ice, water ice, etc., suspended in the air, play a critical role in the thermal equilibrium, circulation, and transfer of momentum in Mars' atmosphere. Cold spot regions are those radiometrically cold areas where the temperature is less than the CO_2 frost point temperature. These regions have the maximum probability of CO_2 ice formation. On Mars, global dust storms (hereafter, GDS) drastically change the microphysical characteristics of CO_2 ice aerosols, besides their geographical and vertical distributions. With the help of the Derived Data Record (DDR) version 5 obtained from the Mars Climate Sounder (MCS) instrument on board the NASA's Mars Reconnaissance Orbiter (MRO) mission, an attempt is made to investigate the origin of cold spots, their spatial and temporal variation, etc. The work focuses on the cold spot regions' vertical, temporal, and spatial variation during the Martian Year 34 GDS. GDS affected the latitudinal variation of ice cap formation and solar insolation, which in turn impacted the cold spot formation. Cold spot regions were found only at the surface levels at the south pole. Most North Pole cold spots formed on the polar nights, and during the global dust storm season, the cold spot regions in the northern hemisphere started to develop outside the polar ring and at lower altitudes as well. Also, during dust storms, there is a high concentration of dust at higher altitudes, which provides a nucleation site for CO_2 ice, leading to the formation of polar hood clouds.

References:

1) Hayne, P., & Paige, D. A. (2008, March). Mars Polar Cold Spots Observed by MRO Mars Climate Sounder. In *39th Annual Lunar and Planetary Science Conference* (No. 1391, p. 2516).

2) Cornwall, C., & Titus, T. N. (2009). Spatial and temporal distributions of Martian north polar cold spots before, during, and after the global dust storm of 2001. *Journal of Geophysical Research: Planets*, *114*(E2).

3) Cornwall, C., & Titus, T. N. (2010). A comparison of Martian north and south polar cold spots and the long-term effects of the 2001 global dust storm. *Journal of Geophysical Research: Planets*, *115*(E6).

4) Weiss, B. P., & Ingersoll, A. P. (2000). Cold spots in the Martian polar regions: evidence of carbon dioxide depletion?. *Icarus*, *144*(2), 432-435.

Elucidating the history of Morella Crater, Mars

Hiral P B [1*], Devika Padmakumar, Sajinkumar K.S.[1]

[1]Department of Geology, University of Kerala, Kariavattom P.O., Thiruvananthapuram-695581, Kerala

*Corresponding Author E-mail: pbhiral@gmail.com

Morella Crater provides an insight to the spectacular catastrophic floods that spawned on Mars from the breaching of its crater lake. Morella crater, a 78 km diameter complex crater, is breached on its eastern side by the Elaver Vallis outflow channel and is nested with an extremely deep collapse structure, called the Ganges Cavus [1]. This crater exhibits temporal and spatial link between diverse features like cavus, water pooling, breaching and outflow channel that indicates its complex history, and thus can shed light on several geological conundrums that modified the Martian surface environment. Thus, the present study focuses on the surface modification processes that was further used for proposing different stages of evolution of Morella crater. Mars Orbiter Laser Altimeter (MOLA) Digital Elevation Models (DEMs), wide and narrow angle Mars Orbiter Camera (MOC) images, High Resolution Imaging Science Experiment (HiRISE) images and MRO Context Camera (CTX) images together with both Thermal Emission Imaging System (THEMIS) visible (VIS) and infrared (IR, both daytime and night time) images, Thermal Emission Spectrometer (TES) and Compact Reconnaissance Imaging Spectrometer of Mars(CRISM) data were used to elucidate the morphological features and processes of Morella crater. Furthermore, a schematic model depicting the entire sequel of the origin of this crater was done using Interactive Erosion simulation in Web Browser (Webgl-Erosion).

This study proposes a five-stage processes that manifest the origin and evolution of Morella crater representing a Hesperian lake basin that was once fed by groundwater. Stage 1 reveals an asteroid impact that formed Morella Crater with extensively fractured terrain in a time period of 5.52×10^1 seconds. The sepulchring of crater was due to filling-up of 2-3 km deposits of sedimentary or volcanic and aeolian origin (stage 2) [2]. Later in third stage, Ganges Cavus, a deep collapsed part (-4000 m), was formed, which is approximately the same as the elevation of the floor of Ganges Chasma. Subsequently, the breakout of confined groundwater produced a lake in Morella and leads to filling of crater, which is depicted in the fourth stage. Eventually, the lake level rose until the wallof Morella crater was overtopped and breached leading to catastrophic release of ponded waters andthe carving of the Elaver Vallis channel complex [3]. By these inferences important clues for the sediment deposits in crater, subsidence of Ganges Cavus, source of water that filled the crater and the catastrophic release of ponded water were revealed with minute details. Thus, this study shed more but convincing evidences on the plausible origin and evolution of Morella Crater

Reference:[1] Michalski, J.R., 2021. The volcanic geology of Morella Crater, Ganges Cavus and Elaver Vallis, Mars. doi.org/10.21203/rs.3.rs-198982/v1

[2] Lucas, A., Ansan, V. and Mangold, N., 2009. New insight on genetic links between outflows and chasmata on Valles Marineris plateau, Mars. *Géomorphologie: relief, processus, environnement*, *15*(1), pp.33-46.

[3] Coleman, N.M., Dinwiddie, C.L. and Casteel, K., 2007. High outflow channels on Mars indicate Hesperian recharge at low latitudes and the presence of Canyon Lakes. *Icarus*, *189*(2), pp.344-361.

A 4-stage model for the formation of Hebes Chasma, Mars

Rahul S.[1*], Devika Padmakumar, Sajinkumar K.S.[1]

[1]Department of Geology, University of Kerala, Kariavattom P.O., Thiruvananthapuram-695581, Kerala

*Corresponding Author E-mail: rahul.s2235@gmail.com

Hebes Chasma is an exclusively endorheic chasma located in the northern side of Valles Marineris, just east of the Tharsis region. The chasma is 315 km long and 126 km wide with a maximum depth of 8 km from the rim. One of the important features that distinguish Hebes Chasma from other Valles Marineris chasmatic system is the presence of a 120 km long plateau, called Hebes Mensa, which is considered to be an interior layered deposit (ILD) [1]. Many scientists have attempted to unravel the mysteries behind the origin of Hebes Mensa; but unequivocal evidence was not so far put forth. Thus, the aim of this study is to put forth a new plausible mechanism of origin for this chasma, which was achieved through morphological comparison with adjacent and similar features. Through this a multiple stage-wise processes for the evolution of Hebes Mensa was suggested. This suggestion will also aid to untangle the mysteries of Valles Marineris' formation. The methodologies used in this study is morphometric and structural identification of myriad features through interpretation of MOLA DEM, topographic profiling using Google Mars and HEC-RAS software, high-resolution imaging studies using CTX and HiRISE, and mineralogical studies using hyperspectral CRISM data and comparison with library spectrum Our study reveals that Hebes Chasma is formed concomitant to Valles Marineris due to the extensional pressure created by Tharsis bulge resulting in rift cracking and valley widening due to normal faulting during late Noachian to early Hesperian. This was followed by volcanism, which filled this widened crack and several layers of pyroclastic materials have been deposited [2]. As there is no evidence of an outflow channel, the pressure generated by the pyroclastic deposit melted the surrounding hydrous minerals like kieserite, epsomite, hexahydrite, and gypsum that increased the pore pressure leading to collapse and piping mechanism escorting the huge amount of materials away from the chasma [3]. Finally, the chasma was subjected to several geologic agents like wind erosion that created the rugged chasma floor; mass wasting along the chasma walls, and fluid overflow all along the chasmaboundary, which as a wholesome created the present topography.

Reference: [1] Schmidt, G., Fueten, F., Stesky, R.,Flahaut, J., & Hauber, E. (2018). Geologyof Hebes Chasma, Mars: 1. Structure, stratigraphy, and mineralogy of the interior layered deposits.Journal of Geophysical Research: Planets, 123, 2893–2919.

[2] Peterson, C. (1981). A secondary origin for the central plateau of Hebes Chasma. Proceedings Lunar Planet Science, XI, 1459–1471.

[3] Jackson, M. P. A., Adams, J. B., Dooley, T. P., Gillespie, A. R., & Montgomery, D. R. (2011). Modeling the collapse of Hebes Chasma, Valles Marineris, Mars. GSA Bulletin, 123(7–8), 1596–1627

Spatial distribution of anomalous impact melt ponds on the lunar farside: Insights fromnew areal coverage map

Satyendra Kumar* and Deepak Dhingra

Department of Earth Sciences, Indian Institute of Technology Kanpur, Kanpur, 208016, India

*Corresponding Author E-mail: sgeo365@gmail.com

An anomalously distinct grouping of smooth impact melt deposits were identified at the antipode of Tycho crater based on high resolution imaging observations [2]. Their smoothness, morphological freshness and crater counts provided a very young age (Late Copernican) for these deposits. The source crater for these deposits has not yet been identified although earlier workers have identified nine plausible source impact craters [2]. We have used multiple morphological criteria to rule out more than half of the craters as a source for these deposits [1, 3].

In the present study, we have carried out a search for the smooth melt deposits beyond the region defined by previous workers and found several new impact melt occurrences. Though the newly identified melt deposits are present all around the previously reported region, a large percentage appears to be concentrated in the eastern side. The revised spatial distribution map of these deposits would help in better understanding of the emplacement of the impact melt.

References: [1] Dhingra et al. 21st NSSS (2022) pp.305 [2] Robinson et al. (2016), Icarus, 273, 121–134. [3] Kumar S. and D. Dhingra, IPSC (2021), pp.97.

Sequels of transformation of Aram Chaos from an ancient complex impact crater into achaotic terrain

Evna Suresh[1]*, Devika Padmakumar[1], Sajinkumar K.S. [1]

[1]Department of Geology, University of Kerala, Kariavattom P.O., Thiruvananthapuram-695581, Kerala

*Corresponding author e-mail: evnasuresh@gmail.com

Aram Chaos, one of the largest and oldest, and most extensively studied impact craters on Mars, is a 280 km diameter complex crater that hosts the second largest-known site of hematite deposits. This crater has undergone several surface modification processes that erased all the crater morphologic features and penultimately depicting a chaotic terrain. The transformation has occurred through several stages. This study narrates the sequels of changes in this massive impact crater. MOLA elevation data, HiRISE and CTX images aidedin creating a 3D model of the crater using ArcGIS and WebGL software.

This study aims to produce the sequence of events the terrain had undergone in stages. Stage 1 depicts the impact collision of the projectile causing a crater formation. Subsequently, the crater has been filled with sediments, preferably by aeolian activity [1], which is narrated in stage 2. The climatic condition of the planet is believed to have a wetter climate than the present condition, in turn making the sediments water saturated. This further leads to the formation of ground ice, depicted in stage 3 [2]. Periodical shifting of climatic condition on Mars has created this event, which might also be the cause for the melting of ice (Stage 4). Stage 5 is the breaching of the crater rims followed by the catastrophic outflow of sediments and water that flows up to Aram Valles. Finally Stage 6 depicts the creation of a chaotic terrain with a rough topography having large slumped and angled blocks [1].

Furthermore, a comparative study on the morphology of craters, similar in size and age, aided in comprehending the past retaining features of the crater and allows constructing a stratigraphy depicting its origin and the evolution. This brings insight of craters of Noachian time and better understanding of the Martian activity that helped in shaping to its current form.

Reference

[1] Glotch, T., Christensen, P., 2005. Geologic and mineralogic mapping of Aram Chaos: Evidence for a water-rich history. J. Geophys. Res. 110, E09006.

[2] Zegers, T.E., Oosthoek, J.H., Rossi, A.P., Blom, J.K., Schumacher, S., 2010. Melt and collapse of buried water ice: An alternative hypothesis for the formation of chaotic terrains on Mars. Earth Planet. Sci. Lett. 297, 496–504

Effect of ion beam on electromagnetic ion cyclotron wave for ring distribution with A.C. electric field in Jovian magnetosphere

R.S. Pandey

Department of Physics, Amity Institute of Applied Sciences, Amity University, Sector – 125 Noida, Uttar Pradesh, India

rspandey@amity.edu

Abstract

The electromagnetic ion-cyclotron waves observed by the Ulysses in Jovian magnetosphere has been investigated in this paper. Various type of large frequency radio emissions by mechanism of resonant interaction has been observed in Jovian magnetosphere. In this paper, the phenomenon of wave-particle interaction between electromagnetic ion-cyclotron waves along with magnetic field lines and fully ionized magnetospheric plasma particles has been considered with parallel propagation of wave to evaluate the detailed dispersion relation with ring distribution in the presence of parallel AC electric field in collision-less magnetoplasma at 17 R_J. Using method of characteristics solution and kinetic approach, expression for relativistic growth rate has been derived. Injection events observed by the Galileo spacecraft through energetic charged particle detector (EPD) in Jovian magnetosphere has been studied. After injecting hot ion beam, parametric analysis of following plasma parameters like temperature anisotropy, AC frequency, relativistic factor etc., has been done and the effect of these plasma parameters on growth rate has been studied via graphs plotted.

Keywords- Electromagnetic ion-cyclotron waves, Ring distribution, hot injection, Jovian magnetosphere

Scaliger Crater Region on the Moon: A Window to the Geological History of the Australe North Basin

Neha Panwar[1,2*], Neeraj Srivastava[1]

[1]Planetary Remote Sensing Section (PRSS), PSDN, Physical Research Laboratory, Ahmedabad

[2]Indian Institute of Technology, Gandhinagar

*nehapanwar20@gmail.com

Australe North (35.5°S, 96°E) is a ~880 km pre-Nectarian impact basin lying to the north of the Mare Australe (38.9°S, 93°E), first identified using the GRAIL data [1]. The basin has no morphological or topographic signatures typically associated with large impact basins on the Moon. Further, the proposed extent of the Australe North Basin does coincide with Mare Australe, which was previously understood as a basin-filling event associated with the Australe Basin [2]. It has been observed that a significant fraction of the Mare Australe basalt lies outside the proposed Australe North Basin. Hence, the relationship of the Australe North Basin with the volcanism in the region is poorly understood.

The Scaliger Crater (27.1°S, 108.9°E) is a ~87 km crater located on the northeastern flank of the Australe North Basin. The unique location of this crater at the intersection of the outer rims of the Australe North and the pre-Nectarian Milne Basin makes it an ideal site to understand the complex stratigraphy of the region. This study employs high-resolution remote sensing data (imaging, topography, and mineralogy) to delineate the geology of the Scaliger Crater and its surrounding region (upto ~6 crater radii) and utilise it to infer the geological evolution of the Australe North Basin. We report extensive magmatism in the area, including the possible intrusion of an Mg-pluton in the subsurface and late-stage volcanism at ~1.7 Ga. The study also establishes the critical role the Australe Basin played in the magmatism associated with the Mare Australe.

Citations: [1] Neumann G. A. et al. (2015) *Sci Adv.* 1(9), e1500852. [2] Whitford-Stark, J. L. (1979) *LPSC X*, 2975-2994.

MAVEN & MEX observations of the Martian upper atmosphere during the passage of stealth coronal mass ejection

V.Venkataraman* and Smitha V Thampi
Space Physics Laboratory, Vikram Sarabhai Space Centre, Thiruvananthapuram
*Corresponding Author E-mail: v.venkataraman@gmail.com

Introduction

Coronal Mass Ejections (CMEs) are energetic events originating from the Sun during which an enormous amount of magnetised solar plasma is ejected into the heliosphere. CMEs releases 10^{14} - 10^{16} g of plasma materials with a typical radial speed of 300 - 500 km s^{-1} (maximum speed at 3000 km s^{-1}) [1]. The source regions of CMEs often consist of complex active regions or filaments [2]. CMEs are classified as halo CMEs, partial halo CMEs, narrow CMEs and CMEs with low coronal signatures based on their morphological evolution. CMEs with no observable signatures at photosphere or lower corona are classified as stealth CMEs, whose speeds are typically ≤ 300 km s^{-1} [3]. Investigation of the interaction of CMEs with planetary bodies provide insights on the evolution of the planetary atmospheres. During the declining phase of solar cycle 24 a stealth CME caused an intense geomagnetic storm at Earth and arrived at Mars. Due to the lack of global intrinsic magnetic fields in Mars, the Martian upper atmosphere and exosphere interacts directly with the solar wind which are in contrast to those of the interaction with Earth's atmosphere. In this study, the response of the Martian upper atmosphere to the impact of CME during 27- 28 August 2018 was investigated.

Observation and data analysis

The in situ data used in the present study were obtained from the various science instruments on board Mars Atmosphere and Volatile EvolutioN (MAVEN) and Mars Express (MEX).

Results and discussion

The Wang-Sheeley-Arge (WSA) model showed the arrival of stealth CME at Mars. MEX observations showed variation in ion and electron fluxes within the plasma boundaries during the passage of ICME. Enhancement in the ion flux was also observed from MAVEN observations during the interaction of the CME with the Martian environment. Energization of planetary ions like O^+ and O_2^+ to hundreds of eV at altitudes below 300 km was observed during the event. The energisation was further supported by the observed enhancement in O^+ pickup ions at energies below 50 keV.

Conclusion

The observed energization and variation in electron flux along the Martian plasma boundaries during the passage of a stealth CME suggest manifestations of significant heating and acceleration during the event.

References

[1] Lamy, P.L., et. al., (2019), *Space Sci. Rev.*,215(5), 39
[2] Gopalswamy, N., et. al., (2006), *Space Sci. Rev.*,123(1 – 3), 303
[3] Webb, D.F., Howard, T.A. (2012), *Living Rev. Solar Phys*,.9(1), 3

Lechatelierite and felsic melt domains within a melt clast: a first report from Dhala impact melt breccias

Jayanta Kumar Pati[1,2,*]

[1]Department of Earth and Planetary Sciences, Nehru Science Centre, University of Allahabad, Allahabad-211002, India

[2]National Centre of Experimental Mineralogy and Petrology, 14 Chatham Lines, University of Allahabad, Allahabad-211002, India

*Corresponding author. E-mail address: jkpati@gmail.com (J.K. Pati)

Abstract

Hypervelocity meteoritic impacts result in the formation of diaplectic ("to destroy by striking"; [1]) glasses (lechatelierite and maskelynite) from commonly occurring silicate minerals on Earth's surface such as quartz and plagioclase feldspar, respectively at pressures of ≥40 GPa accompanied by high residual temperatures (>1500°C; [2]) in the target rock and their presence is considered as impact diagnostic evidence ([3-4]). Unlike actual igneous melting, the diaplectic glasses retain the shape of the precursor mineral grain. However, they are less abundant compared to other unequivocal shock features, such as shatter cones and planar deformation features (PDFs) as they form at relatively higher pressures close to the point of hypervelocity impact ([2]). However, the unequivocal shock features are already reported from Dhala structure [5].

The occurrence of diaplectic glass pseudomorphing various minerals is one of the unequivocal evidences of shock metamorphism. Similarly complete rock melting requires pressure in excess of 60 GPa but the melting processes are not well constrained. Here, the shock melting of a quartzo-feldspathic lithic clast from an impact melt breccia, Dhala structure, India, is presented where multiple felsic melt stringers and a silicic melt (similar to lechatelierite) lens are observed. The felsic melt compositions mimic eutectic melt behaviour similar to synthetic K_2O-Al_2O_3-SiO_2 system suggesting the dominant role of eutectic type punctuated melting rather than instantaneous melt behaviour suggested in impactites, in general.

References: [1] Fritz, J., et al. (2019) *MAPS*, 54, 1533-1547. [2] French, B.M. and Koeberl, C. (2010). *Earth-Science Reviews*, 98,123-170. [3] Goresy, A.E. (1968) *Contr. Mineral. & Petrol.* 17, 331–346. [4] Stöffler, D. (1984) *Journal of Non-Crystalline Solids*, 67, 465-502. [5] Pati, J.K., et al. (2019) *MAPS*, 54, 2312–2333.

Comparative Study of Chandrayaan-3 Prime Landing Sites with Heritage Landing sites

Amitabh, K Suresh, Ajay Prashar, Abdullah S and Kannan V Iyer

Signal and Image Processing Group, Space Applications Centre (ISRO), Ahmedabad-380015
*Corresponding Author E-mail: amitabh@sac.isro.gov.in

The main objective of Chandrayaan-3 mission is to soft and safe landing of a lander on south polar area of lunar surface. The mission goal of soft landing will have to be ensured by an appropriate lander descent trajectory and navigation, guidance and control while the safe landing can be ensured by proper selection of the landing location that meets all the engineering constraints. The Chandrayaan-3 Prime Landing site (69.367621 S, 32.348126E) covering 4km by 2.4km area is situated in the south polar region [1]. This landing area lies between Manzinus U and Bouguslawsky M crater of lunar surface. This site was selected based on terrain parameters and engineering constraints. The basic criteria for landing site selection for chandrayaan-3 includes the local and global slope, sun illumination, radio communication with the earth, crater and boulder sizes. The parameters used are Slope less than 10 deg, Boulders less than 0.32 meter, Crater and boulder density, Sunlit for at least 11-12 days, Visible to Earth for Radio communication, Local terrain features such that they don't shadow the site forlong durations, Distribution of safe grid of 24m x 24m inside 4km x 2.4km landing area [2].

A comparative study has been carried out to compare the Chandrayaan-3 proposed landing sites with respect to the actual landing sites of Apollo and Chang'e missions. This paper provides a comparative study of different terrain parameters like elevation, slope and surface roughness of Apollo-12, 14, 16 and ChangE-4 missions. The LRO-NAC and Chandrayaan-2 OHRC datasets are used for this study. The Digital Elevation Model of heritage sites are generated from LRO-NAC images at the best available resolution (0.6m) while for Chandrayaan-3, 30 cm DEM was extracted from OHRC. Result shows that Chandrayaan-3 proposed site seems to be comparable to other heritage landing sites with respect to terrain roughness parameters even though the heritage sites are situated in the equatorial areas. Figurebelow illustrates the studied landing sites at global scale.

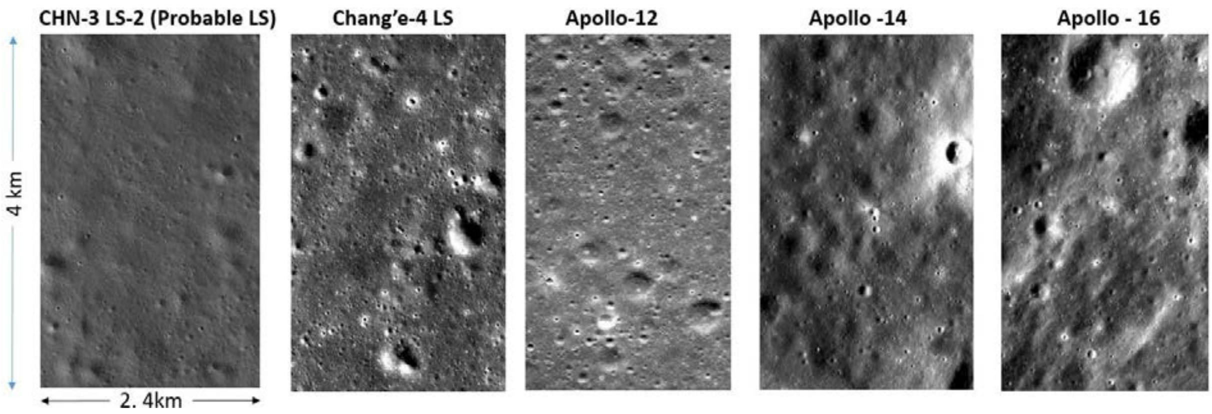

References:

[1] https://www.isro.gov.in/Chandrayaan3_New.html

[2] Amitabh, K Suresh, Ajay K Prashar and Abdullah Suhail A Z, Terrain Characterisation of Potential Landing Sites for Chandrayaan-3 Lander using Orbiter High Resolution Camera (OHRC) Images, LPSC 2023

Effect of MJO Phases on Indian Summer Monsoon onset using OLR and Precipitation

Riddhi D. Prajapati[1], Kamlesh N. Pathak[1*]

[1]Sardar Vallabhbhai National Institute of Technology, Surat-395007, Gujarat, India.
*E-mail: knp@phy.svnit.ac.in

Abstract: The Madden Julian Oscillation (MJO) is characterized by an eastward propagation of strong regions of enhanced convection phase and suppressed convection phase of tropical rainfall, observed mostly over the Indian Ocean and Pacific Ocean. It is defined as a 30–60-day wave in the tropical region. (Confined between latitudes 15°N-15°S). Wind, cloudiness, and rainfall are all associated with the MJO. RMM indices derived from multiple fields of u850-hPa, u200-hPa, and Outgoing Longwave Radiation (OLR) data are used to track MJO. For studying MJO the OLR is an important factor.

The eastward progression of the MJO interacts with the monsoon circulation and modulates the advance, the onset, and the retreat period of the Indian summer monsoon (ISM). Distribute onset year in pre, post, and normal onset years shows the different phase of MJO is responsible for the onset of monsoon. Doing an analysis of OLR and Precipitation data after removing seasonality from it, the relation between the OLR and Precipitation which is associated with MJO has been clearly proven. From this analysis, it has been concluded that OLR anomalies are negative(positive) for above(below) normal rainfall.

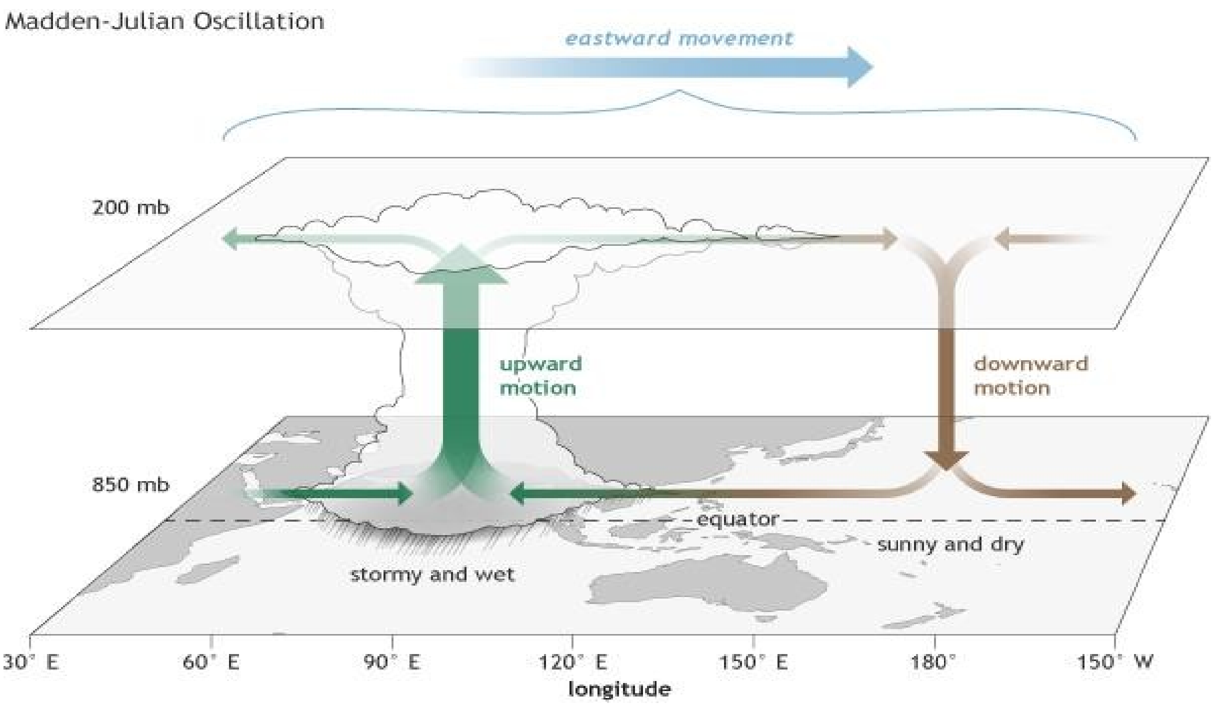

Figure: The structure of MJO. the enhanced convection phase is shown over the Indian Ocean and the suppressed convection phase is shown over the west-central Pacific Ocean. Horizontal left arrows represent wind departures from east to west, and right arrows represent wind departures from west to east. The whole system shifts eastward with time and takes around the globe. (Source: NOAA Climate.gov)

Terrestrial Dyke Swarm Analogues of Prominent Sets of Extensional Lineaments in Eistla Regio Region, Venus

R. K. Srivastava[1], H. El Bilali[2,3], R. E. Ernst[2,3], Twinkle Chaddha[1], Harshita Singh[1],
[1]Department of Geology, Banaras Hindu University, Varanasi, India (rajeshgeolbhu@bhu.ac.in)
[2]Department of Earth Sciences, Carleton University, Ottawa, Canada
[3]Faculty of Geology and Geography, Tomsk State University, Tomsk, Russia.

An elongated equatorial highland on Venus, identified as Eistla Regio, contains abundant radar dark plains and large volcanic edifices [1] and is considered as a broad rise overlying one or more large mantle upwelling [2]. Broadly, it comprises three individual areas of elevated topography, Eastern Eistla Regio, Central Eistla Regio and Western Eistla Regio connected by linear belts of deformation composed of faults and fractures (Fig. 1). Several regions of Eistla Regio, such as Nehalennia, Belet-ili and Gaya (Gaia) coronae, and Anala Mons have been mapped for several thousand of grabens. These grabens, which trend in linear, radial and circumferential patterns, are interpreted to overlie dyke swarms. Such features have been used to identify a number of magmatic centres, and to locate and mantle plumes associated with Eistla Regio.

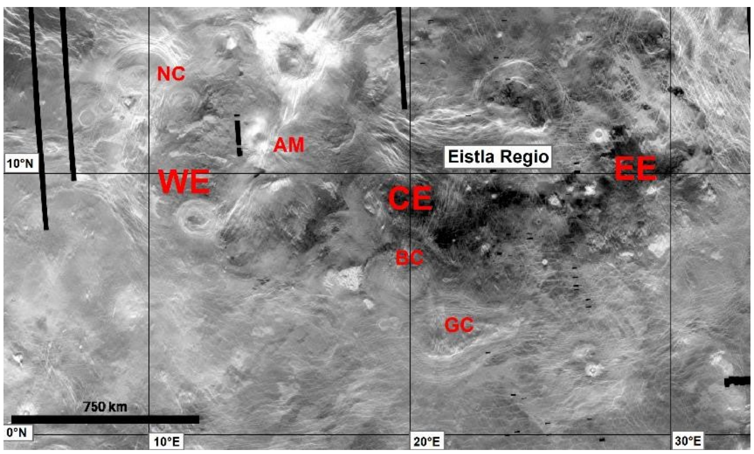

Figure 1: *Eistla Regio image from JMARS [6]. EE – Eastern Eistla, CE – Central Eistla, WE – Western Eistla, AM – Anala Mons, BC – Belet-ili Corona, GC – Gaya Corona, NC – Nehalennia Corona.*

Similar spectacular patterns of dyke swarms are identified on Earth, particularly in the DHABASI Megacraton of the Indian Shield [3,4]. The observed radiating dyke swarm patterns converge on plume centres. The linear swarms might represent part of a larger radiating patterns. Although circumferential dyke swarms are not well preserved in India, they are well exposed in other regions on Earth, for example Lake Victoria magmatic centre in Africa and Keweenawan LIP in North America [5]. This work is an attempt to compare these large linear, radiating and circumferential features, on Venus, with dyke swarms from the Indian shield and elsewhere on Earth.

[1] Basilevsky, A. T., Head, J. W. (1997) *EMP 76*: 67-115. [2] Senske, D. A., et al. (1992) *JGR: Planets* 97, E8, 13395-13420. [3] Samal et al. (2021) *Ore Geol. Rev 131*, 104009; https://doi.org/10.1016/j.oregeorev.2021.104009. [4] Srivastava et al. (2022) *Geol. Soc., London, Sp. Publ. 518*, 175-198. [5] Buchan, K. L., Ernst, R. E. (2021) *Gond. Res. 100*, 25-43. [6] Christensen, P. R. et al. (2009) *AGU Fall Meeting*, Abstract #IN22A-06.

Mapping Magmatic and Structural Units of Belet-ili and Gaya Coronae, Central Eistla Regio, Venus: Dyke Swarm History

Twinkle Chaddha[1], R. E. Ernst[2,3], H. El Bilali[2,3], R. K. Srivastava[1]
[1]Department of Geology, Banaras Hindu University, Varanasi, India (twinkle20.chaddha@bhu.ac.in)
[2]Department of Earth Sciences, Carleton University, Ottawa, Canada
[3]Faculty of Geology and Geography, Tomsk State University, Tomsk, Russia.

Eistla Regio is an important volcanic rise on Venus, and is dominated by enormous radar-dark plains and large volcanic edifices such as Sif Mons, Gula Mons and Sappho Patera [1]. Belet-ili (6.0°N, 20.0°E) and Gaya (Gaia; 3.5°N, 21.5°E) coronae are located about 2000 km east of Gula Mons in Central Eistla Regio [2], within Sappho Patera Quadrangle (previously mapped at 1:5,000,000 scale [3].

In the present study, detailed mapping (1:500,000) is done to develop the geological and tectonic history of the region. Lava flows and graben system (interpreted as the surface expression of dykes), are mapped in order to develop a detailed geological and tectonic history of the Central Eistla Regio (13° to 26°E:0° to 10°N), with a particular focus on Belet-ili and Gaya coronae. Magellan SARdata are used for mapping using ArcMap 10.8.1 software. More than 17,500 grabens are mapped to date, which are revealing multiple linear, radial and circumferential patterns, likely to represent different dyke swarms. These were used to identify at least 11 magmatic centres (see Fig. 1).

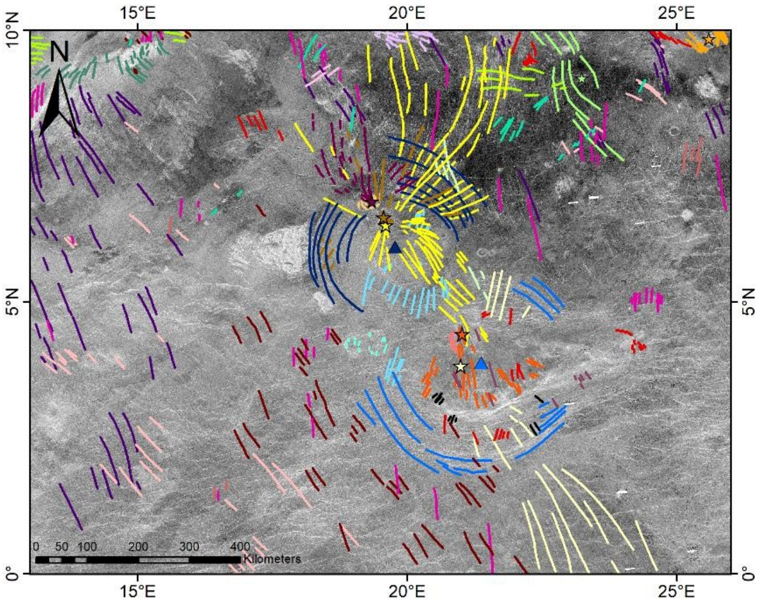

Figure 1: *Geological map of the study area showing generalized graben-fissure systems. Colors represent different dyke swarms. Symbols for magmatic centres: Triangle – circumferential swarm; star – radiating swarm.*

Five different dyke swarms (three radiating and two circumferential) have been distinguished within the Belet-ili Corona along with their magmatic centres. In addition, two other swarms, trending NNE and NNW, are also mapped, however their sources are yet to be determined. The concentric dyke swarm associated with Belet-ili Corona has a diameter of about 360 km. Gaya Corona is an elliptical shaped corona and has diameter of approximately 400-600 km, and include at least one circumferential and three radiating swarms.

[1] Senske D. A. et al. (1992) *JGR, 97*, 13395-13420. [2] Basilevsky, A. T. and J. W. Head (1998) *Earth Moon Planets, 76*, 67-115. [3] McGill, G. E. (2000) *USGS Geol. Invest. Series Map* I-2637; https://pubs.usgs.gov/imap/2637/

Geological Mapping of Nehalennia Corona Region, Central Eistla Regio, Venus: DykeSwarms, Volcanic Flows, and Associated Magmatic and Plume Centres

Harshita Singh[1], R. E. Ernst[2,3], H. El Bilali[2,3], R. K. Srivastava[1]
[1]Department of Geology, Banaras Hindu University, Varanasi, India: harshitasingh8677@gmail.com, [2]Department of Earth Sciences, Carleton University, Ottawa, Canada,
[3]Faculty of Geology and Geography, Tomsk State University, Tomsk, Russia.

The Nehalennia Corona and Anala Mons regions of the Central Eistla Regio, parts of an elongated, equatorial Eistla Regio on Venus, comprise abundant radar dark plains and large volcanic edifices [1]. This work is aimed to provide detailed geological map of the Nehalennia Corona and Anala Mons region on a scale of 1:500,000 for developing its geological and tectonic history. Mapping includes both lava flows and graben systems (interpreted to overlie dykes). Earlier, the Sappho Patera Quadrangle (V–20) is mapped on a scale of 1:5,000,000, which hosts various coronae and volcanic edifices in central region of Eistla Regio [2]. At the first phase of our research, the dyke swarm history of the Nehalennia Corona region, Central Eistla Regio, is presented (Fig. 1). Mapping of lava flows in the region is also in progress; flows are distinguished on differences in radar properties, topography, and morphology. The present mapping uses Magellan synthetic aperture radar (SAR) images and ArcMap 10.8.1 software. In addition, JMARS 5 is used to explore the area and construct topographic profiles**.**

More than 16,500 grabens, mostly interpreted to overlie dykes, have been mapped. This helped to identify a number of magmatic centres in the study region (see Fig, 1). Broadly, the Nehalennia Corona is a large ring-shaped system, which is represented by circumferential and radiating dyke swarms. It is located at 14°N latitude and 10°E longitude and belongs to the Sappho Patera Quadrangle (V–20) of Central Eistla Regio. Nehalennia Corona region is located on a broad topographic rise overlying one or more large mantle upwellings. Through mapping the various mafic dyke swarms, we can infer magmatic centres. Notably, Anala Mons is associated with a giant radiating swarm. This swarm is fanning in the eastern sector of the Nehalennia Corona for a length of more than 1000 km from Anala Mons. A huge NW-trending dyke swarm is also recognized, which is related to the Gula Mons (a large volcanic edifice, located about 1200 km to the NW of the study area). This swarm shows a change in trend at about 1400 km from Gula Mons, near Nehalennia Corona, marking the potential edge of the flattened plume head of Gula Mons.

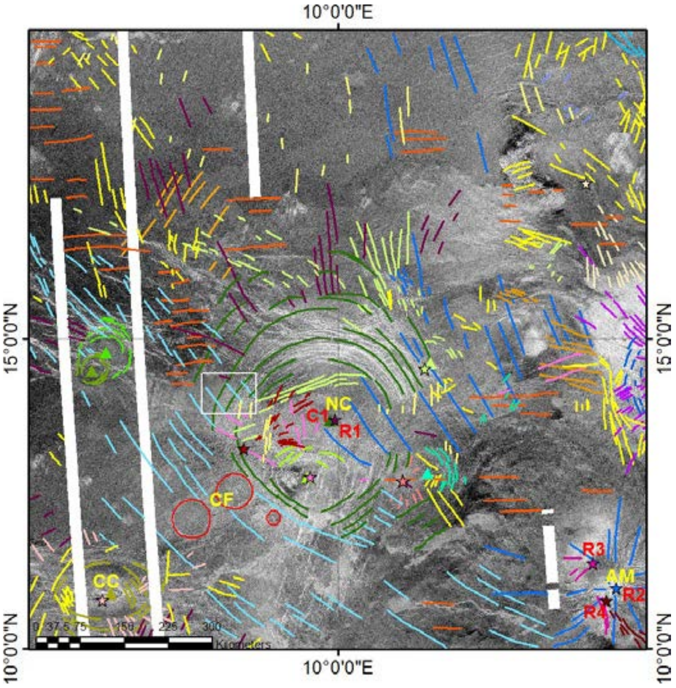

Figure 1: *Generalized map of graben-fissure system, (interpreted to overlie dyke) in Nehalennia Corona region. NC – Nehalennia Corona, CC – Changko Corona, CF – Carmenta Farra, AM – Anala Mons; Symbols for magmatic centres: Triangle – circumferential swarm; star – radiating swarm (R).*

[1] Senske D. A. et al. (1992) *JGR*, *97*, 13395-13420. [2] McGill, G. E. (2000) *USGS Geol. Invest. Series Map* I-2637; https://pubs.usgs.gov/imap/2637/

Abundance and chemical characteristics of micrometeorites from the deep sea and Antarctica regions.

V. P. Singh[1,2,*] and N.G Rudraswami[1,2]

[1]National Institute of Oceanography (Council of Scientific and Industrial Research), Dona Paula, Goa 403004, India

[2]Academy of Scientific and Innovative Research (AcSIR),

Ghaziabad 201002, Uttar Pradesh, India

*Corresponding author E-mail: vijaypratap865@gmail.com

Abstract:

Micrometeorites (MMs) continuously bombard the upper Earth's atmosphere and contribute around 40000 tons of extraterrestrial material annually [1]. These cosmic dust particles, which enter the Earth's atmosphere at a velocity of about >11 km/s, experience a higher degree of heating (up to 3000^0C) because of air molecular frictional force. Therefore they gets altered in their chemical, morphological, and textural characteristics [2]. The cosmic dust particles, which survive the atmospheric hypervelocity impact heating, settle on the Earth's surface and can be collected from various terrestrial environments. However, Antarctica and the deep sea are favourable locations for collecting micrometeorites because of the lower sedimentation rate and minimal anthropogenic activity [3]. Using a Scanning Electron Microscope (SEM) and Electron Probe Micro Analyser (EPMA), we investigated the micrometeorites collected from the deep sea and Antarctica for their morphological, textural, and chemical characteristics. These particles, with their spherical morphology and dendritic, interlocking, and glassy textures, vary in composition from silicate (s-type), nickel bearing iron oxide (I-type) to the mixed composition of silicate and nickel bearing iron oxide (G-type) [4]. Micrometeorites from the deep sea regions suffer harsher conditions during preservation, so they strongly represent etching effects and vary in abundance and alteration from the polar region collections. This article compares the chemical characteristics and abundance of different types of micrometeorites from the deep sea, Antarctica, and rocks of different geological ages, which identifies that carbonaceous chondritic parent bodies contribute the majority of the cosmic dust into the Earth's atmosphere.

References

[1].Love SG and Brownlee DE (1993) Science, 256: 550-553.
[2].Rudraswami, et al., (2015). Astrophys. J., vol.814.
[3].Taylor et al., (2000) MAPS, 35: 651-666.
[4].Genge et al. (2008) MAPS, 43, 497–515.

Application of Machine Learning in Non-Reactive Quantum Dynamics at Low Temperatures for Astrochemical Application

Apoorv Kushwaha[1], T.J. Dhilip Kumar[1*]
[1]Department of Chemistry, IIT Ropar (apoorv.20cyz0021@iitrpr.ac.in)
[*]dhilip@iitrpr.ac.in

The study of non-reactive collision of molecules at low temperatures has a crucial application in astrochemistry. It gives us the cross-sections for rotational excitation/de-excitation of the molecule of interest and thus the rate of rotational transitions. This helps us to determine the internal states of molecules at any temperature range in interstellar medium (ISM). Such studies give us a better understanding of the environment (temperature, abundance, etc.) of the ISM, protoplanetary disks, etc.[1] The study requires an accurate description of *ab initio* potential energy surface (PES) resulting from the collision of any two species, in all possible orientations. Due to poor scaling, computing an accurate PES can be quite challenging as the number of atoms increase.

The current study aims to explore utilization of machine learning (ML) methods for studying such inelastic dynamical processes[2] caused by collision of molecules with hydrogen (H_2) and helium (He) by (a) augmenting the PES, thereby reducing the computation time considerably as ML models takes hours to train compared to months needed for accurate *ab initio* PES calculations by methods such as coupled cluster, and (b) directly predicting rates using ML model such as Gaussian Process (GP) and artificial neural network (NN).

For (a), accurate ML models are created using python library[3] for C_2-He and NCCN-He collision PES utilizing only ∽1% of the required data points which can augment the PES within spectroscopic accuracy (< 1 cm^{-1}). The models are used as benchmark[4-6] to study more complex 4D PES such as collision of NCCN and H_2 (both ortho and para). For (b) the cross section/rate-coefficients of the scattering process will be predicted with the direct knowledge of PES using machine learning models.

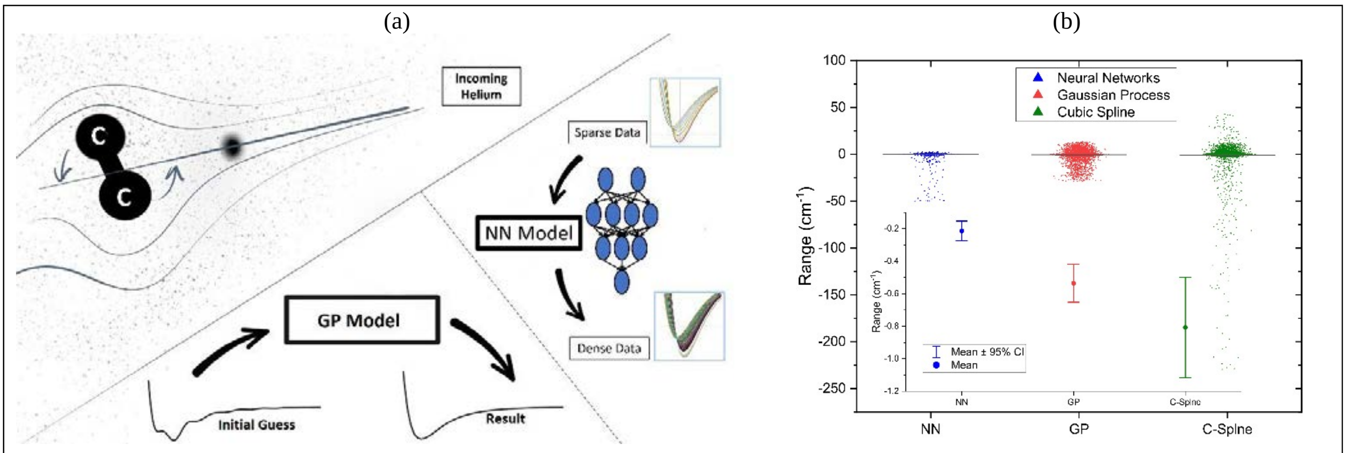

Fig. (a) Schematic diagram of ML methods used to compute PES from sparse data points and (b) Scattered interval plot showing error concentration around means for dynamic C_2-He PES fitted using NN, GP, and Cubic Spline[6]

References

[1] E. Herbst and J. T. Yates Jr, Chem. Rev., **113**, 8707–8709, (2013).
[2] J. Cui and R. V. Krems, Phys. Rev. Lett., **115**, 073202, (2015).
[3] A. S. Abbott, J. M. Turney, B. Zhang, D. G. Smith, D. Altarawy, and H. F. Schaefer III, J. Chem. Theory Comput., **15**, 4386–4398, (2019).
[4] S. Chhabra, A. Kushwaha, R. Kaur, and T. J. Dhilip Kumar, Chem. Phys. Lett. **738**, 136819 (2020).
[5] A. Kushwaha, S. Chhabra, and T. J. Dhilip Kumar, Chem. Phys. Lett. **761**, 138013 (2020).
[6] A. Kushwaha and T. J. Dhilip Kumar, Int. J. Quantum Chem., **123**, e27007, (2023).

Investigating the shielding effect of gamma rays using transparent superlattice structure

Ajaymalolan K.V.1, Sridhar Chandrasekaran1*

1. Center for System Design, Department of ECE,
Chennai Institute of Technology, Kundrathur, Chennai
*Corresponding Author E-mail: sridharc9020@gmail.com

Abstract: In the era of space exploration, we are adding our every single effort to achieve such a milestone with minimal electronic device failure and absorption of harmful radiation inside the space shuttle or space exploration telescopes, or other space vehicles. Our extraterrestrial space ambiance is composed of higher energy radiation such as gamma rays and X-rays. In general, gamma rays are produced by active solar flares, radioactive decay, and black hole. Gamma rays are highly penetrative and can cause harm to humans and other living organisms on prolonged exposure may lead to organ damage and cell mutation [1]. Although harmful, these radiations are used in various applications such as medical treatment and imaging, space exploration, nuclear waste storage, etc. Hence having effective protection against these radiations becomes an act of necessity. Traditionally heavy metals have been used to shield against gamma radiation and have the least possibility of gamma rays penetration through them [2]. Considering environmental safety in mind the use of inorganic materials such as Tungsten, boron, barium sulfate, Tin, bismuth, gadolinium, and antimony are being widely adopted for gamma radiation shielding [3]–[5]. Among them, Tin and its oxides are widely used for radiation shielding to protect onboard electronics from harmful radiation effects [6].

This study is based on analyzing the gamma shielding properties of the transparent glass substrate. The shielding characteristics of Metallic Tin, with Indium Tin Oxide and Tungsten oxide layers coated superlattice structure on glass substrates, are studied in the simulationenvironment. This aims to achieve transparent and non-transparent effective gamma shielding composites. To analyze, the Fresnel equation and radiation heating are simulated in a COMSOL Multiphysics environment. The refracted, absorbed, and transmitted rays are measured at variousangles of incidence and at the boundaries of layers in various combinations to further evidence the shielding effect of the proposed superlattice structure.

Reference

[1] A. Fogtman et al., "Towards sustainable human space exploration—priorities for radiation research to quantify and mitigate radiation risks," NPJ Microgravity, vol. 9, no. 1, Jan. 2023, doi: 10.1038/s41526- 023-00262-7.

[2] B. Muth, W. S. Jung, J. K. Kwak, S. J. Kim, and C. J. Park, "A radiation shielding sensitivity analysis based on metal hydrides multilayers," *Journal of Radiological Protection*, vol. 40, no. 3, pp. 774–789, Sep. 2020, doi: 10.1088/1361-6498/ab9a08.

[3] S. Jayakumar, V. Mani, T. Saravanan, K. Rajamanickam, A. D. Prabhu, and J. Philip, "Multifiller nanocomposites containing gadolinium oxide and bismuth nanoparticles with enhanced X-ray attenuation property," *J Appl Polym Sci*, vol. 138, no. 42, p. 51252, Sep. 2021, doi: 10.1002/app.51252.

[4] P. Kaur, K. J. Singh, S. Thakur, M. Kurudirek, and M. M. Rafiei, “Structural investigations and nuclear radiation shielding ability of bismuth lithium antimony borate glasses,” *Journal of Physics and Chemistry of Solids*, vol. 150, p. 109812, Mar. 2021, doi: 10.1016/j.jpcs.2020.109812.

[5] B. Alım, “A comprehensive study on radiation shielding characteristics of Tin-Silver, Manganin-R, Hastelloy-B, Hastelloy-X and Dilver-P alloys,” *Applied Physics A*, vol. 126, no. 4, p. 262, Apr. 2020, doi: 10.1007/s00339-020-3442-7.

[6] E. Hannachi *et al.*, “Impact of tin oxide on the structural features and radiation shielding response of some ABO3 perovskites ceramics (A = Ca, Sr, Ba; B = Ti),” *Applied Physics A*, vol. 127, no. 12, p. 970, Dec. 2021, doi: 10.1007/s00339-021-05092-6.

Micrometeorites chemical and isotopic changes during atmospheric entry

N. G. Rudraswami*
National Institute of Oceanography (Council of Scientific and Industrial Research),
Dona Paula, Goa 403004, India
Corresponding Author: rudra@nio.org

Abstract:

Micrometeorites (MMs) are extraterrestrial materials in size ranging from a few tens of µm to a few mm and have played a vital role in understanding our solar system. It is the primary source of extraterrestrial material, distantly followed by meteorites. These MMs, as they enter Earth's atmosphere, experience heating leading to a change in their texture, chemical, and isotopic properties, thereby losing their original precursor properties [1-6]. Hence our understanding of the MM's chemical and isotopic properties is limited by the unknown degree of alteration and amount of oxygen isotopic exchange these particles have witnessed [3,4, 6]. To relate it to know meteoritic precursor, it is pertinent to understand the changes related to the chemical and isotopic properties.

The $\delta^{17,18}O$ oxygen isotope of the MMs indicate the wide range in their composition that has a combination of both precursor and atmospheric oxygen composition if one looks at different texture from scoriaceous, porphyritic, relict bearing, glass, barred, and G-type spherules [6]. The large $\delta^{18}O$ composition established within diverse MM types having low oxygen ablation point toward precursor composition and suggest atmospheric oxygen is insignificant during entry. This is supported by the oxygen isotope composition of unmelted MMs that have not exchanged oxygen during atmospheric entry or undergone ablation but have large $\delta^{18}O$ values [3, 6]. The elemental oxygen ablation is negligible (<5%) provided the particle temperature does not experience 2000 K, so scoriaceous, porphyritic, barred and cryptocrystalline particles should have oxygen isotope compositions similar to their parent bodies. The large $\delta^{18}O$ values of MMs from partially heated scoriaceous to glass (except CAT) spherules indicate distinctive primitive carbonaceous chondrites that were altered either by nebular gas or aqueously altered in their parent bodies [3]. This study overall provides insights into the oxygen ablation of the particles during atmospheric entry, oxygen isotopic alteration, and the reservoirs of the diverse extraterrestrial objects that prevailed in the early solar system.

References:

[1] Plane (2012) Chem. Soc. Rev.41, 6507–6518. [2] Genge et al. (2008) MAPS, 43, 497–515. [3] Rudraswami et al. (2022) *APJ, 940(1), 25.* [4] Rudraswami et al. (2020) JGR, 125, e2020JE006414. [5] Brownlee et al. (1997) MAPS, 32, 157–175. [6] Engrand et al. (1999) GCA, 63, 2623–2636.

Study Of Ionospheric Plasma Parameter Using Observation And ModelOver Indian Low Latitude Stations During 2004-2013

Mini Rajput, Sanjay Kumar, A. K. Singh

[1]Atmospheric Research Lab, Department of Physics, Institute of Science, Banaras Hindu University, Varanasi (mini.rajput.2015@gmail.com)

[2]Atmospheric Research Lab, Department of physics, Institute of science, Banaras Hindu University,

Varanasi (sanjay.skitvns@gmail.com)

*abhay_s@rediffmail.com

Ionosphere is part of upper atmosphere having existence of charged particles and neutral. Ionospheric perturbations are well known to affect radio wave communication and navigation system and hence knowledge of ionospheric variability quite significant to improve such radio-based system in different solar and geomagnetic conditions [1-2]. The presented work is an attempt to understand the variabilities of ionospheric Total Electron Content (TEC) over the Indian low latitude regions. In this paper ionospheric total electron content derived from Global Positioning System (GPS) at Indian low latitude station- Bangalore (12.97º N, 77.58º E) have been used to study diurnal, monthly, seasonal and annual variations during the period from 2004 to 2013. Diurnal variations of ionospheric TEC shows typical characteristics of low latitude station such as pre-dawn minimum then broad maximum in noon time followed by a decrease to a minimum during night time. TEC data from ground based GPS measurements has also been compared with those from the IRI-2016 model [3] during 2004-2013. Effect of solar cycle on variability of ionosphere using data from GPS-based observation and the IRI-2016 models has also been studied.

References:

[1] Galav, P., Dashora, N., Sharma, S., & Pandey, R. (2010), Journal of Atmospheric and Solar-Terrestrial Physics, **72**, p 1309–1317.

[2] Kumar, S., Priyadarshi, S., Krishna, G. G., & Singh, A. K. (2012). Astrophysics and Space Science, **339**, p 165–178

[3] Bilitza, D., Altadill, D., Truhlik, V., Shubin, V., Galkin, I., Reinisch, B., & Huang, X(2017), Space Weather, 15, 418– 429).

Deep Machine Learning based Automatic Lunar Craters Detection

Chinmayee Chaini[1*], Dr. Sanchita Paul[1], Dr. Mili Gosh Nee Lala[2] , Dr. C. Jaganathan[2]

[1]Department of Computer Science & Engineering (CSE), Birla Institute of Technology Mesra, Ranchi-835215
[2]Department of Remote Sensing, Birla Institute of Technology Mesra, Ranchi-835215

*chinmayeechaini94@gmail.com, sanchitapaul@bitmesra.ac.in, mili@bitmesra.ac.in, jeganathanc@bitmesra.ac.in

ABSTRACT: Recognizing moon craters is critical in lunar research. We present an integrated framework for the auto-detection of sub-kilometer craters in this research due to the complex morphologies of craters (sites are widely dispersed, overlapped, and highly degraded), which makes human detection difficult and time-consuming and tedious work. The table below demonstrates the research linked to some of the earlier work done in the area of crater detection presented using different Deep Learning and Machine Learning approaches.

Surface Area	Method	Dataset & URL	Advantage	Limitation
Surface Area of Moon [1]	Novel Active Machine (AM) learning approach(Included: the Scalable Template model (STM), Convolutional Neural Networks (CNN), Boosting Algorithm (BA) and Modified Boosting (MB) method, and the Leastsquares Support Vector Machine(LSVM) is used to solve Binary Classification.	Moon data containing HRSC image and the DEM images was downloaded from (http://pds-geosciences.wustl.edu/missions/mars_express/hrsc.htm.100)	1. In this study, Active Machine Learning (AML) reduces thenumber of needed training samples. 2. The features will be easier to describe for taking AML approach. 3. In the training process, the approach actively asks for annotations for the 2-D features derived from imagery with inputs from 3-D features derived from the DEMs due to this model can be retrained.	1. The crater detection rate may increase for Small Craters by incorporating other feature information. 2. There will be no more edge-detection procedure, which may result in extra errors.
Surface Area of Moon [2]	AutomaticDetectionAlgorithm(AD)based on Pattern Recognition and Transfer learning (TL), ML, DL using particular CNN approaches.	Images are obtainedby the fusion of DOM and DEM data (https://github.com/hszhaohs/DeepCraters). The identified lunar craters can be found at (https://doi.org/10.6084/m9) Chang' E-1 and Chang'E-2 data	1. TLbased strategy with a Deep Neural Network (DNN) has properly learned the complex features that define a crater and its age. 2. This method is successfully applied to the problems where sufficient training samples are not available. 3. Using the two-stage Detection and Classification methods, a huge number of craters and their dates were found.	1. The size of small craters in the feature map of the last convolutional layer is too small for accurate detection. 2. The two spatial resolutions of the data, i.e., CE-1 120 and CE-2 50 m, are not enough to deal with the vast presence of craters.
Surface Area of Moon [3]	Using CNN and Custom version of U-NET architecture and Match Template (MT) algorithm from Scikit-image Tuning is typically done via	Dataset is available at available at (..\project chinmayee\papers\highlighted\deep learning review paper.pdf)	1. They have successfully shown Transfer-Learning (TL) from their Moon-trained CNN to Mercury. 2. Despite shortcomings their CNN was still able to understand our	1. Their training data is incomplete, containing many missed craters as well as target

	Backpropagation and goodness of fit is defined through a loss function. They train a DL architecture known as a CNN include convolutional layers, pooling layers, and merge layers to perform crater identification1 on Lunar Digital Elevation Map (DEM) images.		training objective and correlate the binary ring targets with the true rims of the craters.	rings that differ from true crater rims. 2. In this paper Larger filter sizes were tried, butthis significantly increased the number of trainable parameters as well as network capacity, making model tuning more challenging.
Surface of Moon [4]	To detect small craters they proposed Point cloud Semantic Segmentation and Global Feature exchange, as well as HoughTransform. The deep learning model is used to acquire its deep semantic features for preprocessing. Finally, by post-processing the preliminary detection findings, more precise detection results of lunar impact crater are acquired.	Chang'E DEM images with 50 m resolution covering 28 S◦ ∼ 28N◦ area to make a point cloud dataset (Chang'E-2)	1. This twostage detection method based on point cloud semantic segmentation solved the problem of optical image small impact crater is easily affected by the direction of sunlight. 2. In terms of detecting small impact craters, the suggested approach outperforms image-based detection methods.	1. The biggest challenge for computer resource is overlapping problem of super large impact craters and small impact craters. 2. It is difficult to obtain good detection results due to Consideration of spatial distribution information is lost by sampling the point cloud data of the large impact crater.

The Study area (region of extent in terms of latitude/longitude) : Vallis Schroteri: The Lunar "Grand Canyon", the largest rille on the Moon(Chandrayaan-2 Dataset), originates on the Aristarchus Plateau and is comprised of three key morphologic features: the Cobra Head, the primary rille (155 km long), and the inner rille (204 km long). Our proposed model on DEM pictures can identify overlapping and extremely tiny craters, as well as craters within craters, with greater accuracy than others.

Our proposed Algorithm mainly focuses on the following steps:

Algorithm for Craters Detection using Deep Machine Learning:

Input: DEM image

Output: Craters (Overlapping, extremely small and craters within craters)

Step 1: Read the DEM images obtained from chandrayaan-2 payload data.

Step 2: Apply semantic segmentation techniques on DEM images for image segmentation.
Step 3: Extract features using different techniques like (CNN), Gabor filter,Fuzzy C-means techniques
Step 4: Apply various machine learning algorithms like K-nearest neighbor(KNN), Support Vector Machine(SVM), AdaBoost(AB), Gradient Boosting(GB), Decision Tree(DT), Random Forest(RF), and Deep Learning(DL) for classification of extracted features and use a best classifier among them for further analysis.
Step 5:If extaracted oject matches with morphology of crater
Then the identified object might be a crater and Goto **step 6**
Else the identified object is not a crater and Goto **step 11**
Step 6: Apply Match Template algorithm on obtained images in **step-5** to get the craters from the images
Step 7: Get Dimesions and Location of the detected craters
Step 8: Proposed the hybrid classifier with obtained best classifier using Ensemble techniques to increase the accuracy.
Step 9: Performed the **step 5 to 7**
Step 10: Get the highest accuracy of the craters by applying these **step 4 to 7**
Step 11: Stop

Essentially, the performance metrics are dependent on the effective technique that we use to identify different types of craters. Because of enhanced picture segmentation techniques and higherclarity of DEM images, we could theoretically achieve (90-95)% accuracy.

References: [1] Wang, Yiran, and Bo Wu. "Active machine learning approach for crater detection from planetary imagery and digital elevation models." IEEE Transactions on Geoscience and Remote Sensing 57.8 (2019): 5777-5789.[2] Yang, Chen, et al. "Lunar impact crater identification and age estimation with Chang'E data by deep and transfer learning." Nature Communications 11.1 (2020): 6358.[3] Silburt, Ari, et al. "Lunar crater identification via deep learning." Icarus 317 (2019): 27-38.[4] Hu, Yifan, et al. "Detection ofSmall Impact Craters via Semantic Segmenting Lunar Point Clouds Using Deep Learning Network." Remote Sensing 13.9 (2021): 1826.[5]Lemelin, M.; Daly, M.G.; Deliège, A.Analysis of the topographic roughness of the moon using the wavelet leaders method andthe lunar digital elevation model from the lunar orbiter laser altimeter and selene terrain camera. J. Geophys. Res. Planets 2020, 125, e2019JE006105. [6]Salamuniccar, G.; Loncaric, S. Method for crater detection from martian digital topography data using gradientvalue/orientation, morphometry, vote analysis, slip tuning, and calibration. IEEE Trans. Geosci. Remote Sens. 2010, 48, 2317–2329

PHYSICAL PROPERTIES OF LUNAR MAGMAS UNDER HIGH-PRESSURE ANDHIGH-TEMPERATURE CONDITIONS

Nachiketa Rai
Department of Earth Sciences, Indian Institute of Technology Roorkee, India – 247 667
*n.rai@es.iitr.ac.in

Comprehensive models of significant aspects of lunar evolution are hampered by a lack of quantitative constrains on the physical properties of lunar magma at high pressures (P) and temperatures (T). This lack of data plagues the accuracy of models of the physical and thermodynamic properties and resulting dynamics of the lunar interior. For example, the plagioclase-rich crust of the Moon exposed in the highland terranes is widely believed to have formed due to flotation of plagioclase in a global, crystallizing lunar magma ocean. However, dynamic models of this flotation suffer from scarcity of data on the density and viscosity of lunar melts (which determine in part the upward velocity of rising crystals), at lunar high pressure-temperature conditions. The accumulation of dense oxide minerals as they crystallize from magma, likewise critically depends on their settling velocity (v) in less dense silicate melt. The higher the settling velocity, the further the minerals can fall before the melt solidifies, and the more chance they have to accumulate. Viscosity (η) and density (ρ) are critically important physical properties of magma, governing the efficiency, rate and nature of melt transport and affecting the rates of physicochemical processes such as magma crystallization and differentiation. Such melt properties are a consequence of atomic scale transport processes, and therefore directly related to the structure and thermodynamic properties of magma.

Prediction of variations in viscosity and density as a function of pressure, temperature and composition is still highly challenging. In this case, experimental determination of melt properties at high pressure and high temperature conditions relevant to the lunar interiors, through in situ synchrotron X-ray absorption, and in situ viscometry experiments conducted on lunar compositions provide us with the much needed density and viscosity measurements for lunar melts. Constraints from recent experimental measurements of density and viscosity [1,2] for synthetic equivalents of three end-member compositions bracketing the unusually broad range of titanium contents in Apollo samples: Apollo 15C green glass (low titanium content of 0.23 wt% TiO2), Apollo 17 orange glass (intermediate titanium content of 8.8 wt% TiO2) and Apollo 14 black glass (high titanium content of 16.4 wt% TiO2), effect of chemical composition, pressure and temperature on these properties, and its implications as input parameters for an integrated model of the dynamic evolution of the lunar magma ocean will be discussed.

References: [1] Rai N, Perrillat J-P, Mezouar M., Petitgirard S, Colin A, van Westrenen W. (2019). In-situ viscometry of lunar magmas at high pressure and high temperature. Frontiers in Earth Science 7, 94. [2] van Kan Parker M, Sanloup C, Sator N, Guilot B, Tronche EJ, Perrillat J-P, Mezouar M, Rai N, van Westrenen W (2012). Neutral buoyancy of titanium-rich melts in the deep lunar interior. Nature Geoscience doi:10.1038/ngeo1402.

Further evidence for the impact origin of the Ramgarh Structure, India

Shivanshu Dwivedi[1], Anuj Kumar Singh[1], Jayanta Kumar Pati[1,2,*], Wolf Uwe Reimold[3], Ashutosh Pratap Singh[1]

[1]Department of Earth and Planetary Sciences, Nehru Science Centre, University of Allahabad, Prayagraj-211002, India

[2]National Centre of Experimental Mineralogy and Petrology, University of Allahabad, Prayagraj-211002, India

[3]Laboratory of Geochronology and Isotope Geochemistry, Instituto de Geociências, Universidade de Brasília, Brasília, DF, CEP70910-900, Brazil

*Corresponding Author E-mail: (jkpati@gmail.com)

The confirmation of the origin of a structure by meteorite impact is primarily established with the identification of mesoscopic and microscopic, diagnostic shock metamorphic features, and/or chemical traces of a meteoritic projectile in impactites [1-2]. Based on these unequivocal signatures, some 200 meteorite impact structures have been confirmed on Earth to date. India has three confirmed impact structures (Lonar, Dhala, and Ramgarh) so far. The ~10 km diameter Ramgarh structure (25º20'16''N; 76º37'29''E) is a recently confirmed complex impact structure formed in rocks of the Upper Vindhyan Supergroup [3]. The structure is located in the Baran District of Rajasthan, India. Although the impact origin of Ramgarh structure had been repeatedly argued over the last five decades, no unambiguous evidence had been provided until 2020. That year, the unequivocal occurrence of planar deformation features (PDFs), planar fractures (PFs), and feather features (FFs) was documented from sandstones of the Ramgarh structure [3]. The structure displays a prominent, semi-rectangular morphology, with a central depression with a small central mound, which are surrounded by a 3.5 to 4 km wide annular collar. The Ramgarh structure can be easily delineated on Google Earth and other satellite imagery.

In the present study we re-examined twenty-five polished thin sections prepared from representative rock samples that had been collected at Ramgarh in April 2011 [4-5]. Three arenite thin sections were found with notable evidence of shock metamorphism. Microscopic deformation features were recorded in the form of undulous extinction, sub-grain development, brecciation and crushing (cataclasis). Diagnostic evidence of shock metamorphism includes planar fractures (PFs), feather features (FFs), and a single set of planar deformation fractures (PDFs) - all identified in quartz (Fig. 1a-b). Multiple FFs are observed in a given section along with PFs. The detailed examination and subsequent measurement of crystallographic orientations of these micro-deformation features using a universal stage is in progress. This study further supports the meteorite impact origin [3] of the Ramgarh structure.

References: [1] French B. M. and Koeberl C. (2010) *Earth-Science Reviews, 98,*123-170. [2] Gottwald et al. (2020) *Terrestrial Impact Structures, The TanDEM-X Atlas, Part 1 and 2,* Munich: Verlag Dr. Friedrich Pfeil. [3] Kenkmann T. (2020) *MAPS,* 55, 936-961. [4] Singh A.P. (2011) *M.Sc. Dissertation, University of Allahabad,* 76p. [5] Pati J. K. and Singh A.P. (2011) *AICAC-II Symposium, Casablanca, Morocco*.

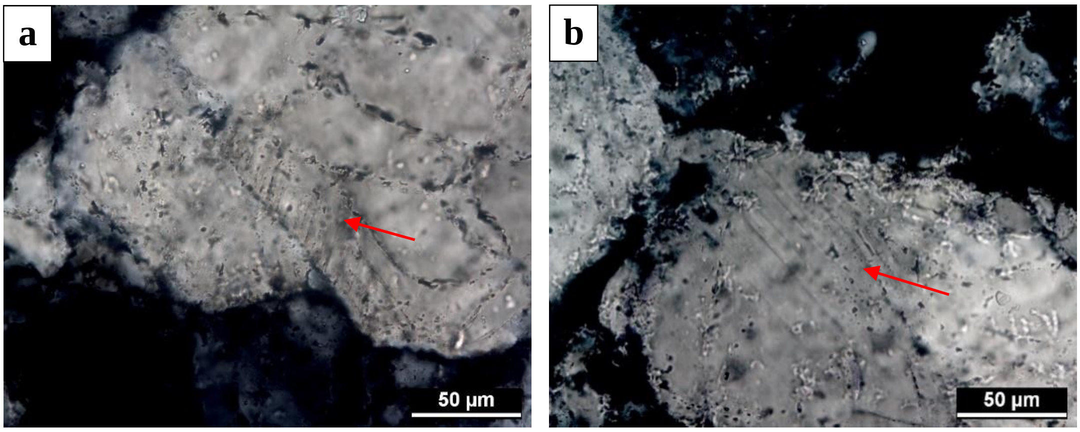

Figure 1: (a) The image shows FF lamellae-oriented NE-SW (marked with red arrow) emanating from a PF within a quartz grain, in PPL. (b) One set of PDF (NW-SE) at the margin of a quartz grain (marked by red arrow) under crossed polarizers.

Effect metallicity on the quenched abundance of the WASP-39 b

Vikas Soni[1*] and Kinsuk Acharyya[1]

[1]Planetary Sciences Division, Physical Research Laboratory, Ahmedabad 380009.

*Corresponding Author E-mail: soniv100@gmail.com

Abstract:

The atmospheric study of exoplanets is at the forefront of modern-day astronomy. The large parametric diversity of these exoplanetary atmospheres degenerates the atmospheric abundance. The atmospheric bulk metallicity significantly affects the atmospheric compositions. In the present work, we have used the quenching approximation to understand the effect of metallicity on the disequilibrium abundance of WASP-39 b. In the quenching approximation, we compare the species' chemical and vertical mixing time scales to find the quench pressure level. Below the quench pressure level, the chemical timescale dominates over the vertical mixing timescale, and the atmospheric composition remains in the chemical equilibrium. Above the quench pressure level, the abundance of species is frozen, with the equilibrium abundance at the quench level. WASP-39 b is among the first exoplanets whose atmosphere has been constrained by JWST. Its observed atmospheric metallicity is found to be 10 x solar metallicity ([1], [2], [3]). We have adopted the thermal profile from [1] and [2] for this study. We constrained the disequilibrium abundance of CH_4 and CO for various vertical mixing strengths for WASP-39 b. We found that the CH_4 and CO mixing ratios are independent of vertical mixing for $K_{ZZ} < 10^{10}$ cm^2 s^{-1}. For high vertical mixing $K_{ZZ}>10^{10}$ cm^2 s^{-1}, the quenched CH_4 mixing ratio can increase by one order of magnitude. We have calculated the equilibrium mixing ratios of CO, CO_2, and H_2O for 0.1, 1, 10, and 100 x solar metallicity. The CO_2, H_2O, and CO abundance profiles for 10 x solar metallicity are qualitatively similar to the retrieved abundance from [2].

References:

[1] Tsai, Shang-Min. et al. (2022) e-prints p. arXiv: 2211.10490

[2] Ahrer. Et al. (2022) e-prints p. arXiv: 2211.10489

[3] The JWST Transiting Exoplanet Community Early Release Science Team. (2022) arXiv e-prints p. arXiv: 2211.10488

Visualization and Characterization of Chandrayaan-3 Landing Site

Hamish Dsouza[1*], Shashi Kumar[1]

[1]Indian Institute of Remote Sensing, Dehradun, India
*Corresponding Author E-mail: hamish.iirs@gmail.com

India's third mission to the Moon, Chandrayaan-3, consisting of a lander and a rover will attempt to land in an area of 4 km x 2.4 km around 69.367621 S, 32.348126 E [1]. The landing site lies near the South Pole of the Moon between Manzinus U and Boguslawsky M craters. Reconnaissance of potential landing sites is necessary not just for selection of suitable regions but also to ensure safe landing and trafficability within the site. In this work, the landing site for Chandrayaan-3 is visualized and characterized using multiple remote sensing datasets. The topology of the region is analyzed using LOLA DEM and its derivatives. The craters and boulders in the region were analysed using LRO NAC images. Data from the hybrid-pol S-band LRO MiniRF was used to study the polarimetric scattering behavior from the surface of the landing site. Average hourly temperatures obtained from the Diviner Lunar Radiometer Experiment is used to study the temperature variations the lander and rover will have to operate in.

The average slope of the landing site is less than 10°, and is considered suitable for roving operations [2]. Varying between around 82K at midnight and 283K at noon, the rover is expected to experience a variation of about 200K throughout the day. S-band SAR data was decomposed using m-chi and m-delta decompositions to study the scattering behavior from the regolith in the landing region. The results of the work, visualized in 3-D view for visual emphasis, present a contextual framework of the prime landing site of Chandrayaan-3.

References: [1] ISRO (2023), *Chandrayaan-3, www.isro.gov.in/Chandrayaan3_New.html*
[2] Kring.D.A. et al. (2012), *A Global Lunar Landing Site Study to Provide the Scientific Context for Exploration of the Moon*

Development of Graphical User Interface for Simulating Meteoroid Ablation

S. Nambiar* and J. P. Pabari

Physical Research Laboratory (Ahmedabad – 380009)

*Email: srirag@prl.res.in

Meteoroids coming from Asteroids and Comets interact with planetary bodies during their evolution within the Solar system. For planetary bodies without an atmosphere like our Moon, these tiny dust particles directly impact the surface. Whereas in the case of bodies with atmosphere, the meteoroid undergoes ablation. The particle deposits metallic ions in the atmosphere during its traverse, which reacts with the ambient atmospheric atoms and molecules and modulates the ionosphere. We have developed a model to simulate this ablation process in planetary environments like Earth, Venus and Mars and some results are presented.

Further, to make the model user friendly, we are developing a Graphical User Interface (GUI) to simulate the ablation process. The GUI will have multiple tunable parameters that the user can set as required and the production rate profile of selected metallic ions and neutrals can be observed as output. More features are being added to this GUI so that it can cater to larger audiences and its an ongoing work.

References: [1] Carrillo-Sanchez et al. (2020), ICARUS, 335, 1-15 [2] J. P. Pabari et al. (2023), PSS, 226,1-14 [3] Crismani et al. (2017), Nat. Geoscience, 10 , 401-404.

Data Logging and Processing using LabVIEW Software for the Lightning Signal

Rashmi[1]*, Jayesh Pabari[1], Sonam Jitarwal[1], Srirag Nambiar[1], Kinsuk Acharyya[1], Trushit Upadhyaya[2]

[1]Physical Research Laboratory, Navrangpura, Ahmedabad
[2]Charotar University of Science & Technology, Changa, Gujarat

*Email: rashmi@prl.res.in

Lightning is a natural phenomenon of large electric discharge that occurs in planetary atmosphere for a very short time duration. In case of earth, the lightning flash rate for intra-cloud and cloud-to-cloud to cloud-to-ground is in the ratio of 3:1 [1]. It is interesting to understand the frequency spectrum, time-frequency localization, time domain characteristics of the lightning pulse, variability of lightning peak frequency over time, variation of flash rate etc. for the lightning on Earth [2,3]. For this purpose, a 1.5 m Vee shaped short dipole antenna is installed on terrace of the main building of Thaltej Campus of PRL, which captures the lightning events during the monsoon. For the continuous monitoring and logging of the captured events, a data acquisition card and LabVIEW software are used. The acquisition card samples the captured signal at desired sampling rate [4]. For visual monitoring of the data, some parameters are plotted in real time, as well. Also, the data is logged into a computer for post analysis or record purpose.

References: [1] Uman, Martin A. (1986), p. 68, Dover Publications, N.Y. [2] S. Jitarwal et al. (2020), VEXAG, #8010. [3] Rakov, V. A., (2003). England [4] Bianchi et al. (2009). Annals of Geophysics, 50.

Investigating Spectral Variability of Mg-Spinel Lithology on the Moon

Garima Sodha, Deepak Dhingra and Somnath Adak*

Department of Earth Sciences, Indian Institute of Technology, Kanpur, India - 208016

*Presenting Author E-mail: somnath22@iitk.ac.in

Remote observations of Mg-Spinel lithology have been an interesting new addition to the lunar crustal compositional diversity [1]. Diverse geologic settings of the global Mg-Spinel occurrences highlight the possibility of compositional variability within Mg-Spinel lithology due to various controlling parameters during their formation. Mg-spinel lithology is identified based on its characteristic broad absorption band at 2-µm and absence of 1-µm absorption in the visible and near-infrared (VNIR) reflectance spectra [1-3]. VNIR spectral response of any mineral is influenced by its chemical composition, grain size, presence of glass, exposure to space weathering and the relative abundance of other constituent minerals. In addition, several external factors such as local topography and illumination geometry also affect the spectral response. However, careful investigation of VNIR spectral response of target lithology may provide insights into its compositional character and variability.

In this study, we are investigating the spectral variability of Mg-Spinel lithology using Moon Mineralogy Mapper (M^3) data at Thomson crater (32° S, 166° E; diameter ~117 km) using different spectral parameters i.e., band minimum position, absorption band depth, spectral slope, absorption band shape and absorption band symmetry. These parameters, especially the band minimum is very sensitive to slight variations in the composition of the lithology. Therefore, spectral variability could be harnessed (with the necessary caution) to infer the compositional diversity of Mg-Spinel lithology. We are trying to quantify these spectral variations to provide better constraints on the compositional character of Mg-Spinel lithology. This work has significant implications for understanding the formation conditions and origin of this lithology on the Moon.

References: [1] Pieters, C. M. et al. (2011) JGR, 116, 4, E00G08. [2] Pieters, C. M. et al. (2014) American Mineralogist, 99, 10, 1893-1910. [3] Cloutis et al. (2004), MAPS, 39, 4, 545-565.

PO^+-He Collision: *Ab initio* Potential Energy Surface and Inelastic Rotational Rate Coefficients

Pooja Chahal[1*] and T.J. Dhilip Kumar[1]
[1]Department of Chemistry, IIT Ropar, Rupnagar 140001
[*]pooja.21cyz0014@iitrpr.ac.in

Recently, PO^+ molecule detected in the interstellar medium (ISM) was reported by Rivilla et al. (2022) [1]. It was detected through four different rotational transition lines towards the G+0.693-0027 molecular clouds. The present work focuses on the calculation of rate coefficients among the rotational levels of the PO^+ molecule in its ground vibrational state in collision with the He atom. A new 2D PO^+ - He potential energy surface (PES) is constructed by employing CCSD(T) method and basis set extrapolated to complete basis set limit (CBS) [2] considering a rigid rotor approximation. The *ab initio* points are augmented by machine learning's neural network code. The PES obtained has a global minimum located at $\theta = 110°$ and R = 3.1 Å. The contour plot for PO^+ ($X^1\Sigma^+$) - He (^1S) [3] collision is shown in Figure. 1. Rate coefficients corresponding to the rotational (de-)excitation of PO^+ by collision with the He atom are obtained from close-coupling quantum scattering calculations [4] of inelastic cross sections. Rate coefficients between the rotational levels were calculated for temperatures ranging from 1 to 200 K. The large asymmetry of PO^+ - He PES includes a propensity rule that favors odd Δj transitions over even Δj. We have reported the new physical insights into the PO^+ molecule collision with the He atom employing new surface and neural network model to compute accurate collision rates. The data collected in this research will allow us to more accurately estimate the PO^+ significant rank for collisional processes, which is crucial for modeling its abundance in the ISM.

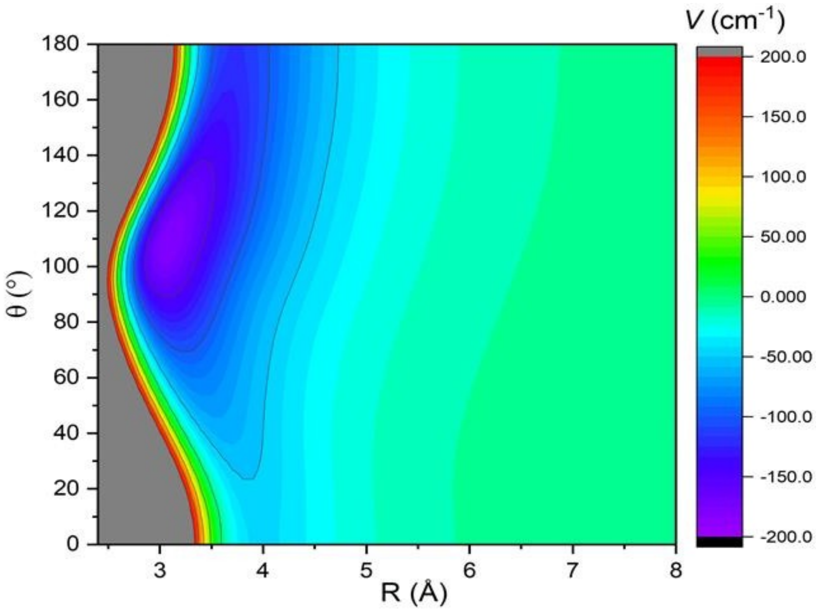

Figure 1. Contour plot for PO^+ - He collision.

References:

[1] Rivilla V.M., et al. (2022), *Front. Astron. Space Sci., 9*. [2] Dunning Jr T.H., (1989), *J. Chem. Phys., 90*, 1007. [3] Metropoulos A., Papakondylis A., Mavridis A., (2003), *J. Chem. Phys., 119*, 5981. [4] Green S., (1975), *J. Chem. Phys., 62*, 2271.

Estimation of Breakdown Electric Field Strength for Venus Environment Simulation Chamber

S. Jitarwal[1]*, J. P. Pabari[1], T. Upadhyaya[2], S. Nambiar[1], Rashmi[1], H. Vaghela[1], R. Mahajan[1] and K. Acharyya[1]

[1]Physical Research Laboratory, Navrangpura, Ahmedabad

[2]Charotar University of Science & Technology, Changa, Gujarat

Email: sonam@prl.res.in*

To simulate Venusian environment, the vacuum chamber shall be filled up with various gases in similar proportion. The facility of Gas manifold system shall be used for insertion of different proportion of gas mixture in planetary environment. The electrodes shall be fitted in within the vessel to create lightning discharge channel within the chamber. The event shall berecorded through PC interface. The lightning is a very transient process, where an ionization front moves rapidly within a locally enhanced electric field that well exceeds the breakdown value. For a given gas, the breakdown voltage is a function only of the product of the pressureand gap length. At higher pressures and gap lengths, the breakdown voltage is approximately proportional to the product of pressure and gap length, and the term Paschen's law is sometimes used to refer to this simpler relation [1]. Venus has ~96 % of CO_2, ~3.5 % N_2 in the atmosphere and ~100-150 ppm of SO_2 in the clouds [2]. The mixture of these gases can have different breakdown strength, however, it is expected that the breakdown is dominated by the CO_2 gas [3]. The combination of various gas mixture shall be carried out within the vacuum chamber using gas manifold system to simulate the Venusian environment and Electric Field strength shall be measured.

In this paper, the breakdown electric field of different gases will be represented. Further, the breakdown electric field strength of different gas mixture in earth and Venusian environment is compared and discussed.

References: [1] Ch. Helling et al. (2013), The Astrophysical Journal,1-44 [2] Lorenz et al. (2018), Earth and Planetary Science, 5(1), 34. [3] P.J. Chantry and R.E. Wootton (1981), Journal of Applied Physics, 52(4), 2731-2739

Spectroscopic and Planetary Perspectives of Tapovan Hot Spring Deposits

Subham Sarkar[1], Dwijesh Ray[1], Satadru. Bhattacharya[2]
[2]Physical Research Laboratory, Ahmedabad, India
[2] Space Applications Centre, Indian Space Research Organisation, Ahmedabad,

*Corresponding author E-mail: subham@prl.res.in

Hot springs have great significance for exploration of extra-terrestrial life forms. Identification of ancient hot spring localities on other planets must necessarily be based on criteria used to detect present and past hot springs environments on Earth. The primary criterion is mineralogical: for instance, a key mineral that is common in almost all hot spring deposits on earth is opaline silica, although not all terrestrial opal is hydrothermal in origin [1]. This is found in great abundance on the Martian surface [2] as well as around the Tapovan hot springs. In this study, we report an analog locality of the Martian surface at Tapovan hot springs, Uttarakhand, India, which hosts opalline silica and calcite. The primary mineral identifications were done using Visible/Near-Infrared (VNIR) (400-2500 nm) spectroscopy, Mid-Infrared (MIR) (4000-400 cm^{-1}) spectroscopy and X-ray diffraction. One of the main reasons for choosing Jezero Crater at the landing site for Mars 2020 Perseverance rover is due to the fact that this hosts the largest known carbonate deposit on the martian surface [3]. Thus, the identification and characterization of opalline silica associated with carbonates in the hydrothermal setting, has an immense significance in astrobiological studies, especially the search for life and suitable places to find life on the red planet and also to reconstruct the worlds paleoenvironmental conditions.

References: [1] McLennan, S. M. (2003). Sedimentary silica on Mars. Geology, 31(4), 315-318. [2] Ruff, S. W., & Farmer, J. D. (2016). Silica deposits on Mars with features resembling hot spring biosignatures at El Tatio in Chile. Nat. Com., 7(1). [3] Farley, K. A. et al., Mars 2020 mission overview. Space Sci. Rev., 2020, 216, 1-41.

Columnar Joints: A comparative study of Martian and Deccan Volcanic province

Aditya Das[1,2*], Subham Sarkar[1], Anil D. Shukla[1], Dwijesh Ray[1]

[1]Planetary Sciences Division, Physical Research Laboratory, Ahmedabad, Gujarat-380058
[2]Indian Institute of Technology Gandhinagar, Gujarat 382355
Corresponding author E-mail *adityadas@prl.res.in

Columnar joints on a basaltic terrain provides preliminary assessment about the water influx and cooling history of the basaltic lava during emplacement. As lava cools, tensional stress come into action contraction, cooling and solidification ultimately leading to the formation of columns [1]. The width of the columns suggests the degree of cooling and the amount of water influx into the basaltic terrain [2,3]. Higher water influx would result in accelerated cooling rates leading to smaller columns (entablature) [2]. Whereas, the thicker and vertical lava column in continental flood basalts is called colonnades. The discovery of columnar joints on multiple locations along the walls of impact craters [4] in Mars by the HiRISE imagery aboard the MRO [5] gives valuable insight to the paleo paleo-volcanological environment on Mars. Most of these jointing characters are exposed along the uplifted walls of the impact craters and regions with intense volcanism in the past.

Similar type of columnar jointing is common in the Deccan Volcanic Province (DVP) at Matanumadh area in Kutch. Both the textural and morphological features of the columns suggest an influx of adequate amount of water seeping into the columnar joints which resulted in accelerated and homogenized cooling and solidification. The spectroscopic [6] and the geochemical similarities [7] between the Deccan and the Martian basalts thus help in carrying out the comparative analogous studies. The morphological and geochemical analysis of the Columnar joints from Kutch would provide important clue to estimate water influx and the rate of cooling that induces the formation of Deccan columns. This study, thus, could be useful in understanding the cooling history of lavas in basaltic planet like Mars and other terrestrial planets where volcanism and emplacement of lava are likely familiar in the “wet” environment.

References: [1] Spry, Alan. "The origin of columnar jointing, particularly in basalt flows." *Journal of the Geological Society of Australia* 8.2 (1962): 191-216. [2] Long, P and Wood, B. *Geol Soc Am Bull*, (1986) 97:1144–1155. [3] Goehring, L, Mahadevan, L, and Morris, S. *PNAS*, (2009) 106:387. [4] Milazzo, M. P., et al. "Columnar Jointing on Mars: EarthAnalog Studies." *43rd Annual Lunar and Planetary Science Conference*. No. 1659. 2012. [5] Milazzo, MP, Keszthelyi, LP, Jaeger, WL, et al. *Geology*, (2009) 37:171–174. [6] Wright, Shawn P., Phil R. Christensen, and Thomas G. Sharp. "Laboratory thermal emission spectroscopy of shocked basalt from Lonar Crater, India, and implications for Mars orbital andsample data." *Journal of Geophysical Research: Planets* 116.E9 (2011). [7] Hagerty, Justin J.,and Horton E. Newsom. "Hydrothermal alteration at the Lonar Lake impact structure, India: Implications for impact cratering on Mars." *Meteoritics & Planetary Science* 38.3 (2003): 365-381.

Understanding Presence of CO_2 in Lunar Exosphere from Experimental Observation of Chandrayaan 2

Swastika Chakraborty[a]

[a*] Narula Institute of Technology, 81, Nilganj Road, Agarpara, Kolkata - 700109, India

Geochemical information of Moon is very essential to understand the early history of the solar system when most of that information has already been erased from Earth. Role of carbon is very important for future mission if help can be taken from localized source for using as rocket fuel, for sustained life on moon, for supply of material for biological use or for robotic movement in a sustained way. Several studies found in literature has investigated the presence of CO_2 in permanent cold traps on the moon. Previously Lunar Reconnaissance Orbiter has indicated the presence of CO_2 from the spectral mixture and called for the necessity of investigation further.

This study presents a spatial distribution of amu 44 in the entire mid latitude region of northern hemisphere of moon for the first time during sunset period of local solar time. The data used for this study is one month observation (September 2019) from the mass spectrometer of CHACE-2(https://pradan.issdc.gov.in/pradan/). Figure below shows entire longitudinal-latitudinal distribution of amu 44 from the available observation in terms of total pressure for northern hemisphere of moon during dusk time. It is observed that there is not much variation of total pressure of amu 44 at 260 degree to 270 degree longitude and 50 degree to 70 degree latitude. Short term analysis of one month observation of CHACE-2 of Chandrayaan 2 is presented for amu 44. Complete quantitative spatial observation at sunset time in northern hemisphere of moon reconfirms the presence of carbon di oxide in lunar exosphere. Long term one year observation of CHACE -2 at different part of northern and southern hemisphere of moon will confirm the abundance of amu 44 and it's diurnal and seasonal variation at local solar time.

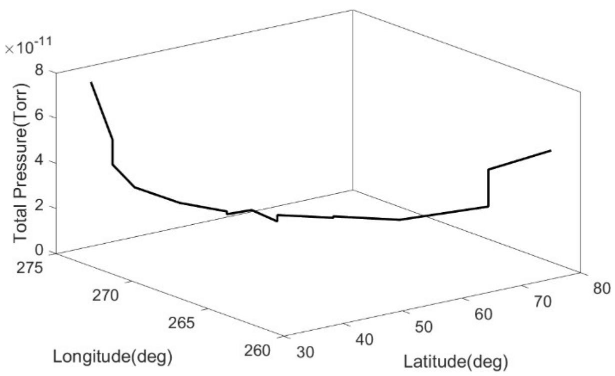

Fig: Latitudinal-Longitudinal distribution of total pressure of amu 44 in northern hemisphere of moon at sunset time

Acknowledgement:This work is supported by Indian Space Research Organization, Department of Space, Government of India (ISRO/SPO/CH-2/AO/7/2022). The significant technical support extended by Chandrayaan 2 Mission Team is duly acknowledged.

An estimation of age and palaeodischarge values across valley networks from the NoachisTerra region of Mars

Supratik Basu[1*], Sudipto Kumar Kolay[1], Satadru Bhattacharya[2], Nilanjan Dasgupta[3], Abhik Kundu[1]

[1]Department of Geology, Asutosh College, 92 S P Mukherjee Road, Kolkata, West Bengal-700026

[2]Space Applications Centre-ISRO, Jodhpur Tekra, Ahmedabad, Gujarat-380015

[3]Department of Geology, Presidency University, 86/1 College Street, Kolkata, West Bengal-700073

*Corresponding Author E-mail: spgeol_rs@caluniv.ac.in

The palaeochannels on Mars and their morphology, drainage, source of water, duration of flow, tectonic implication etc. have been a matter of curiosity among researchers since Mariner 9 mission discovered the water-worn valleys. The region of Noachis Terra, along with Margaritifer Terra, preserve many palaeochannels and therefore are of particular interest for studies on palaeochannel that can unveil history of surface water on Mars [1,2]. Paleochannels are mainly of three types namely outflow channels, valley networks and gullies [2]. Four valley networks from the Noachis Terra region are mapped and palaeodischarge are estimated along with their age. High-resolution CTX images (6m/pixel) and MOLA/HRSC blended digital elevation models are used in this study.

The valleys are estimated to be of early-to-mid Hesperian age (3.84 Ga to 3.32 Ga) [cf., 3,4]. The discharge is calculated using the simple equation of Q=hWu, where ‘h’ is the channel depth or thickness of the water column, ‘W’ is the channel width and ‘u’ represents average flow velocity across the channel cross-section. Palaeoflow parameters like velocity is computed either from Manning or Darcy-Weisbach equations. However, the Darcy-Weisbach equation is preferred over Manning's equation by few previous works as it includes a frictional component that addresses the effect of the valley floor and wall friction on the flowing water [5,6,7]. Thus, palaeodischarge is calculated using the Darcy-Weisbach equation under both bank-full conditions and normal-flow conditions [6]. It is understood that Parana Vallis, which has the lowest mean channel width (245.5 m) had palaeodischarge rates more than Evros and Marikh vallis owing to its higher mean slope (1.838°) and flow depths (7.47 m). Marikh Vallis has the highest mean channel width (535.5 m), however, due to a relatively gentler slope (0.613°) had substantially lower discharge rates under both bank full and normal flow conditions. It is evident from the values of morphometric parameters and data generated that the combined effects of slope and flow depth together had the dominant control on discharge.

References: [1] Grant J. A. and Parker T. J. (2002) *JGR, 107(E9)*, 5066. [2] Carr M. H. and Clow G. D. (1981) *Icarus, 48(1)*, 91-117. [3] Michael, G.G. and Neukum, G. (2010) *EPSL, 294 (3–4)*, 223–229. [4] Kneissl T. et al. (2015) *Icarus, 250*, pp.384-394. [5] Wilson L. et al. (2004) *JGR: Planets, 109(E9)*. [6] Adeli S. et al. (2016) *Icarus, 277*, 286-299. [7] Kleinhans M. G. (2005) *JGR: Planets, 110(E12)*.

Acknowledgement: A RESPOND research grant from Space Applications Centre-ISRO is acknowledged.

Kopargaon in Maharashtra witnessed a recent meteorite fall

Dwijesh Ray and Anil D. Shukla

Physical Research Laboratory, Ahmedabad 380009, India
*Corresponding Author E-mail: dwijesh@prl.res.in

A meteorite is informally known as "free space rocks" and one the most common extra-terrestrial materials readily available for laboratory studies to understand the origin and formation of early Solar System, parent body process, reconstruct the shock-thermal excursion and the cosmic ray interactions during its sojourn in space. Any new meteorite fall is always important due to its pristine essence and dynamic data set on primary mineralogy, textures, whole-rock chemistry. The Indian subcontinent has an exceptional record of meteorite falls (> 700 nos. reported falls and finds) since the first reported fall in Jalandhar, Punjab way back in the year 1621 (Meteoritical Bulletin Data base [1]). On January 24, 2023, a meteorite fell piercing through the roof of Kiran Babanrao Thakre's house, a resident of Bhojade Chauki in the Kopargaon taluka in Ahmednagar district, Maharastra at around 6:50 am IST (Indian Standard Time). The meteorite crashed and piercing through the flat metal roof of the house and then shattered into several fragments once it hit the floor of the bedroom. The high impact of the object produced an impact scar (diameter ~2 inches). Based on the mean olivine (Fa: 29.95 mol%) and low-Ca pyroxene compositions (Fs: 23.97 mol%), the rock belongs to an LL-group of ordinary chondrites and petrologic type 5 [2]. Petrologically, Kopargaon is assigned as LL5, S3 ordinary chondrite breccia [3]. The Kopargaon LL chondrite could be the representative of similar type of S type asteroid probed during the Hayabusa-1 mission [4].

References: [1] https://www.lpi.usra.edu/meteor/metbull.php [2] Van Schmus, W.R. and Wood, J.A. (1967) *GCA, 31*, 747-765. [3] Stoffler, D., Kiel, K. and Scott, E.R.D. (1991) *GCA, 55, 3845-3867* [4] Yoshikawa, M.A., Fujiwara, A. and Kawaguchi, J. (2006) *Proc. Inter Astro Union*, 2(14), 323-324.

Contrasting mineralogy on contemporaneous and adjacent Martian terrains- A CRISM insight

Protiti Roy[1,2*], Dipayan Dasgupta[2], Abhik Kundu[2]

[1]Indian Institute of Technology (Indian School of Mines) Dhanbad, Sardar Patel Nagar, Dhanbad: 826004, Jharkhand; [2]Asutosh College, 92 SP Mukherjee Road, Kolkata: 700026, WB, India.

*Email ID: roy.protiti@gmail.com

Abstract

Much of the Martian crust owes its origin to igneous processes. Previous investigations [1] using gamma-ray spectrometer affirm the origin of volcanic terrains pertaining to partial melting of the Martian interiors. However, such investigative methods are limited in the case of recent Martian terrains (< 3.7 Ga). Recent spectroscopic data from THEMIS, OMEGA, and CRISM have broader applicability in terms of ascertaining the mineralogy across all temporal ranges. The Martian surface bears a resemblance in mineralogy with Plagioclase [2], Pyroxene [3], and/or Olivine [4] bearing basalts on Earth. The OMEGA and CRISM data provide evidences suggesting LCP (low-Calcium Pyroxene) abundance in Noachian Highlands (>~3.7 Ga) compared to Hesperian terrains (<~3.7 Ga, > ~3.2 Ga) with higher concentrations of HCP (high-Calcium Pyroxene) [5].

Our study focuses on two adjacent terrains: Thaumasia Minor (TM) and East Coprates Planum (ECP), both close to the equator. Although these terrains are contemporaneous (Late Noachian), they bear significant differences in their geology. For instance, TM is defined by Late Noachian volcanic unit that bears volcaniclastic lava flows while ECP bears extensively weathered Late Noachian Highlands unit [6]. TM has a higher relief compared to ECP, yet in terms of deformation features, they are equally ornate by faults and impact craters [7]. Spectroscopic analysis using CRISM stamps obtained along these terrains unveil a prominent contrast in the relative abundances of LCP and HCP. Across the TM, HCP is more abundant, while in the ECP, LCP has greater abundance. Volcanism with higher LCP concentrations is often a product of magmatism with elevated H_2O partial pressures [8]. The mantle water leads to higher degrees of partial melting and results in LCP enriched early crust. This is followed by drier events of volcanism under reduced thermal flux and decrease in partial melting, leading to HCP-enriched crust. Therefore, across the TM, magmatism continued till Late Noachian leading to the depletion of LCP; while across the ECP, where magmatism could be recorded until around the Mid-Noachian, is enriched in LCP.

Keywords: LCP, HCP, CRISM, spectroscopy, magmatism

Acknowledgement: ISRO MOM-AO research grant is acknowledged.

References

[1] Baratoux, D. et al. (2011). *Nature, 472*(7343), pp.338-341. [2] Rogers, A.D. and Christensen, P.R. (2007). *JGR: Planets, 112*(E1). [3] Mustard, J.F. et al. (2005). *Science, 307*(5715), pp.1594-1597. [4] Koeppen, W.C. and Hamilton, V.E. (2008). *JGR: Planets, 113*(E5). [5] Poulet, F. et al. (2009). *Icarus, 201*(1), pp.84-101. [6] Tanaka, K. L. et al. (2014). Geologic map of Mars. [7] Dasgupta, D. et al. (2022). *Icarus, 372(January 2020), 114725.* [8] McSween Jr, H.Y. et al. (2001). *Nature, 409*(6819), pp.487-490.

A preliminary investigation of the thermal-contraction polygons along the Martian equatorial region

Sudipto Kumar Kolay[1,2*], Supratik Basu[2], Protiti Roy[2,3,] Dipayan Dasgupta[2], Abhik Kundu[2]

[1]Indian Institute of Technology Kharagpur, Kharagpur-721302, WB, India; [2]Asutosh College, 92 SP Mukherjee Road, Kolkata- 700026, WB, India; [3]Indian Institute of Technology (Indian School of Mines) Dhanbad, Sardar Patel Nagar, Dhanbad: 826004, Jharkhand

**Email ID: kolaysudipto@gmail.com*

Abstract

Previous investigations [1] have reported thermal-contraction polygons in the mid-latitudes to the poles (30° to 80°), in both the hemispheres on the Martian surface and their absence in lower latitudes. The authors [1] have provided detailed insights on their morphology, distinguishing parameters, and genesis. These crack types often show a latitudinal control in terms of their spatial distribution [2] and their genesis often bears direct implications to local climatic controls as well as substrata composition [3]. Previous studies [1] also indicate a roughly symmetrical distribution of flat-topped polygons near the poles to a more peaked and subdued types along the mid latitudes. All of these polygonal cracks are high-centered (elevated polygon faces and depressed rims) early-stage cracks controlled by relative content of ice compared to soil and/or sediment in permafrost ground.

The present study finds polygonal cracks along the equator (0° to 30°) and addresses crack morphologies to explain their genesis. The study was conducted using HiRISE imagery [4]. The subdued type of polygonal cracks, described from mid latitudes, are identified from this region. These cracks are larger in the equatorial region (diameter up to 24m) compared to those in the mid latitudes (diameter up to 16m). Additionally, ice-wedge polygons (low-centered mature stage cracks with depressed polygon faces and elevated rims), a rare type of crack on Martian surface, are also identified from the lower latitudes. These low-centered forms are products of ice sublimation during the late stages of polygon formation [5]. Spatial variation in crack morphology within the same HiRISE image is a common observation and is attributed to local heterogeneity in substrata and micro-climatic controls. The study finds a greater frequency of high-centered cracks over the low-centered cracks. This indicates dominant control of substrata type, compared to micro-climate parameters, on the genesis of polygonal cracks along the lower latitudes.

Keywords: Polygonal crack, substrata, micro-climate

Acknowledgement: RESPOND Research Grant from SAC-ISRO is acknowledged.

References

[1] Levy, J.S., Marchant, D.R. and Head, J.W. (2010). *Icarus*, *206*(1), pp.229-252. [2] Kreslavsky, M.A. and Head III, J.W. (1999). *JGR: Planets*, *104*(E9), pp.21911-21924. [3] Marchant, D.R. and Head, J.W. (2003). *AGU Fall Meeting Abstracts* (Vol. 2003, pp. C12C-06). [4] McEwen, A.S. et al. (2007). *JGR*, *112*. [5] Mangold, N. (2005). *Icarus*, *174*(2), pp.336-359.

Jarosite: a possible indicator for the history of temperature spikes on Martian surface

Debdatta Banerjee[1*], Swastika Chatterjee[1]

[1]Department of Earth Sciences, Indian Institute of Science Education and Research Kolkata, Nadia 741246, West Bengal, India

[*]db20ip003@iiserkol.ac.in

Jarosite, a mineral in the alunite supergroup with a general formula $AB_3(TO_4)_2(OH)_6$ (A = Na, K, Ag, Tl, H_3O, NH4, Pb; B = Fe, Al; and T = S, As, P) [1] has been found to be abundantly present on Martian surface [2,3]. It has also been recently reported to be found deep in the Antarctic ice[4]. This mineral group mainly finds application in acid mine drainage[5], in the mobility of toxic elements[6] and metallurgical processing[7].

Jarosite ($KFe(SO_4)_2(OH)_6$) has been found to decompose into yavapaiite, hematite and water at about 18℃ under Martian conditions [8]. With the aid of ab-initio quantum chemical density functional theory, we have calculated the thermodynamic stability of jarosite, when the composition is varied within permissible limit. The stability of jarosite on the martian surface is important as it carries information regarding the chemical, isotopical and potentially biological activity of the past. Our calculations indicate that incorporation of Na^+ at K^+ sites and Al^{3+} at Fe^{3+} sites both increase the stability of Jarosite.

With the decomposition of jarosite into its end products,we have evaluated the isotopic fractionation of $^{56}Fe/^{54}Fe$ among its Fe containing end products, namely, yavapaiite($KFe(SO_4)_2$) and hematite (Fe_2O_3), with the help of statistical mechanics. As expected, the fractionation is a function of temperature and it has been modeled to an isotopic thermometric equation. From this model we conclude that since thermodynamic decompositions may take place at relatively high temperatures (~18℃) as compared to the average surface temperature of Mars (~ -50℃), the study of the temperature dependence of the isotopic fractionation of Fe among the relevant end products, can give us an idea of the history of temperature spikes on the surface of the planet Mars.

References :

[1]S.J. Mills et al. (2009)*European Journal of Mineralogy*, 21, 1073–1080
[2]P.R. Christensen et al. (2004) *Science*, 306,1733–1739
[3]G. Klingelhöfer et al. (2004) *Science*, 306,1740–1745.
[4]Baccolo, Giovanni, et al. (2021) *Nature Communications* 12.1 : 436.
[5]Nordstrom et al. (2000)*Environmental Science and Technology*, 34, 254–258
[6]Kolitsch and Pring (2001)*Journal of Mineralogical and Petrological Sciences*, 96, 67–78
[7]Dutrizac and Jambor (2000)*Reviews in Mineralogy and Geochemistry, Mineralogical Society of America*,vol. 40, p. 405–452
[8]Navrotsky et al. (2005) *Icarus* 176.1: 250-253.

Landslide susceptibility assessment using frequency ratio model and analytical hierarchy process, in Mahendragiri hill ranges, Odisha

Rajat Kumar Pattanaik[1], Dr. Yengkhom Kesorjit Singh[2]

1Research Scholar, School of Earth Ocean and Climate Sciences, IIT Bhubaneswar, 752055
2Assistant Professor, School of Earth Ocean and Climate Sciences, IIT Bhubaneswar, 752055

*Corresponding Author: Rajat kumar Pattanaik, E-mail: rkp14@iitbbs.ac.in

Slope failure in the mountainous region is a major problem. Numerous landslides occurred in the Mahendragiri hill ranges in the Ganjam district of Odisha in 2013 and 2018, during the Phailin and Titli cyclones respectively, causing enormous damage to the area. Landslide susceptibility index maps are very efficient and effective tools for planning, management and mitigation of disasters like landslides. This study aims to prepare the landslide susceptibility map in the Mahendragiri region using the frequency ratio (FR) model and the analytical hierarchy process (AHP) model. Thirteen causative factors are considered for landslide in this study, such as, slope, aspect, curvature, rail fall, normalized differentiated vegetation index (NDVI), land use and land cover (LULC), lineament density, distance from the lineament, stream density, distance from the stream, elevation, geology and topographic wetness index (TWI). The landslide inventory map is prepared by comparing the Landsat-8, and Sentinel-2 natural color images, google earth images and field surveys. 205 landslide points are identified out of which 154 points are used as training data for the preparation of the model and 51 points are used for the validation of the model. The success rate curve shows that FR model and the AHP model have success rates of 87% and 62% respectively. The findings indicated that, the accuracy reached by the frequency ratio model was somewhat better than that of the AHP model. The study area is in the initial stage of development, but with increase in the construction activity in the area, the frequency of the landslide could increase which will impact the local community as well as the development works. The final susceptibility map could be used by the development planners, contractors or engineers, which will help them to develop better planning for the construction activities in the area and will help in the disaster risk reduction.

Key words: Landslide, Frequency ratio model, analytical hierarchy process, susceptibility map

Seasonal Occurrence of Ionospheric Plasma Bubbles During Ascending Phase of 25th Solar Cycle Over Varanasi

Mukulika Mondal[1], Sanjay Kumar[1], A. K. Singh[1*]

[1]Banaras Hindu University (missmukulika@gmail.com)
* singhak@bhu.ac.in

Ionospheric plasma bubbles are plasma density depletions and accompanying plumes of irregularities that give rise to severe radio signal disruptions [1]. These plasma bubbles are mostly observed in the pre-midnight period [2]. Radio signal suffers fluctuations in both phase and amplitude during their passage through these plasma bubbles. These fluctuations in phase and amplitude of the signal are known as phase and amplitude scintillations respectively [2]. The present study is carried out to observe the variation of occurrence of amplitude scintillations during ascending phase of solar cycle from November 2020 to October 2021 over equatorial anomaly region Varanasi (latitude 25.31° N, longitude 82.97° E). We have taken GNSS data from multifrequency GNSS receiver to study the occurrence of amplitude scintillation index S_4. To study the seasonal variation of S_4, three seasons of year are considered i.e., winter (November, December, January and February), Equinox (March, April, September and October) and summer (May, June, July and August). Diurnal and monthly variation of S_4 index is also analysed. Analysis found maximum scintillation occurrences during the equinox season. The scintillation activity is more prominent during night-time hours than daytime. To study the effect of geomagnetic activity on S_4, we have taken moderate class geomagnetic storm occurred on 14th March, 2022 ($DST_{minimum}$ = -85 nT). The geomagnetic storm modulates the scintillation occurrences

References:

[1] Burke, W. J. et al., ***J. Geophys. Res***. 108(A5), 1221 (2003).
[2] Aarons J., ***Space Sci. Rev***. 63, 209 (1993).

Geomorphological characterization of complex crater central peaks on the Moon

Roshan A. Shukla* and Deepak Dhingra

Department of Earth Sciences, Indian Institute of Technology Kanpur, UP 208016
*Corresponding Author e-mail: roshanadarshshukla@gmail.com

We are using high-resolution datasets from multiple missions for the detailed morphological characterization of central peaks of complex impact craters on the Moon. The dataset includes high resolution imaging at different spatial scales and topography from several missions including Lunar Reconnaissance Orbiter (LRO) [1] and Kaguya SELENE (Seleneological and Engineering Explorer) [2]. The objective of our study is to identify and analyze the systematics of morphological parameters related to central peaks and utilize the obtained trends for understanding their formation process. Our global survey of lunar complex craters (±60° latitude) has revealed interesting geomorphological diversity of the central peaks [3]. This diversity is exhibited in numerous forms including location of the peak with respect to the crater center, shape of the peak and number of peaks in a given crater. Our work is building on the work carried out by earlier workers using earth-based photography, images from lunar orbiter and other missions [4, 5]. We are adding new dimensions to this previous work along with evaluation of the data at much higher spatial resolution and global coverage.

We would present the progress in this direction with a focus on the shape of central peaks.

References: [1] Chin et al. (2007). Lunar reconnaissance orbiter overview: The instrument suite and mission. Space Sci. Rev. 129, 391–419. [2] Haruyama, J. et al. (2008). Global lunar-surface mapping experiment using the lunar imager/Spectrometer on SELENE. Earth Planets Space 60, 243–256 [3] Shukla, R.A. and D. Dhingra (2022). National Space Science Symposium pp.315 [4] Allen, C. C. (1975). Central peaks in lunar craters. The Moon, 12(4), 463-474. [5] Hale, W., & Head, J. W. (1979). In LPSC Proceedings Vol. 10, pp. 2623-2633.

Variation of Ar-40 in Lunar Exosphere

C.P.Pabari[1*], J.P.Pabari[2] , S.Nambiar[2]

[1]St. Xavier's College (Autonomous), Ahmedabad-380009.

[2]Physical Research Laboratory, Ahmedabad-380009.

*E-mail: chandanipabari60@gmail.com

A thin, outermost gaseous envelope around the Moon is known as the lunar exosphere. It consists of variety of species, gases and water. NASA's Lunar Atmosphere and Dust Environment Explorer (LADEE), the first mission in the Lunar Quest series, was designed to orbit the Moon, and to study its thin atmosphere and the lunar dust environment—specifically to collect data on the global density, composition, and time variability of the exosphere [1]. NMS is an instrument on the LADEE spacecraft designed to analyze the composition of the lunar exosphere (neutrals and ions) during the mission [2]. It has provided observations of gases like Ar, Ne, He etc. in the lunar exosphere. In present work, the derived data as .csv fileprovided by NASA PDS is used to analyse the variability in the density of Argon gas present in Lunar Exosphere [3]. Also, we have analyzed one month data to obtain the Argon-40 profilein the exosphere and estimated the scale height. It is found that the scale height is approximately48 km and the surface density is of the order of 10^4 for the Argon-40. The results could be useful to understand variation of Argon-40 in the exosphere. Similar approach may be used forother gases.

References:

[1]Online a, 8 February 2023. Available: https://solarsystem.nasa.gov/missions/ladee/in-depth/

[2]Online b, 14 April 2015. Available: https://atmos.nmsu.edu/PDS/data/PDS4/LADEE/nms_bundle

[3] Benna M., Lyness E. (2014), *NASA PDS,* https://doi.org/10.17189/1518943.

Influence of space event/weather (CME) on Upper Martian Atmosphere:A supportive study to show the anomaly at different atmospheric level

Marylina Das*, Jyotirmoy Kalita, Anirban Guha

[a]*Department of Physics, Tripura University (A Central University), Suryamaninagar, Agartala, Tripura-799022, India*
marylinadas@gmail.com (Corresponding Author)

Abstract: In this investigation, we have shown ICME/ Space weather events followed by an increment of water ions (H^+, OH^-, H_2O+) as well as enhancement on the ionosphere as appearance of an oblique echo. The climate sounders used to capture data regarding the recombination of water ion as water ice particles specifically at a significant height from the Martian surface that appear as cloud and also reported by previous literature (*Lavega et al., 2015, Andrews et al., 2016*). We also analyzed NGIMS and MARSIS data to confirm our investigation related to the ionosphere of Mars. We found that during the appearance of high-altitude clouds, the number of water ions became less or recombined. For ion mass 19, the amount had been decreased from 5.1×10^{-23} g/cc to 4.2×10^{-24} g/cc. Also, during CME, we observed strong echoes in the ionosphere corresponding to the ion density up to 9×10^6 cm^{-3}. The observation is self-explanatory that at the height of 170 km we may see an increase in ion density which further decrease at the height of 230 km to create H_2O+, H+ abundance. Our current work tries to relate this space weather with the anomaly at different Martian atmospheric level.

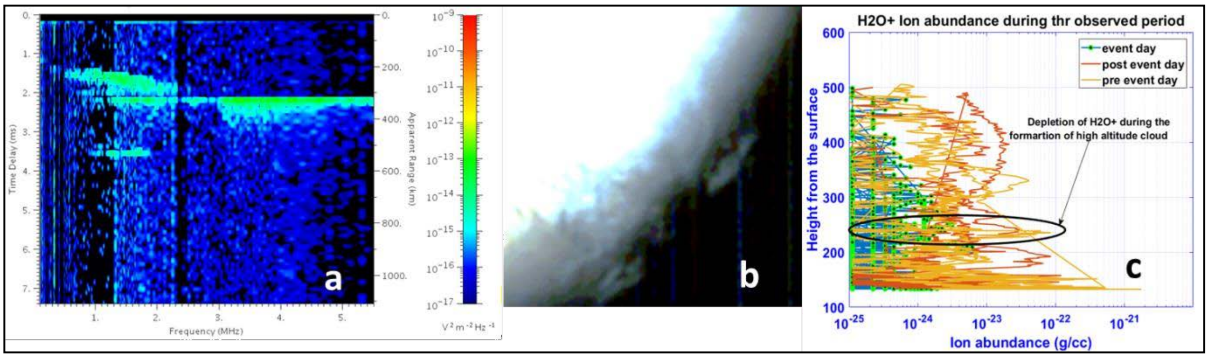

Figure 1: (a) illustrating the echoes formed due to CME event; (b) Illustrate the formation of high-altitude water ice cloud (the detached portion) at the edge of the planet; (c) NGIMS the showing the decrement and recombination of water ion to form water-ice cloud in the upper atmosphere.

References:

1. Sa´nchez-Lavega, A., et al., 2015. An extremely high-altitude plume seen at Mars' morning terminator, Nature,
518, 525-528.
2. Andrews, D. J., André, M., Opgenoorth, H. J., Edberg, N. J. T., Diéval, C., Duru, F., et al. (2014). Oblique reflections in the Mars Express MARSIS data set: Stable density structures in the Martian ionosphere. Journal of Geophysical Research: Space Physics, 119, 3944–3960. https://doi.org/10.1002/2013JA019697

Automatic Contrast Enhancement of Permanently Shadowed Region Images on Lunar Poles using reference-less dynamic range adjustment

Alik Mondal[1], Rishitosh Kumar Sinha[2], Sandeep Kumar[3]

[1]Bsc(H) Physics Student at Bhaskaracharya College of Applied Science, Delhi University (Sector-1, Dwarka, New Delhi, Delhi)

[2]Scientist/Engineer SE at Physical Research Laboratory (Navrangpura, Ahmedabad)

[3]Assistant Professor of Physics at Bhaskaracharya College of Applied Science, Delhi University (Dwarka, New Delhi, Delhi)

Edualik801@gmail.com, rishitosh@prl.res.in, sandeep.kumar@bcas.du.ac.in,

Abstract: The study proposes an automatic contrast enhancement technique for improving the visibility of Permanently Shadowed Region (PSR) images on the Lunar poles. PSRs are the areas on the Moon that are never illuminated by sunlight, resulting in images with low contrast and visibility. Thus, are challenging to image. The proposed technique is based on reference-less deep curve estimation, which utilizes a deep neural network to estimate the high-order curves for the input PSR image. The estimated curve is then used to adjust the pixel intensity values of the image, enhancing its contrast. The proposed method does not require any reference image because of modified non-reference loss functions, to cater this specific problem, making it suitable for processing PSR images where no reference image is available. The performance of the proposed method is evaluated on a dataset curated from Chandrayaan-2 OHRC images, and the results obtained are quite promising based on significant low training time.

Future work will be focused on improving the model's performance by further incorporating different deep learning architectures (preferably a Diffusion model) and hyperparametertuning.

The proposed approach offers a means to enhance the quality of PSR images, enabling more accurate scientific exploration, surface morphology analysis, and mapping of the lunar surface. Furthermore, the methodology can be applied to enhance images of other airless planetary bodies, thereby broadening the scope and potential impact of this work.

References:

[1] Bickel, V. T., et al. (2021). Peering into lunar permanently shadowed regions with Deep Learning. Nature Communications

[2] Guo, C., et al. (2020). Zero-reference deep curve estimation for low-light image enhancement. 2020 IEEE/CVF Conference on Computer Vision and Pattern Recognition (CVPR).

[3] Moseley, B., et al. (2021). Extreme low-light environment-driven image denoising over permanently shadowed lunar regions with a physical noise model. 2021 IEEE/CVF Conference on Computer Vision and Pattern Recognition (CVPR).

Characterization of Potential Landing Sites on de-Gerlache – Shackleton Ridge for the Upcoming Lunar Missions

S. A Sathyan[1*], M. Chowdhury[2], M. Bhatt[1], S. Narendranath[3], N. Srivastava[1]

[1]Physical Research Laboratory, Ahmedabad, Gujarat 380009
[2]Onshore Construction Company Pvt. Ltd., Powai, Mumbai- 400072.
[3]ISRO Satellite Centre, Vimanapura, Bangalore-560 017
*Corresponding Author E-mail: sachana@prl.res.in

Numerous studies have been initiated in the past years, making use of the abundant remote sensing datasets, to highlight potential regions of interest for future lunar landing missions with a stronger focus on the South Pole [1, 2, 3]. Situated within the outer portion of the South-Pole Aitken (SPA) basin, the South Pole offers a unique opportunity to explore the basin's compositional maturity and diversity, structure and age making it a remarkable location for landing [4]. The polar landing sites though scientifically interesting but are technically challenging due to the difficult terrain and limited information available. Moreover, because of the low obliquity and topographic highs, illumination is a major constraint for landing in lunar poles.

This study focuses on geological characterization of four important sites placed between the Shackleton (89.9°S, 0.0°E) and the de Gerlache (88.5°S, 87.1°W) craters mainly considering the importance of this region as candidate regions in future landing missions [5]. The three sites, S (89.46°S, 158.10°W), C1 (89.24°S, 136.12°W), C2 (89.17°S, 113.46°W) in the vicinity of Shackleton crater are taken from [6] and the fourth site named as site D (89°S, 87.1°W), introduced in the present study, belong to the de Gerlache crater. All the selected sites offer nearly persistent illumination (>50%). Maps representing general terrain of the area, slope, aspect, roughness and temperature have been generated with the aid of LOLA DEM to study the topography. Adopting methodology from [7], site specific geomorphology maps have been prepared using LROC NAC [8] and OHRC [9] images. To highlight safe traverse regions, a trafficability map is prepared based on slope, roughness and illumination datasets. Following the same methodology, a PSR map was also prepared emphasizing on micro cold traps surrounding each landing site using LRO-Diviner and illumination datasets. The potential of these micro cold traps has been evaluated with respect to LRO-Mini RF Circular Polarization Ratio (CPR) map, M^3 OH/H_2O abundance and LPNS hydrogen abundance. A proximity analysis of these micro PSRs with respect to the corresponding landing sites was carried out to understand the degree of accessibility. Apart from PSR exploration, factors like ejecta from multiple impact events, lunar hematite, PAN were incorporated while prioritizing the sites and hence making them much more prospective in nature.

Based on technical (landing feasibility) and scientific exploration potential, two of the landing sites (C1 and D) have been found to be most promising for the future landing missions as they depict less slope, maximum illumination and are located nearer to hematite deposits and PSRs with potential water ice and volatiles reservoirs. These results have direct implications to future landing missions like Artemis and LUPEX that consider the studied landing sites as their prime landing hotspots.

References: [1] Kumari N. et al. (2022) Planet. Sci. J. 3, 224. [2] Flahaut J. et al. (2020) Planetary and Space Science, 180, 104750. [3] De Rosa D. et al. (2012) Planetary and Space Science, 74, 224–246. [4] Spudis P. D. et al (1994) Science, 266, 1848-1851. [5] https://www.nasa.gov/specials/artemis/. [6] Glaser P. (2018) Planetary and Space Science 162, 170–178. [7] Bernhardt H. et al. (2022) Icarus, 379, 114963. [8] Robinson M. S. et al. (2010) Space Sci Rev 150, 81–124. [9] Chowdhury A.R. et al. (2019) Current Science, 117 (7), 560-565.

Place the title of your abstract here (Times New Roman, font size 12pt Bold)

Vidhi Panchal[1*], Shail Pandey[1]

[1]Sardar Vallabhbhai National Institute of Technology(full mailing address)
*Corresponding Author E-mail: vidhhipanchal@gmail.com

A dusty plasma electric propulsion scheme has been studied. An argon based plasma uses its thermal energy to charge the micrometer sized dust particles injected into the system. The potential gets developed between plasma and dust particles as they get charged. The potential difference creates Electric field and corresponding Electrostatic force accelerate the particles to produce thrust while stripping of charge before the exhaust. The effect of introduction of dust particles on the plasma has been observed and analyzed. Factors such as, dust particle size, density and temperature of plasma affects the charge accretion on dust particles which has been also studied. As a consequence of the change in the charge accretion, the plasma potential and ultimately plasma parameters such as ion density, electron density and neutral density gets affected. The changes in plasma parameters have been studied as well. The dust particle size and density should be chosen considering the Debye length of plasma to get the maximum thrust. Theoretically, thrust and specific impulse of the mentioned thruster has been obtained which are comparable to Xenon based thruster.

References: Use the brief numbered style common in many abstracts, e.g., [1], [2], etc. References should then appear in numerical order in the reference list, and should use the following abbreviated style:

[1] Author A. B. and Author C. D. (2019) *GRL, 90,* 857-870. [2] Author E. F. et al. (2015) *Current Science, 102(1), 34-55* [3] Author G. H. (2016) *47th LPSC,* 1344–1345.

Bi-LSTM deep learning based Martian Ionosphere Electron Density prediction model using Mars Global Surveyor mission data observations

T. Venkateswara Rao[1,2], D. Venkata Ratnam[1] and M. Sridhar[1]

[1]Department of Electronics and Communication Engineering, Koneru Lakshmaiah Education Foundation (KLEF), Deemed to be University, Guntur, India-522302.

[2]Balloon Facility of Tata Institute of Fundamental Research (TIFR), ECIL Post 5, Hyderabad - 500 062, India.

Corresponding Author E-mail: tanneeru@tifr.res.in

Abstract

The Martian ionosphere is a significant area of study for planetary scientists and space agencies due to its potential impact on future missions to Mars. The electron density is an important parameter to measure in the Martian ionosphere, as it can affect satellite communication and navigation. The influence of solar, geomagnetic activity, and extreme space weather events on the Martian ionosphere can be portrayed and predicted by the Martian ionospheric electron density parameter. The complex and non-linear variability of the Martian ionosphere can be accurately predicted by machine learning models. In this research, we propose the development of a deep machine learning Bi-directional Long Short-Term Memory (Bi-LSTM) model algorithm to predict the ionospheric electron density at a given location and time on Mars. The Mars Global Surveyor (MGS) mission data samples are considered in the present analysis for the training and testing of the proposed model performance. About 5600 electron density profiles recorded by the MGS during the year 1998 to 2005 which was the 23rd solar cycle major period are considered to prepare the input variables such as solar zenith angle (SZA), electron density, latitude, longitude, altitude, local true solar time and solar longitude to the Bi-LSTM model. The performance of the Bi-LSTM model is evaluated and compared with the Bagged Trees prediction model in terms of prediction metrics such as Mean Absolute Error (MAE) and Root Mean Square Error (RMSE). The results of this research could have important implications for future Mars missions, as accurate predictions of ionospheric electron density will be crucial for ensuring reliable communication and navigation. Additionally, the proposed machine learning algorithm could be applied to other planets and moons in our solar system, providing a valuable tool for future planetary science missions.

Study of impact parameters due to hypervelocity dust impact on spacecrafts

Aarti Yadav[1]*, J. P. Pabari[1]
[1]Physical Research Laboratory, Ahmedabad, 380058, Gujarat
*E-mail: aarti@prl.res.in

Interplanetary dust particles can cause electrical damage due to hypervelocity impact. Many of the spacecrafts undergo system failure due to such impacts. The impactors can be meteoroid and orbital debris having the velocity 11-70 km/s and around 10 km/s, respectively [1]. Here, we study different parameters of the dust impact to understand its further effect on the surface of spacecrafts. We calculated the impact charge production Q [1], which has a range along with a range of parameters [2] it includes. Also, the crater diameter [3] and penetration depth [4] are estimated. When a hypervelocity impact hits the metallic surface it also produces high density plasma, which expands and rarifies [1]. We also calculated some characteristic parameters of this plasma such as thermal velocity, oscillation frequency, and the distribution function of electrons and ions [1]. The results can help in designing and operation of the space missions to reduce the threat of system failure and other anomalies.

References: [1] Nicolas Lee, Sigrid Close, Ashish Goel (2013), Phys. Plasmas 20, 032901. [2] N. McBride and J. A. M. McDonnell (1999), Planetary Space Sci. 47, 1005. [3] Paul, K. G., Igenbergs, E. B., Berthoud. L. (1997), Int. J. Impact Eng. 20. [4] J. P. Pabari, S. A. Haider (2018), Planetary and Space Science 161, 68-75.

Prototype of plane parallel impact ionization dust detector

Shivani J. Singh[1, 2]*, Jayesh P. Pabari[2], Srirag N. Nambiar[2], Sonam Jitarwal[2] and Rashmi[2]

[1]BVM Engineering College, Vallabh Vidyanagar, India
[2]Physical Research Laboratory, Navrangpura, Ahmedabad, India

*E-mail: shivaniasdfgh@gmail.com

Interplanetary Dust is a dust complex which includes variety of dust such as asteroid dust, cometary dust, Kuiper belt and many such contributors [1]. To detect the interplanetary dust, a three-channel impact ionization dust detector has been in use for a long time, customarily. One such detector is under development at PRL [2]. To make a miniaturized version of it for resource limited application, we carried out work on a two-channel dust detector [3]. The advantages of two-channel detector are lower mass and compact size. Whenever a dust particle travelling at very high velocity hits the detector target, it instantaneously vaporizes and converted into electrons and ions. The charge carriers are collected by appropriately biased electrodes and processed in the electronics. We present the concept of a plane parallel impact ionization dust detector, its mechanical design, electronics design and initial results. Further work is underway at PRL.

References:

[1]Espy, A. J. et al. (2009), *AAS/Division for Planetary Sciences Meeting Abstracts# 41, 41, 16*-33. [2] Pabari et al. (2018), *Planetary and Space Science, 161, 68-75*.[3] Nambiar S. et al. (2021), *52nd LPSC*, 2548 .

Study of Impact and Escape process on the Lunar surface and Estimation of CriticalProjectile Mass

Aanchal Sahu[1]* and J.P. Pabari[1]
[1]Physical Research Laboratory, Navrangpura, Ahmedabad-380009, India
*E-mail: aanchalsahu@prl.res.in

There is a continuous shower of micrometeorites in planetary system [1] and a planet encounters the dust particles during their spiral-in motion towards the Sun. In case of Moon, all incoming particles can reach the surface without ablation owing to the absence of atmosphere [2]. Due to impact of hypervelocity dust particles on lunar surface, ejecta comes out in the lunar environment. For the ejecta created due to an impact on lunar surface, the total ejected mass has been estimated [3]. Also, it was found that the ejected velocity from a few m/s to a few km/s is inversely proportional to the fragment size [4].

In the present work, we have revisited the estimation of total ejected mass due to an impactor. It is further plotted as a function of incoming micrometeorite mass and its velocity to understand contribution in ejecta from different size of particles. We have considered a wider particle mass range from 10^{-18} kg to 10^{-12} kg and incoming micrometeorite velocity from 1 to 50 km/sec. Using a given relation [5], we have plotted the variation of size of ejected fragment as a function of the velocity. In addition, we found the critical IDP mass for a net escape from Moon, from the escape rates of regolith and water ice for q = 2.75 and q = 3.5 [6]. The results can be useful to understand the net escape and critical size of impactor.

References: [1] Love and Brownlee (1993), Science, 262, 5133. [2] J. P. Pabari et. Al. (2019), Icarus, 338. [3] Gault et al. (1963), NASA-TN-D-1767. Online 21st February 2023. Available: https://ntrs.nasa.gov/search.jsp?R=19630004711. [4] Grades and Miller (2015), ESABASE2/Debris Release 7.0 Technical Description (2015) Online 1st October 2018. Available: http://esabase2.net/wp-content/uploads/2015/12/ESABASE2-Debris-Technical-Description.pdf. [5] Rival and Mandeville (1999), Space Debris, 1 (1), 45-57. [6] Asada, N. (1985), J. Geophys. Res., 90, 12445-12453.

Character of Water-Ice Detections at Lunar North Polar Crater Peary: Implications for Buried Volatiles

Mishal K.T and Deepak Dhingra

Department of Earth Sciences, Indian Institute of Technology Kanpur, UP-208016

*mishalkt@iitk.ac.in, ddhingra@iitk.ac.in

Topographical depressions on the lunar poles which do not receive direct sunlight are excellent locations to trap volatiles [1]. These dark locations (with temperatures < 110K) have not received direct sunlight over geological time scale (millions of years) and are referred to as permanently shadowed regions (PSRs). The PSRs at the lunar poles are expected to evolve with respect to large scale geological events that can alter the topographic depressions. These include processes such as impact cratering and volcanism, which are common, pervasive and have occurred over the geological history of the Moon [2]. Large craters near the lunar poles, which are filled to different extent represent the influence of various geological events. Originally, these craters must have been very deep and might have hosted considerably large PSRs during the early lunar geological time. The series of depositional events in such craters might have subsequently reduced or completely obliterated the PSRs and buried the harbored volatiles over the geological time. Accordingly, North Polar crater Peary (Diameter: ~78 km, Latitude: ~88.6^0, Longitude: 24.4^0) might have hosted a larger PSR than crater Shoemaker (Diameter: ~51 km, Latitude: ~-88.1^0, Longitude: 45.9^0), which currently hosts one of the largest PSRs (1075 km^2) on the Moon. Comparative analysis based on crater topographic profiles indicate that the floor of crater Peary has been buried with thick deposits (> 2.5 km) in contrast to depth of younger craters with similar diameter [3]. We are evaluating the reported volatile detections at crater Peary from multiple remote sensing instruments to understand the character of potentially buried volatiles. The large number of radar anomalous craters detected inside Peary [4] suggests the possible presence of such volatile reservoirs. Lunar Prospector Neutron Spectrometer has also detected the presence of hydrogen -bearing deposits in the upper 1 meter of this infilled crater [5], Interestingly, these locations can be correlated with the ejecta of superposed younger craters that might have tapped and therefore exposed the buried volatile deposits. The surface detection of volatiles from Moon Mineralogical Mapper [6] and Lunar Orbiter Laser Altimeter [7] within superposed younger craters on Peary further illustrate the possibility of tapping of the volatiles by the younger crater formation events. Even though there are other possibilities for deposition of volatiles at these sites, the potential correlation of volatile detections from multiple instruments with buried volatiles cannot be ignored. In-situ measurements could be considered during the future missions to better constrain the potential presence of such deeply buried ancient volatile deposits.

References:[1] Watson, K. et al (1961) JGR, 66(5), 1598-1600. [2] Mishal K. T and Deepak Dhingra (2022) NSSS, # 394. [3] Mishal K. T and Deepak Dhingra (2022) LPSC 54, # 2559. [4] Spudis, P. D et al (2013). JGR: Planets, 118(10), 2016-2029. [5] Feldman, W.C. et al (2001). JGR:Planets, 106(E10), 23231-23251. [6] Li, S. et al (2018) PNAS, 115(36), 8907-8912. [7] Fisher, E.A et al (2017). Icarus, 292, 74-85.

Perseverance rover observation changes the hydrological status of the depositional systemof Jezero crater: from open lake to closed lake delta

Moinak Sinha*[1], Priyabrata Das[2], Amit Basu Sarbadhikari[3]

[1] Centre for Advanced Studies, University of Delhi, Chhatra Marg, Faculty of Science, University Enclave, Delhi, India-110007

[2]IIREES Edutech Private Limited, Durgapur, West Bengal, India-713201

[2]Physical Research Laboratory, Ahmedabad, Gujarat, India-380009

*moinak2013@gmail.com

Jezero crater is a Noachian basin (45 km in diameter) at the western edge of Isidis Planitia, which lies north of the Martian equator in the Nilli Fossae region within the Syrtis major quadrangle. Orbiter data has long suggested that two input valleys have entered the crater from the west and north, depositing sediment at their mouths.

Recent rover observations by Perseverance have further allowed us to classify the Jezero fan deposit as a Gilbert-type delta (Mangold et al., (2021)[1]). Previous studies have suggested that Jezero crater hosted an open-lake system with a water level at an elevation of ~ -2395 m (Fassett and Head, (2005)[2;] Schon et al., (2012)[3]. Although orbiter images have allowed us to constrain the outer channel at ~ -2390 m, Mangold et al., (2021) studied the rover images of Kodiak butte (erosional remnant of delta scarp) some of whose topmost units were deposited at about ~ -2490 m to ~ -2500 m ~100m below the previously accepted open lake level, thus re-defining it to be hydrologically closed at the time of progradation of the delta. Further observations reveal that the topmost unit in some of the scarp remnants, erosionally truncates the horizon below (sand and gravel) and consists of unsorted conglomerates, which contain boulders up to 1.5 m on the long axis implying a marked change in depositional conditions. Such observations point to a temporal change in the energy regime of the fluvial systems feeding the western fan, from episodic high discharge fluvial flows capable of entraining and mobilizing meter-scale rounded boulders over large distances from its source to sustained fluvial activity that built the fan deposits prograding into the Jezero crater lake. Deciphering the provenance of these detrital boulders can aid us to constrain the depositional process and history associated with these episodic high energy flows—something which may further be translated to constrain and understand the paleoenvironmental conditions during the progradation of the delta.

References

[1]Mangold et al. (2021), Perseverance rover reveals an ancient delta-lake system and flood deposits at Jezero crater, Mars (711-717), Vol 374, Science

[2]Fluvial sedimentary deposits on Mars: Ancient deltas in a Crater Lake in the Nili Fossae region, Caleb I. Fassett and James W. Head III, (2005), Vol 32, Geophysical Research Letters

[3]An Overfilled Lacustrine system and progradational delta in Jezero Crater Mars: Implications for Noachian climate; Samuel C. Schon (2012), (28-45),Vol 67, Planetary and Space Science, Elsevier

Spectral Reflectance Studies of Nernst crater on Moon Using Chandrayaan-1 M3Datasets

Keerthana R [1]*, Annadurai R [1] and Kusuma K.N [2]

[1] Department of Civil Engineering, SRM Institute of Science and Technology, Kattankulathur - 603 203

[2] Department of Earth Sciences, Pondicherry University, Puducherry – 605 014

*Corresponding author email –keerthicivil10@gmail.com

Nernst impact crater is located in the highland region and has a diameter of 116 km. It is situated on the northwestern limb of the Oceanus Procellarum [1]. It has a Floor Fractured Crater (FFC) associated with a series of concentric fractures and a domical floor profile. This study investigates the morphology and mineralogy of the crater. From the mineralogy, analysis was carried out in the present study area to identify various minerals such as LCP, Highland Material, and Plagioclase. Using M3 datasets, an Integrated Band Depth-based Color Composite Image was generated to differentiate among similar spectral profiles [2] [3]. The Nernst crater lies on the feldspathic Highland Terrane, which exhibits an anorthosite signature on the crater rim, floor, and central peak. The morphological analysis was carried out using Lunar Reconnaissance Orbiter and Kaguya DEM images identified features such as uplifted central peak, dome, fractures, rilles, rim, rolling stone, Double Impact crater, convex floor, and wall terrace are marked on the morphological map. There is an additional impact crater, Nernst T just on the western rim edge of the Nernst crater. Nernst T crater contains rolling stone, rock boulders, domes, lunar slump, and minerals such as Low Calcium Pyroxene (LCP) and Pure Crystalline Plagioclase. The integrated analysis reveals that anorthosite was present in and around the Nernst crater and that the study area is classified as a class 2 floor fractured crater.

References:

[1] Donaldson et al. (2014) *Journal of Geophysical Research Planets,119 1516–1545,* [2] Mustard. (2011) *Journal of Geophysical Research, 116.* [3] Besse et al. (2011) *Journal of Geophysical Resource, 116, 1-15*

Volcanic craters and cones in central Kachchh mainland, western India:potential analogue for the Martian studies?

Anil Chavan[1]*, K.B. Kimi[1], K.S. Sharini[1], S. Vijayan[1], Subhash Bhandari[2]

[1]Planetary Science Division, Physical Research Laboratory, Ahmedabad, India.
[2]Department of Earth and Environmental Science, K.S.K.V. Kachchh University, Bhuj, India
*Corresponding Author E-mail: asac.anil@gmail.com; anilchavan@prl.res.in

A peri-cratonic rift basin in western India, the Kachchh Basin displays a broad array of geodiversity dating back 200 million years, from the Jurassic Period to the present. For the study of planetary science, the Kachchh basin has retained numerous terrestrial analogue locations [1, 2, 3]. Kachchh Basin has been more or less like Mars' Noachian-Hesperian transition since the Cenozoic epoch [4]. The basin has a number of possible locations that might be explored as Martian counterparts [3]. The northwestern Deccan Continental Flood Basalt Province (CFB) (65-68 Ma) is linked to the magmatism in Kachchh. These are the foundation of the local Deccan stratigraphy, and their volcanological context is poorly understood. Apart from the flow, there are isolated hills of volcanic rocks, which have stood against the erosional processes that occurred in the basin.

This study provides an overview of features indicative of the interaction between water and lava and/or magma in Kachchh and their suitability as analogue for Mars. We have surveyed < 22 craters/cones within the basin for their relevancy as planetary analogue. Evaluated during field investigations and satellite imagery for structures, physiography, geologic setting, and concerning climate change from its evolution. The weathering profile and altered aqueous minerals are also proven analogues from the basin [5, 6]. We propose the Dhinodhar,Varar, and other basaltic vents as an analogue for the Ceraunius, Hecates Tholus, and Volcanic Rootless Constructs (VRCs) of Mars. Though there is no scale-to-scale match, this study focuses more on the geological processes responsible for forming similar landforms on Mars and Earth.

Keywords: Kachchh Basin; Noachian Hesperian transition; Planetary analogue; Ceraunius Tholus; Volcanic Rootless Constructs (VRCs)

References

[1] Chavan and Bhandari 2019, *9th Internal. Conf. on Mars*, Rept. 2089, 6076p; [2] Chavan, et al., 2022, I*carus*, 385, p.115118; [3] Chavan, et al., 2022, Geoheritage, 14(1), p.33; [4] Ray et al., 2021, *Planet Space Sci* 197:105163; [5] Shukla et al., 2014, 8th Internal. *Conf. on Mars*. Pasadena, California, pp 1194; [6] Bhattacharya et al., 2016, *J. Geophys Res: Planets* 121(3):402–431.

MEMS FOR SOLAR PANEL DEPLOYMENT ON A SPACECRAFT

Shryas Bhurat[1], Shreesha S[2], Shubham Das[3*]

[1]Aerospace Engineering, R. V. College of Engineering (shryasbhurat.ae19@rvce.edu.in)
[2]Aerospace Engineering, R. V. College of Engineering (shreeshas@rvce.edu.in)
[3]Aerospace Engineering, R. V. College of Engineering (shubhamdas.ae19@rvce.edu.in)

This paper investigates the potential of Micro-Electro-Mechanical Systems (MEMS) technology to improve the performance of solar panels for spacecraft. The paper examines how the integration of mechanical elements, sensors, actuators, and electronics on a small scale can lead to the creation of tiny solar cells that are integrated into a larger panel, providing increased efficiency and weight reduction. Additionally, the paper demonstrates how MEMS technology enables the creation of solar cells that can track the sun, increasing the overall energy captured by the panel. The paper includes an examination of the manufacturing process and a basic MATLAB code that demonstrates how to control the movement of the panel using options to deploy, expand, turn and compress with a control feedback mechanism. The paper also includes an explanation of how to plot the results of a MEMS-based solar panel and how to handle the warning message of function shadowing. The paper concludes with a summary of the potential benefits of using MEMS technology for solar panels for spacecraft, providing cost savings and increased energy output with comparison to current solar panels.

Micro Actuator Technology used in Soft Robotics Engineering for Space Technology Applications

Shubham Das[1], Shryas Bhurat[2], Prof. Shreesha S[3]

[1]Department of Aerospace Engineering, RV College of Engineering, Mysore Road, Bengaluru-560059, Karnataka, India

[2]Department of Aerospace Engineering, RV College of Engineering, Mysore Road, Bengaluru-560059, Karnataka, India

[3]Professor, Department of Aerospace Engineering, RV College of Engineering, Mysore Road, Bengaluru-560059, Karnataka, India

*Shubham Das, Email ID : shubhamdastwo@gmail.com

Soft robotics is a rapidly growing field that leverages soft, compliant materials to create robots that are highly adaptable and capable of performing a wide range of tasks. One key component of soft robots is the use of micro actuators, which are small, precise devices used to control and adjust the position and other physical parameters of the robot. The actuators can be of piezoelectric, hydraulic or pneumatic type which can be embedded in soft materials to provide controlled movement, shape-changing or force generation. Soft robots used for space technology applications need to be designed as highly energy-efficient, robust, and capable of operating in harsh environments. These actuators embedded in the soft robots are able to achieve high levels of precision in their movements, making them suitable for tasks that require fine control and adjustment. In addition, micro actuators can be used in developing soft robotics based devices for space technology applications since they can be easily integrated with sensors and control systems to provide closed-loop feedback and precise control for robotic movements, making them a popular choice for use in various fields such as mechanical, hydraulics, thermal and electronics. This paper has tried to provide an overview of the current state of the art in micro actuators technology used in soft robotics for space technology based applications, including a discussion of the key features and capabilities of these devices and their future potential applications in this domain.

Keywords: Soft Robotics, Micro Actuators, Space Technology

References:

[1] B. Kim, J. Kim, and B. Lee, "Soft actuators for space applications," in Proceedings of the International Conference on Robotics and Automation, 2019, pp. 1278-1283.

[2] L. Spobia, A. C. Stefanescu, and A. E. Tarniceru, "Development of a soft pneumatic actuator for space robotic applications," in Proceedings of the International Conference on Robotics and Automation, 2019, pp. 1071-1076.

[3] R. Shepherd, D. Rus, and M. Cutkosky, "Design and control of soft robotic systems for space applications," in Proceedings of the International Conference on Robotics and Automation, 2020, pp. 947-952.

[4] L. Spobia, A. E. Tarniceru, and A. C. Stefanescu, "Development of a soft robot for space debris removal," Journal of Intelligent Material Systems and Structures, vol. 27, pp. 1009-1017, 2016.

[5] S. Kim, S. Cho, and J. Kim, "Design and fabrication of soft pneumatic actuators for space robots," Journal of Intelligent Material Systems and Structures, vol. 23, pp. 819-825, 2012.

Radar Scattering Properties of Lunar Impact Craters and Associated Ejecta Facies

T. Samaddar[1*], J. Mehar[1], R.S Chatterjee[1]
[1]Indian Institute of Remote Sensing, Dehradun
*Corresponding Author E-mail: (tamalsamaddar@gmail.com)

Abstract: Radar remote sensing in lunar study has provided us with a greater understanding of the physical properties of the lunar regolith. Synthetic Aperture Radar due to its penetrative nature help in the detection and study of the lunar regolith at near subsurface depths. The Miniature Radio Frequency (Mini-RF) onboard the Lunar Reconnaissance Orbiter (LRO) gives an ideal chance for such studies. It provides almost global coverage of the lunar surface operating at the S-band (12.6 cm). We have utilized Mini-RF radar imagery to investigate the impact craters Aristarchus (23.7°N 47.4°W) and Giordano Bruno (35.9°N 102.8°E) in depth, identifying and characterizing different crater facies units such as rough boulder units/blocks, impact melts, and melt flows. We present our observed results showing characteristic radar signatures of these impact crater features.

Data & Methodology: In the case of the Mini-RF data, we utilized the Map projected calibrated dataset (MAPCDR) product, particularly the derived products of the Stokes parameters (S1,S2,S3,S4) [1]. LROC Wide Angle Camera (WAC) imagery was utilised as the basemap, while LROC Narrow Angle Camera (NAC) imagery was used for thorough analysis and comparison with the observed radar signals. The Stokes parameters were used to derive the Stokes child parameters such as degree of polarization, m, and the Poincare ellipticity, χ, have been utilized to derive the m- χ decomposition technique [2]. Based on the different scattering mechanisms due to the physical properties of the lunar surface, double bounce, volumetric and single bounce scattering of the radar waves take place, which are represented by the red, green and blue colors respectively in the m-χ RGB image generated.

Discussion: Initial results observed through the m-chi decomposition provide characteristic signatures for mapping different ejecta facies such as the impact melt flows and the rough/blocky boulder units. Due to the rocks acting mostly as smooth reflectors in the case of large blocks, the highly rough and large size boulders/blocks present on the lunar surface exhibit a significant amount of odd bounce scattering appearing blue in the case of theGiordano Bruno crater rim. However, in case of the Aristarchus crater, the boulder units beingrelatively smaller in comparison and more closely placed result in more diffuse scattering amongst themselves appearing green. Although the impact melts and flows appear smooth in optical images, they are highly rough particles, similar to the rough proximal ejecta blanket just outside the crater rim. Because of the numerous rock particles and fragments present in the lunar regolith, impact melts and flow units exhibit considerable volumetric scattering. The features identified with the radar data show very good correlation upon thorough comparison with the 0.5 m/px NAC imagery.

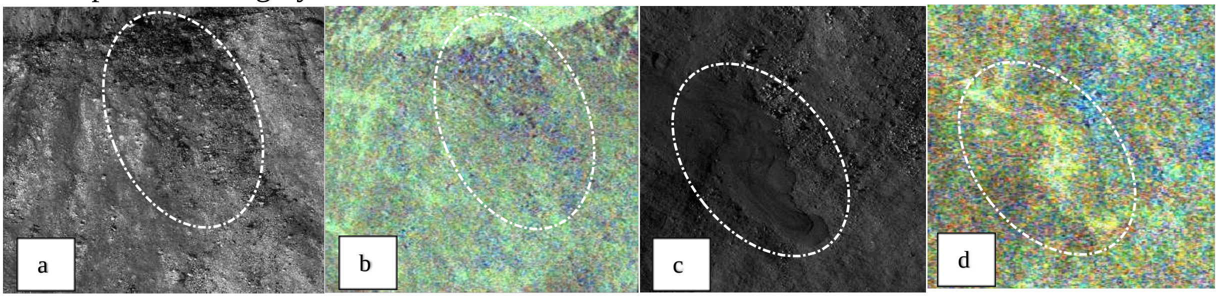

Figure 1 - m-χ radar signatures showing characteristic features along with the corresponding NAC imagery. a-b) showing the southern portion of the Giordano Bruno crater and the bluish appearing rough boulder units. c-d) showing the rough impact melt flow appearing bright with the curved flow pattern visible.

References: [1] Stokes, G. G. (1852). The Illumination and polarization of the sunlight sky on Rayleigh scattering. *Trans. Cambridge. Phil. Soc, 9*, 399 [2] Raney, R. K. et al. (2012). The m-chi decomposition of hybrid dual-polarimetric radar data with application to lunar craters. *Journal of Geophysical Research: Planets, 117* (E12), 0–21

Measurable Schumann Resonance on Martian Surface

Anushka Singh[1,2*], Jayesh P. Pabari[2] and Siddhi Shah[2]

[1]National Institute of Technology, Patna, India
[2]Physical Research Laboratory, Navrangpura, Ahmedabad, India

*E-mail: (anushkas.ug19.ec@nitp.ac.in)

Lightning has been studied on Earth since a long back and can be observed on other planets in the Solar System [1]. Unlike the lightning on Earth, which is due to a naturally occurring discharge between two electrically charged regions in the atmosphere temporarily, lightning on Mars can be conclusively expected as a result of electrical activities associated with the Martian Dust Devils. The low atmospheric pressure and arid, windy environment on Mars suggest that dust in the dust devils is more susceptible to triboelectric charging, leading possibly to the lightning [2]. The extremely low frequency electromagnetic waves generated as a result of the lightning discharge are reflected from the Martian ionosphere and interfere inthe mars-ionosphere cavity, giving rise to Schumann Resonance in the lower altitude region [3]. The calculation of Schumann Resonance across various altitudes can be an effective tool in order to determine lightning characteristics on Mars [4].

In this work, we have represented a model in order to calculate the Schumann Resonance frequency in the Martian ionospheric cavity. During the dust devils, the permittivity and conductivity of the medium are modified due to the presence of dust [5]. We have studied the variation of Martian Schumann Resonance for different conditions, which may be measurable by in-situ experiment on Mars. This work can help in designing the instrument for future mission.

References:

[1] Nickolaenko, A. P. and Rabinowich, L. M. (1982) *Kosmicheskie Issledovaniya, 20(1),* 82-88. [2] Krauss, C. E. et al. (2006) *Journal of Geophysical Research, 111(E2).* [3] Haider, S. A. et al. (2019) *Advances In Space Research, 63(7),* 2260-2266. [4] Bliokh, P. V. et al. (1977) *Naukova dumka, Kiev 199,* l0. [5] Pabari, J. P. and Sana, T. (2021) *Current Science, 121(6),* 769-774.

Geological evolution of Mare Nectaris: Insights from diverse degraded craters

Sharini K.S.[1], Kimi K.B.[2,3], Harish[4], Tuhi S.[5], R.K.S. Priya[1], Vijayan S.[2*]

[1]College of Engineering, Guindy, Anna University, Chennai, India, [2]Physical Research Laboratory, Ahmedabad, India, [3]Indian Institute of Technology, Gandhinagar, India, [4]Space and Planetary Science Center and Department of Earth Sciences, Khalifa University, Abu Dhabi, UAE, [5]Department of Geosciences, Auburn University, Auburn, AL, USA.

*Corresponding Author E-mail: vijayan@prl.res.in

Impact craters are the most common feature found on all terrestrial planetary bodies, including the Moon. After the formation of the crater, it can undergo extensive modifications due to magma intrusion [1,2], lava infilling [3], and the reactivation of existing impact fractures [4]. In this study, we aim to understand the modification processes of deformed craters located in Mare Nectaris on the Moon. To analyze the geomorphology of the craters, we used the Lunar Reconnaissance Orbiter's (LRO) Wide Angle Camera's (WAC) global mosaic of ~100 meters/pixel [5]. High-resolution images from LRO's Narrow Angle Camera (NAC) with a spatial resolution of ~0.5 m/pixel [5] and Chandrayaan-2's Terrain Mapping Camera-2 with a spatial resolution of ~5 m/pixel [6] were also used. We used SLDEM2015 for topography analysis, which has a spatial resolution of ~59 m/pixel and a vertical accuracy of ~3–4 m [7]. To analyze the mineralogy, we used Chandrayaan-1's M^3 [8] data. Impact craters on the mare-highland boundary of the Nectaris basin have undergone extensive modification due to significant topographic differences between the two regions. They were modified due to magmatic intrusion, volcanism, fractures, lobate scarps and wrinkle ridges. The craters Fracastorius, Bohnenberger A and Beaumont are located in the mare-highland boundary of the basin, and their floor is flooded due to the low elevation of the rim which caused it to breach and allow lava from the basin to flow into the crater. Lava can breach the rim from the basin to the crater or vice versa. Similarly, due to the location of the Daguerre crater within the mare region, the entire crater is breached and only some parts of the lava-covered rim and floor are visible. Several other craters have also formed within the mare region of the Nectaris basin. Magmatic intrusion can cause domical shape of the floor of craters [2] forming domical craters, which is seen in both Bohnenberger and Bohnenberger A. Fractures on the floors of the Fracastorius, Bohnenberger, Bohnenberger A and Beaumont craters plausibly indicate intrusions and mare infilling. We have observed wrinkle ridges in a concentric pattern on the basin floor that passes through the Fracastorius crater, indicating reactivation of an existing fracture in the basin. Gaudibert and the unnamed crater located near its southwestern rim have undergone intensive deformation when compared to other craters, due to material slumping. The obtained spectra from the mare region of the Nectaris basin shows absorption at ~1 μm and ~2 μm, which is due to the presence of iron. In this study, we observed diverse morphological features associated with different geological processes, which suggest multiple localized activities in Mare Nectaris.

References: [1] Schultz, P. H. (1976). [2] Jozwiak, L.M. et al. (2012) Journal of Geophysical Research: Planets 117. [3] Kimi KB et al. (2023) Icarus, v390 115298. [4] Nypaver, C. A. and Thomson, B. J. (2022) v49, e (17) [5] Robinson, M. S. et al. (2010) Space science reviews 150, 81–124. [6] Chowdhury A.R. et al. (2020) Current Science 118(4):566. [7] Barker, M. K. et al. (2016) Icarus 273, 346–355. [8] Pieters, C. M. et al, (2009) Current Science 500-505.

Parameters contributing in the initiation of lightning

Janki Jigar Shah[1,2*], Jayesh Pabari[2], Srirag Nambiar[2], Sonam Jitarwal[2], Rashmi[2], Kinsuk Acharyya[2] and Trushit Upadhyaya[3]

[1]L.D. College of Engineering, Ahmedabad, India
[2]Physical Research Laboratory, Navrangpura, Ahmedabad, India

[3]CHARUSAT, Changa, India

Corresponding Author E-mail: (jankishah2002@gmail.com)

Lightning has been proved as one of the most destructive natural disasters accompanying the thunderstorms. It is a phenomenon of electrical discharge that occurs in nature between clouds or between clouds and the ground [1]. Along with the continuous economic and social development, the personal safety and property damage caused by lightning have attracted people's attention. It is therefore, necessary to study the inter-relations between lightning and its causative factors [2]. Significant progress is being made in forecasting of lightning across the world. The forecasting of lightning includes statistical methods, conventional machine learning methods, and most recently, deep learning methods [3]. The lightning frequency, is governed by the parameters like pressure, temperature, windspeed and humidity. Recent researches have also stated the governance of lightning by the effect of some surface parameters [4].

In this work, a dataset of all features is created for predicting the lightning activity, by classifying the dataset into lightning active and in-active classes. Data preprocessing to remove any missing or invalid data is a preordained step before moving to the model formation for lightning prediction [5]. Electric Field Strength and Lightning Activity are the parameters which are generated synthetically with reference to the values of Precipitation and Electric Field Strength respectively. The results for some parameters have also been plotted. The results shall further be used to study lightning occurrences and its effects beyond earth system requirements.

References:

[1] Saunders, Clive. (2008), *Planetary Atmospheric Electricity, 335-353.* [2] Chakraborty et al. (2021), *Atmospheric Chemistry and Physics, 21, 11161-11177.* [3] Bouchard, Aurélie. et al. (2022*), Natural Hazards, 1-37* [4] Dewan, Ashraf. et al. (2018), *Theoretical and Applied Climatology, 134, 347-362.* [5] Mostajabi, Amirhossein. et al. (2019), *Npj Climate and Atmospheric Science, 2,1- 41.*

Constraints on the Chemical Composition of the Bulk Silicate Earth from volatile element abundances. G. Srinivasan. Centre for Space Science & Earth Habitability, E5/11 Arera Colony, Bhopal 462016, , India. gopalan.srinivasan@gmail.com.

To understand the planetary differentiation resulting in chemically distinct reservoirs it is important to establish the bulk planetary chemical composition and the time scales of processes [1]. The nebular material, similar to Sun, was subjected to various differentiation processes (e.g., evaporation, condensation, impact collision, aggregation, etc.,) prior to its incorporation in planetary bodies. These processes took place in various settings (nebula, planetary bodies, and some via collisions of planetary bodies). Due to formation at different distances from the Sun meteorite constituents experienced varied temperatures, evaporation and condensation histories. Chondrites also record different chemical and isotopic compositions [2]. Comparison of the bulk Earth composition with that of primitive chondritesreveals that the building blocks of the Earth deviate from the primordial composition representing the "Sun". The first order similarities between chondritic composition, and moreparticularly that of CI chondrites with that of the Sun, their use to model the composition of planetary bodies [3,4]. Whether the current collection of chondritic meteorites is a representative proxy from which Earth formed is an open question. Nonetheless, it is possibleto quantify the relative abundances and bulk composition of the different materials that contributed to the growing Earth / rocky planets [5]. In an extremely simple scenario - Earth mass increased due to monotonic accumulation of parcels of matter with a composition similar to primitive chondrites. The deviations of the observed from the predicted composition could be used to infer constraints. The alternative would be to consider that building blocks comprising the Earth were depleted in volatile elements relative to CI chondrite composition as is observed in other carbonaceous chondrites. Such an alternative scenario could be parsed into three main epochs: i) a main growth scenario resulting in formation of proto-Earth (80-85% of bulk Earth mass); this was followed by core-mantle separation; ii) material less depleted in volatile material is accreted via the Moon forming impact of Theia. This last step results in accumulation of 99% of the mass and was followed by segregation of sulfide melt known as "Hadean matte" [6]; and iii) the remainder of Earth mass was aggregated later and is popularly labelled as "*late veneer*" [e.g., 7]. The motivationfor a phased scenario arises from mantle abundances of highly siderophile elements (HSE) exceeding equilibrium metal-silicate partitioning. Alternative scenarios for partition under higher T-P conditions or late accretion have been proposed to account for such abundances.

This study explores the abundances of few volatile elements (e.g., In, Cd, Sn, Pb). from the impact addition of Theia to the present-day mantle. Mass balance calculation for end member scenarios is explored to constrain the processes involved. For example: starting with bulk Earth Sn and Pb abundance of 0.240 ppm and 0.608 ppm and applying the $D^{met/sil}$ partition coefficient of 400 and 28 [8] the anticipated mantle concentrations are 0.002ppm and 0.0547ppm, respectively. Yet the estimated abundances in mantle for both Sn and Pb are 0.130 ppm [9] and 0.185ppm [10] respectively are higher. Ideas to explore a way around this discrepancy will be discussed..

References: [1] H. Palme, H. O'Neill (2014) in *Treatise on Geochemistry,* vol. 3, pp. 1–38 [2] P.H.Warren (2011) *Earth Planet. Sci. Lett.* **311** 93–100. [3] H. Wänke and G. Dreibus (1988) *Philos. Trans. R. Soc.,* **325** 545–557. [4] D.C. Rubie, et al (2011) *Earth Planet. Sci. Lett.* **301** 31–42. [5] C. Liebske, A. Khan (2019) *Icarus* **322** 121–134. [6] H.S.C. O'Neill (1991) *Geochim. Cosmochim. Acta* **55** 1159–1172. [7] K. Mezger, et al. (2020) *Sp ace Sci. Rev.* **216** 27-51. [8] K. Righter et al. (2018) *Met. & Planet.Sci.* 53, 284–305. [9] K. P. Jochum et al (1993) *Geochim et Cosmochim. Acta* **57** 3585–3595 [10] Galer, S.J.G., Goldstein, S.L., (1996) in *Reading the Isotopic Code* (eds. A. Basu, S. R. Hart), AGU, **95**, pp. 75–98.

Constraints on the Chemical Composition of the Bulk Silicate Earth from volatile element abundances. G. Srinivasan. Centre for Space Science & Earth Habitability, E5/11 Arera Colony, Bhopal 462016, , India. gopalan.srinivasan@gmail.com.

To understand the planetary differentiation resulting in chemically distinct reservoirs it is important to establish the bulk planetary chemical composition and the time scales of processes [1]. The nebular material, similar to Sun, was subjected to various differentiation processes (e.g., evaporation, condensation, impact collision, aggregation, etc.,) prior to its incorporation in planetary bodies. These processes took place in various settings (nebula, planetary bodies, and some via collisions of planetary bodies). Due to formation at different distances from the Sun meteorite constituents experienced varied temperatures, evaporation and condensation histories. Chondrites also record different chemical and isotopic compositions [2]. Comparison of the bulk Earth composition with that of primitive chondritesreveals that the building blocks of the Earth deviate from the primordial composition representing the "Sun". The first order similarities between chondritic composition, and moreparticularly that of CI chondrites with that of the Sun, their use to model the composition of planetary bodies [3,4]. Whether the current collection of chondritic meteorites is a representative proxy from which Earth formed is an open question. Nonetheless, it is possibleto quantify the relative abundances and bulk composition of the different materials that contributed to the growing Earth / rocky planets [5]. In an extremely simple scenario - Earth mass increased due to monotonic accumulation of parcels of matter with a composition similar to primitive chondrites. The deviations of the observed from the predicted composition could be used to infer constraints. The alternative would be to consider that building blocks comprising the Earth were depleted in volatile elements relative to CI chondrite composition as is observed in other carbonaceous chondrites. Such an alternative scenario could be parsed into three main epochs: i) a main growth scenario resulting in formation of proto-Earth (80-85% of bulk Earth mass); this was followed by core-mantle separation; ii) material less depleted in volatile material is accreted via the Moon forming impact of Theia. This last step results in accumulation of 99% of the mass and was followed by segregation of sulfide melt known as "Hadean matte" [6]; and iii) the remainder of Earth mass was aggregated later and is popularly labelled as "*late veneer*" [e.g., 7]. The motivationfor a phased scenario arises from mantle abundances of highly siderophile elements (HSE) exceeding equilibrium metal-silicate partitioning. Alternative scenarios for partition under higher T-P conditions or late accretion have been proposed to account for such abundances.

This study explores the abundances of few volatile elements (e.g., In, Cd, Sn, Pb). from the impact addition of Theia to the present-day mantle. Mass balance calculation for end member scenarios is explored to constrain the processes involved. For example: starting with bulk Earth Sn and Pb abundance of 0.240 ppm and 0.608 ppm and applying the $D^{met/sil}$ partition coefficient of 400 and 28 [8] the anticipated mantle concentrations are 0.002ppm and 0.0547ppm, respectively. Yet the estimated abundances in mantle for both Sn and Pb are 0.130 ppm [9] and 0.185ppm [10] respectively are higher. Ideas to explore a way around this discrepancy will be discussed..

References: [1] H. Palme, H. O'Neill (2014) in *Treatise on Geochemistry*, vol. 3, pp. 1–38 [2] P.H.Warren (2011) *Earth Planet. Sci. Lett.* **311** 93–100. [3] H. Wänke and G. Dreibus (1988) *Philos. Trans. R. Soc.*, **325** 545–557. [4] D.C. Rubie, et al (2011) *Earth Planet. Sci. Lett.* **301** 31–42. [5] C. Liebske, A. Khan (2019) *Icarus* **322** 121–134. [6] H.S.C. O'Neill (1991) *Geochim. Cosmochim. Acta* **55** 1159–1172. [7] K. Mezger, et al. (2020) *Sp ace Sci. Rev*. **216** 27-51. [8] K. Righter et al. (2018) *Met. & Planet.Sci.* 53, 284–305. [9] K. P. Jochum et al (1993) *Geochim et Cosmochim. Acta* **57** 3585–3595 [10] Galer, S.J.G., Goldstein, S.L., (1996) in *Reading the Isotopic Code* (eds. A. Basu, S. R. Hart), AGU, **95**, pp. 75–98.

Comparative Geology and Mineralogy of Lunar South Pole for Chandrayaan-3 andArtemis III Landing Sites using M3 and IIRS Data

Prateek Tripathi[1*], Rahul Dev Garg[2]

[1,2]Geomatics Engineering, Department of Civil Engineering, Indian Institute of Technology, Roorkee
*Corresponding Author E-mail: (ptripathi@ce.iitr.ac.in)

he potential landing sites for the Chandrayaan-3 (Ch-3) and Artemis III missions are located near the Manzinus crater located~650 Km from south pole and within 6 degrees latitude of the lunar south pole, respectively, falling under the 25 degrees latitude of the lunar south pole [1,2]. Geology and mineralogy are crucial factors in deciding the science activities to be carried out and In-Situ Resource Utilization (ISRU) [3]. Therefore, it is important to examine the geology, mineralogy, and morphology of the vicinity of these two potential landing sites to support both robotic and future manned missions. In this study, data from the Moon Mineralogy Mapper (M3) of Ch-1 (up to 3000 nm) and Imaging Infrared Spectrometer (IIRS) from Ch-2 (up to 5000 nm) were used to compare the geology and mineralogy of the lunar south pole, covering the Ch-3 and Artemis III potential landing sites.

The IIRS radiance data available at the PRADAN portal was processed to reflectance [4], and vertical spectral profiling was conducted for both M3 and IIRS datasets to evaluate the effects of space weathering and changes in mineralogy. The absorption bands at 790 nm, 1980 nm, and 2180 nm are shifted (south of the Ch-2 landing site), suggesting varying degrees of space weathering in that direction. The medium reflectance values between 450 nm and 800 nm indicate the presence of highland materials. A shift is observed in the 1090 nm, 1940 nm, and 2140 nm for the Artemis potential landing sites. No mafic minerals are observed in the Integrated Band Depth map. Anorthosite is seen on the Shackleton crater rim and on the southern and western sides of the Chandrayaan-3 landing site. M^3 revealed high values of plagioclase band depth and low FeO % values in the region. As most of the IIRS data is in shadow, the lunar hydration feature was checked at M3 ice exposures [5] in the vicinity of Artemis III landing sites and Ch-3 landing site..

References: [1] Amitabh et al. (2023) 54^{th} LPSC, 1037 [2] NASA (2022) NASA Identifies Candidate Regions for Landing Next Americans on Moon [3] Anand M. et al. (2012) *PSS, 74(1), 42–48* [4] Chauhan P. et al. (2021) *Current Science, 121(3), 391-401* [5] Shuai Li et al (2018) *Lunar Polar Volatiles, 5010.*

Structural control on polygonal impact crater rim geometry from Mare Crisium

Joyita Thapa[1*], Tanumoy Majumder[2], Rwiti Basu[1], A.S Arya[3], Abhik Kundu[1]

[1]Department of Geology, Asutosh College, 92, S.P. Mukherjee Road, Kolkata, 700026, West Bengal, India; [2]Indian Institute of Technology Dhanbad, Sardar Patel Nagar, Dhanbad, 826004, Jharkhand, India; [3]Space Applications Centre, ISRO, Ahmedabad, Gujarat, India.

*E-mail: joyita.thapa11@gmail.com

Abstract: Polygonal impact craters (PICs) with characteristic polygonal rim geometry are frequent on the surface of terrestrial planets and their respective natural satellites. Trends of their rim segments are considered to reflect the orientations of fractures/weak zones present in their vicinity. Mare Crisium (Fig.1) is a Nectarian-aged lunar basin (3.9 Ga) with a diameter of 740 km, present on the near side. Wrinkle ridges and polygonal impact craters, both simpleand complex, are widely present on this mare. It has been proposed that the 45° relation of simple PICs to weak structural planes does not hold everywhere, and the crater rim segments may show parallelism with fault strikes as both simple and complex PICs rims show similar trends [1]. In the case of Mare Crisium, we correlated the trends of 114 PICs (110 simple PICs;4 complex PICs) with wrinkle ridges using rose plots and frequency plots (Fig. 1). It has been observed that the dominant trend of wrinkle ridges is NE-SW (45^0-60^0) followed by NNW-NNE (330^0-345^0) and NW-SE (300^0-315^0, 315^0-330^0). Other trends include ~N-S (0^0-15^0, 345^0-0^0). Simple and complex PICs both show dominant trends in the NW-SE (315^0-330^0 for SPICs and 300^0-315^0 for CPICs) direction with subordinate orientation in the NE-SW (45^0-60^0) and ~N-S (0^0-15^0) direction. To ascertain if the trends of PIC rim segments and straight segments of tectonic structures (wrinkle ridges) had the same or different variabilities, F-tests with confidence levels of = 0.05, 0.025, and 0.01 were performed using the null hypothesis. The statistical correlations between simple and complex PICs with wrinkle ridges are accepted for all three confidence levels. It can be concluded that both simple and complex PICs align with the two dominant trends of the wrinkle ridges in Mare Crisium. Moreover, from the F-test, it can be ascertained that the wrinkle ridges possibly had control on the PIC rims' geometry, provided the null hypothesis for "the match of variation in trends of PIC rim segments (simple and complex separately) with the trends variation of straight segments of wrinkle ridges" is accepted. Further, geological and geophysical investigations are required to understand the extent of the control of such tectonic features on the rim orientation of polygonal impact craters.

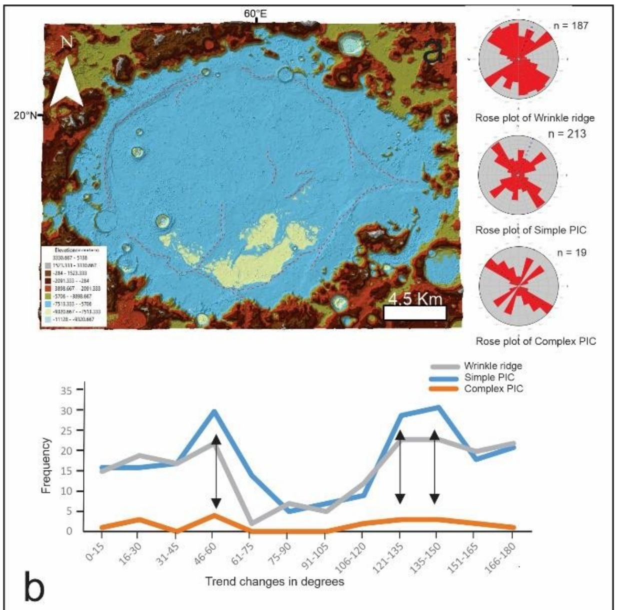

Figure 1: (a) Colored SLDEM of Mare Crisium with marked wrinkle ridges (dotted red lines); (b) Frequency plot of trend values (at 15° intervals) of deformational structures (wrinkle ridges here) and PICs' (simple and complex) rim segments from the Mare Crisium basin to understand the patterns and relationships among these features.

Acknowledgement: Research grant from SAC ISRO Ahmedabad is acknowledged.

References: [1] Öhman, T. et al., 2008 *Meteoritics & Planetary Science*, *43*(10), pp.1605-1628

Curved Prism based Imaging-spectrometer Design in a CubeSat format for Planetary Studies

Jenilkumar Changela[1,2,*], Vaibhav Dixit[2]

[1]St. Xavier's College, Navrangpura, Ahmedabad
[2]Physical Research Laboratory, Navrangpura, Ahmedabad

[*] jenilchangela1@gmail.com

Although grating-based spectrometers provide much higher spectral resolution than prisms, they suffer from the problem of low throughput. Recent advances in optical manufacturing technology have once again revived interest towards prism-based spectrometers of which several designs have employed curved prisms based on the aplanatic principle [1]. Curved prism-based imaging spectrometers offer better performance, no higher-order interference, are easier to manufacture, and can be fitted into compact spaces making them well suited for use in small spacecrafts such as CubeSats. Such devices can mainly be used for mineralogical studies of planetary bodies, but are not limited to, can also be used to determine the composition of planetary atmospheres, etc. We shall present a preliminary optical design of a curved prism based imaging spectrometer that can be accommodated in a 4U-6U CubeSat. The instrument would be sensitive in the visible waveband and provide moderate spatial resolution. The short development time and low cost will make these types of instruments attractive options for future planetary missions.

References:

[1] Compact prism spectrographs based on aplanatic principles
Author David W. Warren,John A. Hackwell and David J. Gutierrez
Optical Engineering, Vol. 36, Issue 04, (April 1997) https://doi.org/10.1117/1.601237

Development and Characterization of a Multichannel Large Area X-Ray Spectrometer using Silicon Drift Detectors with ASIC Based Readout

Nishant Singh[1*], M. Shanmugam[1], Arpit Patel[1], Sushil Kumar[1], Deepak Kumar Painkra[1], Tinkal Ladiya[1], and S. Vadawale[1]

[1]Physical Research Laboratory, Ahmedabad

*nishant@prl.res.in

Abstract

The use of silicon-based X-ray spectroscopy has been increasingly widespread in various fields such as planetary elemental studies, solar studies, X-ray imaging, and astronomical observations. We have already developed a single-channel X-ray spectrometer with discrete components- Solar X-ray Monitor, flown on Chandrayaan-2 orbiter. In this work, we have developed a large area Silicon Drift Detector (SDD) based X-ray spectrometer using multiple SDDs and which are readout by a multi-channel Application Specific Integrated Circuit (ASIC). This will be compact instrument with very low power consumption. The developed system employs the VERDI ASIC, which is capable of readout from eight detectors simultaneously. The ASIC comprises of a preamplifier, a shaper with adjustable shaping times, and a peak stretcher with a baseline holder in each channel. The system enables to stack multiple SDD modules in a compact assembly with excellent energy resolution in the range of 0.5 keV to 15 keV with fast readout.

The performance of the large area X-ray spectrometer was characterized for various electrical parameters such as shaping time, channel gain, detector temperature and dynamic range of the ASIC. The spectrometer provides an energy resolution of ~145 eV at 5.9 keV with 5 detector channels for the optimum shaping time of ~2 μs, at a detector temperature of approximately -30°C. The instrument is an excellent candidate for future planetary exploration missions and X-ray astronomy missions. The performance and results from the instrument will be presented at the conference.

Design aspects of Venus Radiation environment monitor (VeRad) for the Venus orbiter mission

Sushil Kumar[1], Deepak K. Painkra[1], M. Shanmugam[1], D. Chakrabarty[1], Arpit Patel[1], Shiv K. Goyal[1], Tinkal Ladiya[1], N. Singh[1], Abhishek J. Verma[1], Neeraj Tiwari[1], Varun Sheel[1], Santosh Vadawale[1], Nandita Srivastava[1], Aveek Sarkar[1], Sanjay K Mishra[1], Anil Bhardwaj[1]

[1]Physical Research Laboratory, Ahmedabad

*sushil@prl.res.in

It is important to study the effects of energetic particles on the ionosphere of Venus as this has a significant impact on the fundamental atmospheric properties of the planet. Till now, no measurement of charge particle radiation exists around the Venus. The Venus Radiation environment monitor (VeRad), one of the selected instruments of future Venus orbiter mission of India, aims to detect energetic particles around the Venus to study the effects of these particles on the ionosphere of the Venus. VeRad instrument is configured as two packages, each with three detector units and its readout electronics, covering six different directions. The detector units of the instrument consist of a stack of two Si PIN detectors each with a depletion depth of 300 microns to cover particles in the energy range of 20 keV to 100 MeV. Various laboratory tests were conducted to characterize the detectors and optimize their performance, in terms of the leakage current, its performance with temperature, energy resolution, and low energy threshold. Additionally, simulations were carried out to finalize the number of detectors and their thickness to be used in each detector unit.

The results of the laboratory tests and simulations, as well as the detailed design aspects of the VeRad instrument will be presented in the conference.

Discovery of a close-in massive giant planet around a sub-giant star

***Akanksha Khandelwal**, Rishikesh Sharma, Abhijit Chakraborty, Priyanka Chaturvedi, Solène Ulmer-Moll, David R. Ciardi, Andrew W. Boyle, Sanjay Baliwal, Eike. W. Guenther, Allyson Bieryla, David W. Latham, Neelam J.S.S.V. Prasad, Ashirbad Nayak, Monika Lendl, Christoph Mordasini*

The classification of massive giant planets (with masses between 4 and 13 times that of Jupiter) as either planets or Brown dwarfs has long been debated, and their presence in close proximity to their stars has always puzzled astronomers. Recently, we have discovered a massive giant planet orbiting a sub-giant F-type star TOI-4603 by NASA's Transiting Exoplanet Survey Satellite (TESS). In this talk, I will discuss the discovery and characterization of this newly discovered exoplanet. The planet has a radius of 1.043 times that of Jupiter and an orbital period of 7.24 days. Through radial velocity measurements using the PARAS (PRL) and TRES spectrographs, the planet's mass was determined to be 12.89 times that of Jupiter, resulting in a bulk density of 14.1 g/cm3. This makes it one of the few massive giant planets with extreme density and situated in the transition mass range between massive giant planets and low-mass brown dwarfs, an important addition to the population of fewer than five objects in this mass range. Furthermore, the planet is currently undergoing high eccentricity tidal migration, which can provide insights into planet migration theories. Detecting such systems can help us better understand the processes governing massive planets and improve our understanding of their dominant formation and migration pathways.

Advancing the public reach of India's planetary science and space exploration activities

Jatan Mehta

Globally published, independent Space and Moon Exploration Writer, Mumbai, 400068

E-mail: hey@jatan.space

Abstract: The pursuit of space exploration and its related sciences are resource-intensive endeavors. To that end, these activities are primarily publicly funded, including here in India. And yet our citizens at large have little insight into, or understanding of, the breath and depth of India's space exploration activities. This issue is particularly poignant in the case of planetary science and astrophysics, where neither the Indian taxpayers nor the international scientific community for that matter are aware of *and* able to leverage the full extent of space research being carried out in our country. Since public awareness is what ultimately influences through policy the scope and quantity of funding available for our space science endeavors, orchestrated efforts in that direction will greatly improve our collective space exploration output, as has been proven in the case of other space agencies such as NASA and ESA.

Based on my experience as a globally published space exploration writer[1], who regularly covers worldwide lunar exploration updates[2], Indian space activities[3] as well as planetary exploration[4], I wish to demonstrate how various international space institutes & organizations integrate science communications into their operations, and how they distinctly benefit from it. Moreover, I will also discuss several established mechanisms by which our country's individual scientists can formally, responsibly help writers & journalists broaden the reach of their own work and field at large, especially on the global arena.

References: [1] Jatan's Space writings: https://blog.jatan.space/about

[2] Moon Monday archive: https://blog.jatan.space/s/moon-monday/archive

[3] Indian Space Progress: https://blog.jatan.space/indian-space

[4] Space exploration & planetary science articles: https://blog.jatan.space/s/articles/archive

Exploration of the Microbial Community and Physicochemical Characteristics of a hypersaline lake and its Implications for Astrobiological Exploration on Mars

Deepali Singh[1,2]*, Priyadarshni Singh[1], Nidhi Roy[1], Saumitra Mukherjee[1],

[1]School of Environmental Sciences, Jawaharlal Nehru University, New Delhi, India

[2]Physical Research Laboratory, Ahmedabad, Gujarat, India

*E-mail: deeps301090@gmail.com

Sambhar Lake is a hypersaline playa that has undergone several cycles of desiccation and re-filling, sharing its climate-controlled history with that of several paleolakes on Mars which makes it a desirable location to study extremophiles and their adaptation to changing environmental variables. This study was carried out within Sambhar Lake to identify the major microbial communities present within saline settings and consequently determine the physicochemical factors that play a significant role in shaping the community. We analyzed four different types of samples from the area including water samples from the lake and a salt pan nearby, a sediment, and a salt sample. Biological characterization of the samples showed that *Archaea* dominate the community composition in most samples closely followed by *Proteobacteria*, *Actinobacteria*, and *Firmicutes*. Despite the sampling sites being in proximity to each other, they shared only seven common genera. The sediment sample had maximum species richness while the lake water had maximum species evenness. The taxonomic composition of the lake differed significantly from the samples collected from the salt pan indicating that geochemistry plays a significant role in shaping the microbial community. To explore this idea further, we collected physicochemical and taxonomic data from other saline lakes around the world and carried out correlation analysis and Canonical Correspondence Analysis. Chloride ions, elevation, depth, sodium ions, alkalinity, and salinity were identified as the major factors that influenced the microbial community composition in saline settings. These variables can be explored further for in-situ or simulation studies while designing payloads for future exploratory missions and considering possibilities of habitability on Mars.

Keywords: Mars, terrestrial analog, astrobiology, biosignatures, saline lakes

The Effect of Ions and Electric Field in the Nucleation Process of Clouds

M. Chandra[1] and N Singh[2]

[1]Poornima Institute of Engineering & Technology, Jaipur

[2] CSJM, University Kanpur
mksh.rpt@gmail.com

Abstract

It has been found that for ion induced nucleation at a given supersaturation, the Gibb's free energy of formation of a critical water nucleus, its radius, and also the number of water molecules in it are comparatively smaller than those in a very classical nucleation case. As a result, equilibrium concentration and, therefore, the rate of nucleation are found to increase. The ion induced nucleation has been found to be simpler at low supersaturations (even Sv,w <1) and the effect decreases for larger nuclei. It's been shown that in ion induced nucleation, even the smaller nuclei (10^{-8} cm) are stable at Sv,w <1, while in homogeneous cases they cannot exit. Except for larger radii (10^{-7} cm), where ions have no effect, the supersaturation required for a given small radius is far less in ion-induced nucleation than in the homogeneous case. It is also been found that the physical change of vapour is more favoured by negative ions than that for positive ions. The speculation of drop growth within the presence of an electrical field has been applied to the nucleation process in vapour condensation and ice glaciations. The comfort time is found to vary inversely with the electrical field for a given size of the nucleus. Also, the critical nucleus of a given radius is made at a lower supersaturation than in force field free nucleation. The speed of nucleation within the presence of an electrical field is found to extend by over 100 times at electric fields near breakdown for dry and varies linearly with the electrical field. The effect is more pronounced in heterogeneous nucleation as compared to a homogeneous one.

Keywords: Supersaturations, Nucleation, glaciation, electric field

References:

1. Sapkota, B.K., and Varshneya, N.C.: 'On the global atmospheric electrical circuit', J. Atmos. Terr. Phys. 52, 1–20, 1990.
2. Santos, L.P.; da Silva, D.S.;Galembeck, A.; Galembeck, F. Electric Fields Enhance Ice Formation from Water Vapor by Decreasing the Nucleation Energy Barrier. Colloids Interfaces, 6, 13, 2022.

Exploring Mars, its analogues and future landing sites

Vijayan S[1], Kimi KB[1], Sharini KS[2], Tuhi S[3], Harish[4], Anil Chavan[1]

[1] Planetary Sciences Division, Physical Research Laboratory, Ahmedabad, India.

[2]College of Engineering Guindy, Anna University, Chennai, India

[3] Department of Geosciences, Auburn University, Auburn, AL, USA

[4]Space and Planetary Science Center and Department of Earth Sciences, Khalifa University,

vijayan@prl.res.in

Mars host features like valleys, channels, and fan/delta deposits which provide evidence for its past water-rich history compared to present-day dry and cold conditions. Mars is also known for its diverse records of geological activities that resemble the Earth. The preserved water modified landforms and their presence on the dichotomy boundary and elsewhere will provide some crucial clues to the source for water and their rapid activities [1]. Impact craters with inlet channels and severely breached rims, withhold vital geological evidence for the fluvial activities either by flood carved or witnessed outburst flood through subsurface or rapid snow melt. Abundant geologic evidence in the form of massive fan/delta deposits, fluvial channels/drainage networks and numerous preserved hydrated mineral deposits indicate that at some point in Mars history its climate was comparable to the current terrestrial conditions. Such water altered landforms are potential regions of interest to compare them to their terrestrial counterpart for understanding any potential bio signature presence. In addition, the region with hydrous minerals exposures, adjacent to fan/delta deposits, magmatic hydrothermal region with channels on volcanic slopes are widespread on Mars and identifying such diverse landforms region on both the planetary bodies will provide an insight into understanding the biosignature sites on Mars. The lacustrine environment of Mars and some potential high altitude lakes present in India comparable to such environment will act as a potential analogue. Moreover, the different comparable geologically evolved landform and their modification are widespread in the Indian subcontinent like fan/delta deposits, fluvial channels, hot springs, brines, dunes and volcanic landforms. Exploring such analogues within the Indian subcontinent will also help to understand the past environment of Mars and such site can be potential targets for future Indian and international missions to decide the landing site on Mars.

References: [1] Carr and Head (2010), EPSL 294 3-4),185-203.

Development of SiPM based scintillator readout technique for future planetary missions

Deepak Kumar Painkra[1], Sushil Kumar[1], Nishant Singh[1], Dr. M Shanmugam[1], Arpit Patel[1], Tinkal Ladiya[1], Shiv K Goyal[1]

[1]Physical Research Laboratory, Ahmedabad (deepakp@prl.res.in)

Silicon Photomultipliers (SiPM) have recently emerged as a promising alternative to traditional photomultiplier tubes (PMTs) for various space applications due to their high sensitivity, low-voltage operation, insensitivity to magnetic fields, mechanical robustness, and excellent uniformity of response.

In this study, we have characterize the On-semiconductor made Micro C- series SiPM (Area: 3mmx3mm , Microcell size: 35 µm) over a wide temperature range (-30^{o}C to 70^{o}C) to measure V-I characteristics and the variation in breakdown voltage at different operating temperatures. The characterization is crucial to asses the temperature stability of SiPM, which is essential for space application. Furthermore, we have developed the LM6172 IC based front end electronics (FEE) for spectroscopic measurements using Thallium doped Caesium Iodide (CsI(Tl)) and plastic (BC-408) scintillator. FEE consists of a Charge sensitive pre-amplifier (CSPA) and a shaper circuit to enhance the signal to noise ratio (SNR) of the detector signal. With this readout method, we have achieved the energy resolution of 7% FWHM and 12% FWHM with CsI(Tl) and BC-408 respectively, using Am -241, 5.49MeV Alpha source. The SiPM based scintillator readout technique offer advantages such as high detection efficiency, low power consumption, and compact size. These techniques also have the potential to improve the performance of future planetary missions where size, weight, and power consumption are critical factors.

Constraining physical properties of lunar impact melts using dual-wavelength radar and meter-scale topography data

Sriram Saran Bhiravarasu*, Rohit Nagori, Tathagata Chakraborty, Dharmendra Pandey, Anup Das, and Deepak Putrevu

Space Applications Centre (ISRO), Ahmedabad – 380015

*Corresponding Author E-mail: sriram.saran@sac.isro.gov.in

Lunar impact melt deposits have unique physical properties compared to other lunar terrain. They have among the highest observed S-band (12.6 cm wavelength) radar returns on the surface of the Moon (e.g. [1, 2]), including the circular polarization ratio (CPR) values near or exceeding one (e.g., [3]). When observed in radar and high-resolution optical imagery, the ejecta blankets around fresh craters also appear 'rough' at these scales; however, the lunar impact melt flows appear smooth at the meter scale [3, 4]. In many cases, it has been observed that the morphologies of impact melt flows appear very similar to those of terrestrial lava flows, although they also exhibit distinct features such as erosional channels [5]. However, the surface characteristics of lunar impact melt flows – rough at decimeter scales and smooth at meter scales – are unlike any terrestrial lava flows yet studied [6]. Questions still remain to explain this dichotomy: Is this phenomenon due to (a) differences in post-emplacement modification processes? Or (b) fundamental differences in the surface texture of the melt flows?

In this work, we extend the results obtained by [6], by comparing the meter-scale roughness (RMS slope 'C_s' and Hurst exponent 'H' parameters, from LROC NAC Digital Terrain Models) to the decimeter-scale roughness of three lunar impact flow features obtained from L-band (25 cm wavelength) DFSAR and S-band Mini-RF (LRO) radar observations. These results obtained for melt flows associated with King, Tycho, and Korolov X craters are further compared to the meter-scale roughness of terrestrial lava flows from topographic profiles acquired in the field and the decimeter-scale roughness of terrestrial lava flows (Craters of the Moon Monument – COTM, Kilauea and Mauna Ulu in Hawaii, Holuhraun in Iceland) derived from L-band UAVSAR and AIRSAR radar data sets as presented in [6], [7].

Preliminary results indicate that the L- and S-band CPR values for the three lunar impact melt flows are comparable (individually), although the radar data was observed at much different incident angles (26° of DFSAR vs. 49° of Mini-RF). At the centimeter to decimeter scale, all the three lunar impact melts look most like blocky terrestrial lava flows, but at the meter scale, they appear most like smooth Hawaiian pāhoehoe (Mauna Ulu, in Figure 1). Only the COTM blocky lava approaches the CPR values of the impact melts. Moreover, the moderate to high CPR values for the three melt flow regions analyzed here indicate that the radar may be sensing the disrupted surface of the melt flows (wavelength-sized blocks), broken apart by impact gardening and covered with a thin regolith. However, their different meter-scale roughness ($H>0.8$, $C_s< 4°$) may also indicate that the lunar impact melt flows have a different surface texture owing to the different surface cooling conditions compared to the terrestrial lava flows (e.g. [6]). Additional characterization of all the features analyzed in this work using full polarimetric radar parameters is in progress, which might provide further constraints on their physical properties.

References: [1] Campbell B. A. et al. (2010) Icarus 208, 565–573. [2] Neish C. D. et al. (2014) Icarus 239, 105–117. [3] Campbell B. A. (2012) JGR 117, E06008. [4] Ghent, R. R. et al. (2010) Icarus 209, 818–835. [5] Denevi B. W. et al. (2012) Icarus 219, 665–675. [6] Neish C. D. et al.

(2017) Icarus 281, 73–89. [7] Campbell B. A. (2002) Cambridge University Press, Cambridge, U.K.

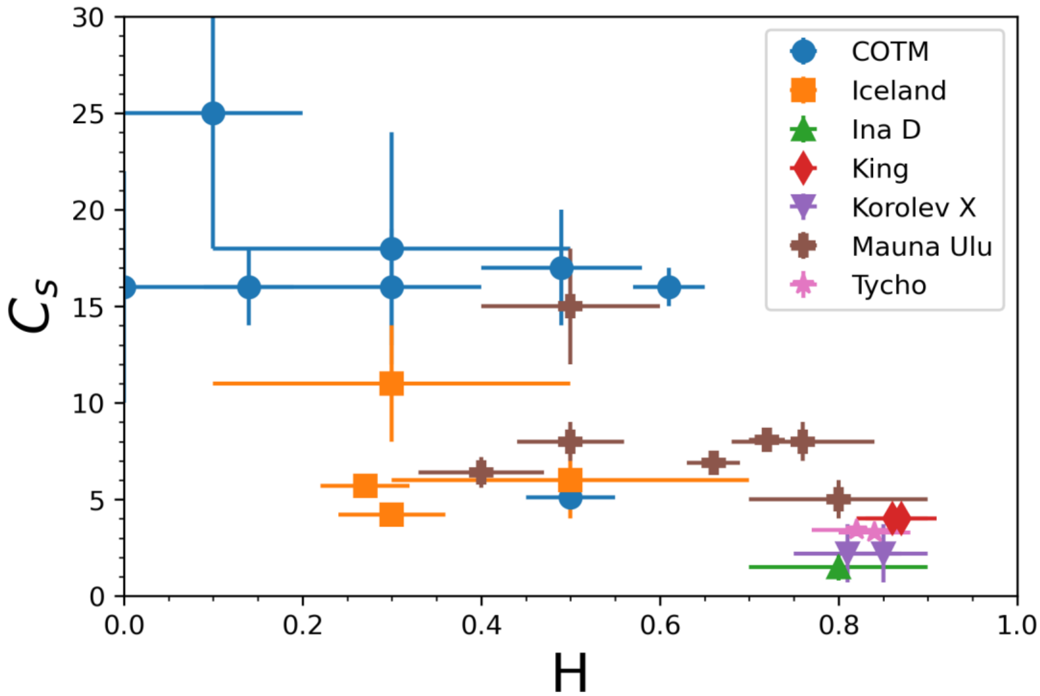

Figure 1 Root mean square (RMS) slope C_s (in degrees) at 1 m reference scale versus Hurst exponent (H) for three lunar impact melt flows (King, Tycho, Korolov X) over 2 m to 12 m range of step size. For comparison, the additional data presented here are from Hawaiian lavas (Kīleaua), reported in [7]; the values for Hawaiian lavas studied in Mauna Ulu, transitional lava flows at COTM, the new lava flow at Holuhraun in Iceland, a lava flow at Ina D (irregular mare patch feature), and the impact melt flow at Korolev X are reported in [6]. The values of H and RMS slope are determined from linear fits to the variogram and the 1 sigma standard deviation of the fit is given as error for each point.

Glacial Lakes in Northwestern Himalayas: Potential analogues to understand Martian history

Thahira U[1*], Tuhi S[2], Kimi KB[3]., Sharini KS[4], Harish[5], Anil Chavan[3], Vijayan S[3]

[1] Dept. of Remote sensing, Bharathidasan University, Trichy, India.

[2] Department of Geosciences, Auburn University, Auburn, AL, USA

[3] Planetary Sciences Division, Physical Research Laboratory, Ahmedabad, India.

[4]College of Engineering, Guindy, Anna University, Chennai, India

[5]Space and Planetary Science Center and Department of Earth Sciences, Khalifa University,

*Corresponding Author E-mail: thahira04032002@gmail.com vijayan@prl.res.in

Glacial lakes form in the depressions or voids created by the melting of glaciers. The Northwestern Himalayan region consists of glacial lakes of various types: including supraglacial, subglacial, proglacial, periglacial, cirque, moraine-dammed, and ice-dammed lakes. Cirques are bowl-shaped depressions formed due to glacial erosion that can store water and form cirque lakes (Tarn) [1]. Such cirques are also possible on Mars, which will us an insight into the Mars glacial activity. Global climatic conditions and stability are key factors for surface ice erosion and expression on terrestrial planets such as Mars and Earth. Our study focuses on comparing the analogous glacier environments in the Northwestern Himalayan Stretch to past glacial environments on Mars. The spatio-temporal analysis of glacial lakes of the Northwestern Himalayas in Chamoli and Pithoragarh districts of Uttarakhand using remote sensing and GIS techniques was carried out using Landsat 5, 7, and 8 imagery from1994, 2000, 2010 and 2020[2]. Upon regional analysis and applying the Normalized Difference Water Index(NDWI), we chose three glacial lakes that showed significant spatio-temporal changes in the study area. The three lakes that were chosen show an increase in lake area instead of the typical shrinkage of lake area. These lakes area variation from 1994 to 2020 are as follows, GLake1-1, 0.0707 to 0.1808 sq. km, GLake2- 0.116 to 0.242 sq. km, GLlake3-0.086 to 0.239 sq. km. These three glacial lakes have nearly doubled in their spatial extent. GLake1 have shown tremendous growth in the interim period from 2010 to 2020, which is interpreted to be due to the rapid melting rate of surrounding glaciers. The geomorphology of this area with high relief landforms and distinct deformation patterns support further studies for effective comparison with the Martian glacial environment and will help decipher their past variation in snow melt and runoff. Despite the presence of a lacustrine environment and glacial lakes on the surface of the Mars in the past, evidence for several glacial related phenomena is missing or hindered due to their post modification. The identification of cirques on the Martian counterpart is probably one open area of research, where the post modification of the glacial surface and significant dust cover hindering their presence. The dichotomy boundary at mid-latitudes is a potential region to anticipate cirques on Mars, which acts as a paleo environmental indicator for past glacial activity.

References: [1] Govindha Raj K, Babu & vinod Kumar, Kumranchat. (2016). Inventory of Glacial Lakes and its Evolution in Uttarakhand Himalaya Using Time Series Satellite Data. Journal of the Indian Society of Remote Sensing. 44. 959-976. 10.1007/s12524-016-0560-y.

[2] Basak et al (2022). "Spatio-Temporal Analysis of the Glacial Lakes of the Western Himalayas in Chamoli and Pithoragarh Districts of Uttarakhand Using Remote Sensing and GIS." In Artificial Intelligence for Societal Development and Global Well-Being, pp. 222-240. IGI Global, 2022.

Distinct Variations in Surface Temperatures of Diverse Sites on the Moon

G Ambily[1*], K Durga Prasad[2]

[1,2]Physical Research Laboratory, Ahmedabad, India
*Corresponding Author E-mail: ambilyg@prl.res.in

Lunar surface temperatures show significant variations as a function of its latitude, local relief and thermophysical properties [1]. Daytime temperature are determined by the incoming solar flux and illumination angle, while nighttime temperatures are dictated by mainly the thermophysical properties of the surface [2]. Even though there is abundant data on global regolith temperatures, local and regional scale variations are still less explored, unless for some certain landing sites [3,4]. Since the temperatures can vary considerably due to the topography of a site, understanding the thermal environment on local scale (within few kilometers) is crucial for future operations and resource prospecting. We have processed LOLA & Diviner datasets onboard LRO, of a set of geologically distinct sites and diurnal temperature variations of the lunar surface were analyzed.

The sites are selected in such a way that a pair of sites represent same latitude, but of diverse geology and local relief. They are distributed across latitudes ranging from $20^0 – 90^0$ and are either geologically, morphologically or thermophysically distinct. The sites selected are Apollo-17 Landing site [6], Aristarchus Crater [4], Ryder Crater, Von Karman Crater, CB-Thorium Anomaly hotspot [7], Dugan J Crater, Malapert E Mons [8] and Cabeus Crater [8]. The topography is obtained from LOLA DEM files and real-time brightness temperatures observed by Diviner for an interval of 3.00 hours local time, are taken from NASA – PDS [5]. The maximum and minimum temperatures at each local time are identified and plotted along with the actual temperature maps overlaid on topography files.

A significant temperature variation is observed across all sites on a diurnal basis, which can be attributed to its topography. It is also observed that sites at the same latitudes, situated few kilometers apart, show large difference in temperature at same local time, due to the topography. Therefore, it is inferred that understanding the topological effects on temperatures is essential for any site-specific studies and operations in future. The detailed results will be presented and discussed.

References: [1] Vasavada, Ashwin R., et al. Journal of Geophysical Research: Planets 117.E12 (2012). [2] K. Durga Prasad et al., Earth and Space Science (2022): 9, e2021EA001968. [3] Williams, Jean-Pierre, et al. Earth and Space Science 9(2) (2022). [4] K E Bauch et al., 2011(LPSC). [5]https://pds-geosciences.wustl.edu/missions/lro/ [6] Apollo 17 Preliminary Science Report Robert A. Parker et al., 1973. [7] Lawrence, D. J., Geophys. Res. Lett., 34, L03201, doi:10.1029/2006GL028530. [8] Myriam Lemelin et al., 2014.

Martian erosional valley formation - Interpretation based on drainage density analysis

Dibyendu Ghosh[1]*, Alok Porwal[1], Guneshwar Thangjam[2], Malcolm Aranha[1,3]
[1]Indian Institute of Technology Bombay, Mumbai- 400076, India
[2]School of Earth and Planetary Science, NISER, HBNI, Bhubaneswar-752050, India
[3]Oulu Mining School, University of Oulu, Finland
*Corresponding Author E-mail: ghosh.dibyendu@iitb.ac.in

Studying the Martian drainage density is crucial to understanding the red planet's erosional history and surface processes [1]. Drainage density, defined as the total length of all channels divided by the total area of a given basin [2], gives an idea about the frequency of the occurrence of the stream on a land surface; therefore, it represents the relationship between the erosive force and ground resistance [1]. Since Mariner 9 discovered the valley network on Mars, understanding the erosive agents that form these valley networks has become a central research theme. Considering drainage density is highly dependent on many factors like slope, permeability, and rainfall, it is an important parameter for understanding the past climate and the agents that created the Martian valleys. Based on available datasets, previous researchers [3-5] used various methodologies to identify the catchment area and estimate the drainage density. Results indicate a higher drainage density during Noachian than Hesperian and Amazonian times. Valleys around volcanoes also have the highest drainage density.

This study utilized high-resolution global-scale imagery and the DEM dataset (CTX and MOLA-HRSC blended DEM). The drainage densities have been studied in conjunction with other morphometric parameters to comprehend the formation of valley networks in the Thaumasia highland and surrounding regions. A combined manual and automated approach has been used to delineate the valleys and the catchment basins, in order to estimate drainage densities. The geological map for the Thaumasia region [6] was used to mark the ageboundaries and determine the age of the valley networks. The highest drainage density was observed in the geologic units belonging to Noachian (unit Nfc), and the Noachian-Hesperiantransitional period (unit HNpld and unit HNfc). Valleys in the Nfc unit are located on the flanksof elevated mountain-shaped features and display a parallel drainage pattern along with relatively higher drainage density. The drainage patterns in the valleys of HNpld and HNfc units indicate topographic and structural control. Besides higher drainage density, sinuosity isalso observed in the valleys of HNpld, and valleys tend to widen as they approach their lowerreaches. Despite all these features indicating valley formation under a fluvial regime, geomorphological features associated with ice, such as concentric crater fill and alcove heads,located around the valley heads and surrounding areas, suggest that both fluvial and ice- dominated erosional regime may have contributed to valley formation.

References:

[1] Huggett, R. J. Routledge fundamentals of physical geography series. [2] Horton, R. E. (1945). Geol. Soc. Am. Bull., 56(3), 275-370 [3] Carr, M. H., & Chuang, F. C. (1997). JGR: Planets, 102(E4), 9145-9152. [4] Luo, W., & Stepinski, T. F. (2006). Geophys. Res. Lett., 33(18). [5] Hoke, M. R., & Hynek, B. M. (2009). J. Geophys. Res. Planets, 114(E8). [6] Dohm, J. M., et al. (2001). ASSEMBLAGE, 2(5), 16.

Probing Late Irradiation Scenario Using ^{36}Cl-^{36}S Isotope Systematics

Advait Unnithan*, Kuljeet Kaur Marhas (Times New Roman, font size 12pt)
Physical Research Laboratory, Ahmedabad, Gujarat, India 380009.
*advait@prl.res.in

Isotopic studies of meteorites exhumed excesses in specific isotope(s) of element(s), which were demonstrated to have originated from the decay of radionuclide(s) [1]. The Genesis of these parental short-lived now-extinct radionuclides (SLNs), having half-life in the range of a few days to millions of years, has been a subject of research investigation for all these six decades. Several astronomical, observational, theoretical and isotopic studies of meteorites suggest that our Sun, during its infancy (4.56 Ga years ago), was very active, resulting in several episodes of intense flaring with copious production of enhanced solar energeticparticles and X- and UV rays. These solar energetic particles (SEPs), on interaction with ambient gas and dust in the early Solar system, can produce SLNs such as ^{7}Be ($t_{1/2}$=53 days), ^{36Cl} ($t_{1/2}$=0.3Ma), ^{26Al} ($t_{1/2}$=0.72Ma), ^{10Be} ($t_{1/2}$=1.38Ma) etc. [2, 3]. These isotopes generated in the late stage (>5 Ma after the birth) irradiation events can get incorporated in the early solar system solids forming larger bodies, asteroids, planetesimals etc. This late irradiation event is hypothesised to make a small but significant contribution to a few of these SLNs. Calcium-Aluminium rich Inclusions (CAIs), being one the first forming solids in the Solar system, are important suites of objects to understand the earliest history of solar system events and processes. Sodalite ($Na_8Al_6Si_6O_{24}Cl_2$) and Wadalite ($Ca_6Al_5Si_2O_{16}Cl_3$), chlorine (Cl) bearing metasomatically generated secondary minerals found in some CAIs have been studied for traces of SLN ^{36}Cl [4]. These studies have found a range of excesses in the measured ^{36}S/^{32}S corresponding to (^{36}Cl/^{35}Cl) = (3.7 ± 0.8) ×10^{-6} for sodalite and (1.81 ± 0.13) ×10^{-5} for wadalite [5, 6, 7]. The observed ^{36}Cl/^{35}Cl in a few studied CAIs do not correlate linearly with their respective ^{26}Al/^{27}Al abundances. The short half-life ^{36}Cl coupled with a later formation of the phases evince production of ^{36}Cl during an event termed the "late irradiation event". Previous studies suggest ^{36}Cl originated from different reservoirs. An extensive petrographic, mineralogic, and isotopic analysis of a wide range of altered CAIs and their secondary minerals is currently being pursued to constrain the genesis, chronology, duration, and cosmolocation of these events forming the CAIs.

References:

[1] Goswami J. N., Marhas K. K., Chaussidon M., Gounelle M. and Meyer B. S. (2005), *Chondrites and the Protoplanetary Disk, vol. 341 pp. 485–527* [2] Marhas K. K., Goswami J. N. and Davis A. M. (2002), *Science 298, 2182–2185* [3] Mishra, R.K., Marhas, K.K. (2019) *Nature Astronomy* ***3****, 498–505* [4] Krot, A.N., Petaev, M.I. & Nagashima, K. (2021) *Prog Earth Planet Sci* ***8****, 61* [5] Hsu, W. B., Guan, Y. B., Leshin, L. A., Ushikubo, T. & Wasserburg, G. J. (2006) *Astrophys. J.* ***640****, 525–529* [6] Jacobsen B, Matzel J, Hutcheon ID, Krot AN, Nagashima K, Ishii HA, Ramon E, Meyer BS, Davis AM, Ciesla FJ, Yin Q-Z (2011) *Astrophys. J. Lett.* ***731****, 28–33* [7] Lin Y, Guan Y, Leshin LA, Ouyang Z, Wang D. (2005) *ProcNatl Acad Sci U S A. Feb 1;102(5):1306-11*

V_0 layer in the Venusian ionosphere: How the forcing from the lower atmosphere modulates it?

Keshav R Tripathi[1], R. K. Choudhary[1], and Ambili KM[1]

[1]Space Physics Laboratory, VSSC, Trivandrum, Kerala, India-695022
*Corresponding Author E-mail: (tripathikr95@gmail.com)

Venus was known to have the sporadic presence of enhanced electron density below the 120 km altitude [1]. Recent measurements using radio science (RS) payload onboard the Akatsuki orbiter has now shown them to occur across the entire Venusian ionosphere, irrespective of solar zenith angles, and geographical limitations. Such enhancements are now known as a new ionospheric layer, the V_0 layer [2]. Though the origin of this layer in the Venus ionosphere still remains unclear, it is found that the shape of the V_0 layer is not uniform and changes with time. This study attempts to figure out the potential source for the different shapes of the layer.

Akatsuki has an inclined elliptical orbit around Venus which limits the number of occultation events. To increase our statistics we have retrieved atmospheric parameters (electron density profiles of the ionosphere, neutral density, temperature, and pressure profiles of the lower neutral atmosphere) from the frequency residual observed by Venus Radio Science Experiment (VeRa) onboard Venus Express (VEX) orbiter too. Technical details of the instruments used in VeRa experiments are given elsewhere [3]. The phase change in radio signals due to the Venusian atmosphere (i.e. frequency residual) for most of the radio occultation (RO) experiments are available from (ftp://psa.esac.esa.int/pub/mirror/VENUS-EXPRESS/VRA).

Based on the available statistics, the effect of forcing from the lower atmosphere has been explored. We show that the Gravity waves (GW) play a crucial role in determining the shape of the V_0 layer. For the solar zenith angle (SZA) less than 40^o, when the average gravity wave potential energy (AGPE) is less than 4.7 Joule/kg, V_0 has a single well-defined peak. For SZA > 40^0, and AGPE > 4.7 Joule/kg, a mostly wave-like feature at the base of the V0 layer emerges. We surmise that though GW does not control the formation of a V_0 layer, they surely control its shape and altitude of occurrence.

References:

[1] Pätzold, M., Tellmann, S., Häusler, B., Bird, M.K., Tyler, G.L., Christou, A.A. and Withers, P., 2009. A sporadic layer in the Venus lower ionosphere of meteoric origin. *Geophysical research letters*, *36*(5).

[2] Tripathi, K.R., Choudhary, R.K., Ambili, K.M., Imamura, T. and Ando, H., 2022. Characteristic Features of V0 Layer in the Venus Ionosphere as Observed by the Akatsuki Orbiter: Evidence for Its Presence During the Local Noon and Post-Sunset Conditions. *Geophysical Research Letters*, *49*(7), p.e2022GL097824.

[3] Häusler, B., Pätzold, M., Tyler, G.L., Simpson, R.A., Bird, M.K., Dehant, V., Barriot, J.P., Eidel, W., Mattei, R., Remus, S. and Selle, J., 2006. Radio science investigations by VeRa onboard the Venus Express spacecraft. *Planetary and Space Science*, *54*(13-14), pp.1315-1335.

The Detection and Characterization of Transiting Exoplanets

Sanjay Baliwal[1,2,*]

[1]Physical Research Laboratory, Ahmedabad 380009, India

[2]Indian Institute of Technology, Gandhinagar 382355, India

[*]sanjaybaliwal@prl.res.in

Exoplanets are planets located outside our solar system. The first exoplanet was discovered in 1995 by Michel Mayor and Didier Queloz, around a Sun-like star named 51 Pegasi, which earned them the 2019 Nobel Prize in physics. Since then, the field of exoplanets has progressed significantly, with a large amount of research being conducted in this area. The detection and characterization of exoplanets provide an essential step towards the goal of discovering habitable planets and improving our understanding of the formation and evolution of planetary systems. Because of their star's bright glare, exoplanets are challenging to spot directly. Scientists have developed various indirect methods for detecting them, including the Transit and Radial Velocity (RV) techniques being the most successful.

Various space and ground-based transiting surveys such as Kepler, TESS, and SuperWASP make detecting these exoplanetary systems easy. But, about 40% to 50% of them are observed to be false positives. Radial velocity follow-up of these candidates are needed to rule out this scenario and find the nature of the transiting astrophysical body (exoplanet or brown-dwarf or an eclipsing binary system of low mass M-dwarf). In order to contribute to this field, PARAS and PARAS-2 high-resolution spectrographs have been designed for radial velocity follow up observations in PRL, which will target Jupiters to super-earth type exoplanets.

In the talk, I will briefly overview exoplanets, their detection methods, and how the PARAS-2 spectrograph will contribute to the discovery of exoplanets.

Geological investigation of scarps in the vicinity of the primary landing site of the Chandrayaan-3 mission

Rishitosh K. Sinha[1*], Alka Rani[1], Trishit Ruj[2], Anil Bhardwaj[1]

[1] Physical Research Laboratory, Ahmedabad 380009, Gujarat, India

[2] Institute of Space and Astronautical Science (ISAS), Japan Aerospace Exploration Agency (JAXA), 3-1-1 Yoshinodai, Sagamihara, Kanagawa 252–5210, Japan

*Corresponding Author E-mail: (rishitosh@prl.res.in)

Abstract: The proposed coordinate of primary landing site (PLS) of ISRO's Chandrayaan-3 lander-rover-based mission is 69.36° S, 32.34° E, located in between Manzinus and Boguslawsky craters in the southern high latitude of the Moon. We have found morphological evidence of scarps at two locations: (1) ~6 km in the west and (2) ~100 km in the southwest of the PLS. Since, scarps are geologically recent potential thrust fault-derived tectonic structures [1-3], of which a large number of them are seismically active recently [4-5]. Therefore, it is worth to investigate the morphology, topography, formation age, and associated seismic activity of the scarps in detail to gain new insights into their probable influence on the PLS of the Chandrayaan-3 mission. Moreover, this will help to understand the potential of the seismometer instrument for Lunar Seismic Activity (ILSA) onboard the Chandrayaan-3 lander in detecting seismicity within the PLS concerning the potential shallow moonquakes related to the movements along scarps [6].

Our investigation of the scarps reveals that the scarp located at ~6 km in the west of PLS does not have the morphologic and topographic characteristics of typical lobate scarps, implying that it is a non-fault related scarp flanking the southwest edge of an isolated, degraded massif. The scarp located at ~100 km in the southwest of PLS is a cluster of typical lobate scarps. At the conference, a more detailed presentation of the findings related to the estimation of moment magnitude associated with the scarps and the potential formation period of the scarps will be presented and discussed. Furthermore, we will discuss our inferences about the safety of the PLS from any potential seismic hazards and examine the potential of ILSA in characterizing the spatiotemporal patterns of potential shallow moonquakes occurring currently at a focal depth of <1 km around the PLS.

References: [1] Binder, A.B. (1982) *The Moon and the Planets, 26(2)*, 117-133. [2] Watters, T.R. et al. (2015) *Geology, 43(10),* 851-854. [3] van der Bogert, C.H. et al. (2018) *Icarus, 306*, 225-242. [4] Nakamura, Y. et al. (1979) *LPSC*, 2299-2309. [5] Watters, T.R. et al. (2019) *Nat. Geosci., 12(6)*, 411-417. [6] John, J. et al. (2020) *Current Science, 118(3).*

Venus Solar Soft x-ray Spectrometer (VS^3) on board Venus OrbiterMission

M. Shanmugam, Varun Sheel, Arpit Patel, Hitesh kumar Adalaja, Nishant Singh, Tinkal Ladiya, S. V. Vadawale, Bhuwan Joshi, N. P. S. Mithun and A. Bhardwaj

In the Venus daytime ionosphere, V1 is the secondary layer produced by the solar soft X-rays is typically situated at around 125 km. It is poorly understood, as electron densities at this altitude are strongly influenced by the intensity of ionizing solar soft X-rays and hence by the solar cycle. In the absence of their measurements, theoretical estimates of the soft x-ray flux are considered in ionospheric models. To understand the effect of solar flares on the V1 peak and its variation with different solar flux conditions, it is proposed to have continuous measurements of solar X-ray spectrum in the energy range 0.5 –15 keV. In this direction, Venus Solar Soft x-ray Spectrometer (VS3) has been planned for the upcoming Indian Venus Orbiter mission. This measurement will also be important for the independent solar studies such as evolution of non-thermal processes associated with the solar flares, elemental abundance in solar corona and the non-thermal component in the quite sub spectra. This also provides unique opportunity to carry out solar observation from different vantage points (Venus orbiter, Ch-2, Aditya-L1 etc.).

VS^3 uses Silicon Drift Detector (SDD), which has unique capability of providing high energy resolution at very high incident count rates expected from Solar X-rays. The developed instrument provides energy resolution of ~180 eV at 5.9 keV, when the SDD is cooled to -35^{o}C and for the pulse peaking time of 0.4 μs. The science aspects and the instrument design details of VS^{3}will be presented in the conference.

Understanding Tectonism in Smythii Basin on the Moon using Remote Sensing Data

Dimple Sharma*, Neha Panwar, Neeraj Srivastava
[1]Gujarat University, Navrangpura, 380009
[2]Physical Research Laboratory, Navrangpura, 380009
dimplesharma241097@gmail.com

Tectonic landforms on the Moon, such as grabens, lobate scarps and wrinkle ridges, act as windows to understand the tectonic regime of the Moon. The Moon has been in a continuous compressive state since 3.6 Ga [1,2]. Wrinkle ridges are complex tectonic landforms found exclusively within the mare regions, interpreted to be formed due to contractional tectonics. They can serve as one of the important structural features that can be utilized to understand basin-related tectonics owing to their occurrence within the mare-filled impact basins on the Moon. Smythii Basin (1.3°N,87.5°E) is a ~880 km, partially filled multi-ring basin located along the equator on the easternmost edge of the lunar nearside. Most wrinkle ridges within the basin are situated on the northeastern side, where the mare basalts are present inside the inner depression. The length (L) and maximum displacement (d_{max}) of wrinkle ridges were estimated from the topographic measurement. The length of the wrinkle ridge is directly proportional to the maximum displacement of the thrust fault, which can be represented by the relationship $d_{max}=\gamma L$, where γ is a constant determined by rock type and tectonic settings [3]. This relationship can be used to calculate the strain accumulated in the region associated with wrinkle ridge formation and may connect with basin characteristics [4]. This study intends to use the d_{max}-L ratio obtained through high-resolution Kaguya and LOLA-derived SLDEM2015 data to understand stress variation and structural formation to decipher the tectonic history of the basin. The longest running wrinkle ridge in the Smythii Basin is 85.20 km long having a d_{max} value 478.87 m. Preliminary investigation reveals that the γ-value for the Smythii Basin wrinkle ridges is $\sim 5.6 \times 10^{-2}$.

References:

[1]. Solomon, S. C., & Head, J. W. (1980). Reviews of Geophysics and Space Physics, 18, 107–141. [2] Watters T.H. et al. (2012), Nat. Geosci.,5,181-183. [3] Cowie, P. A. and Scholz, C. H. (1992). J. Struct. Geol., 14(10), 1149-1156. [4]. Li.B. et al. (2018) J. Struct. Geol., 109, 27-37.

Insights into the magmatic evolution of Mars from the geochemical studies ofMartian shergottites

V.M. Nair[1,2,*], Y. Srivastava[1,2], A. Rani[1] and A. Basu Sarbadhikari[1]

[1]Physical Research Laboratory, Ahmedabad 380009, India.
[2]Indian Institute of Technology Gandhinagar, Gujarat 382355, India.
*** E-mail:** varsha@prl.res.in

Significant insights into the chemical and mineralogical characteristics of the Martian surface have been gleaned by in-situ and remote analysis done by Landers, Rovers, and Orbiters over the past few decades. However, the instruments that are deployed by landers and rovers on the surface of Mars lack the precision and accuracy of analytical techniques used in laboratories on Earth and are unable to examine multiple physical or geochemical sample parameters that will shed light on the evolution of the planet. In the absence of a sample return mission, Martian meteorites serve as the sole source for in-depth laboratory investigations and give information on a variety of geological processes and the evolution of Mars.

The shergottites are the most abundant type of Martian meteorites. Using coupled variations in Incompatible Trace Elements, including bulk rock rare earth elements (REEs) [1,2] and radiogenic isotopic [3] compositions, shergottites are geochemically classified into different types, and these compositional changes are predominantly inherited from their mantle sources [4]. Shergottites can also be classified into different groups according to their texture, and different textures represent mineral formation and emplacement in the shallow subsurface or perhaps eruption at the surface, which gives an understanding of the igneous emplacement history of Martian magma. As a result, the study of Shergottite samples provides various insights into the Martian interior and the extent of its heterogeneity.

In this study, we will be discussing the textural and geochemical characteristics of different Shergottite samples using in-situ geochemical analytical methods. The petrology has been used to identify the magmatic processes and the igneous emplacement history of the meteorites.

References:[1] Basu Sarbadhikari, A. et al. (2009) GCA, *73*(7), 2190-2214. [2] Basu Sarbadhikari, A. et al. (2011) GCA, *75*(22), 6803-6820. [3] Day, J.M.D. et al. (2018) Nat. Commun., *9*(1), 1-8. [4] Udry, A. et al. (2020): e2020JE006523.

Thermodynamic and Optical properties of water clusters at various temperatures andpressures and implications for atmospheric chemistry.

Ranga Subramanian[1*]
[1]Dept. of Chemistry, Science Block IIT Patna

*ranga@iitp.ac.in

The atmospheric new particle formation (NPF) creates secondary aerosols from gaseous vapors that go through gas-to-particle (GTP) conversion. We have used water clusters to investigate the principles of intermolecular interactions, including the formation of hydrogen bonds and cluster structure, as well as phenomena like solvation and nucleation that are important to atmospheric transitions from the gas phase to clusters to aerosol particles. We will discuss water clusters of Methanol, Ethanol, and Formic acid [1, 2]. We have predicted optical and thermodynamic properties, which will be discussed in detail.

References:

1. Pal J., Patla A., and Subramanian R., (2021), Chemosphere, 272, 129846-129858.
2. Patla A., and Subramanian R., (2023), Phys. Chem. Chem. Phys., 2023, DoI: 10.1039/D2CP03908G

INSIGHTS TO LUNAR CRUSTAL DIVERSITY AND MAGMATIC HISTORYFROM LUNAR REGOLITH BRECCIA METEORITES

Y. Srivastava[1,2*], V.M. Nair[1,2], A. Rani[1] and A. Basu Sarbadhikari[1]

[1] Physical Research Laboratory, Ahmedabad 380009, India
[2] Indian Institute of Technology Gandhinagar, Gujarat 382355, India
* E-mail: yash@prl.res.in

The geological history of the Moon and its interaction with the dynamic solar system environment are recorded on its lunar surface. Through remote sensing missions, scientists have discovered compositional variations across the lunar surface, leading to the classification of three distinct and broad geologic terranes: the Procellarum KREEP Terrane (PKT), which was examined during the Apollo and Luna missions; the South Pole-Aitken basin (SPA), the largest impact basin of the Moon; and the Feldspathic Highlands Terrane (FHT) [1]. Lunar regolith breccia meteorites, which could have potentially originated from any part of the Moon, provide valuable insights into significant processes that have shaped the lunar surface, including meteoroid impacts and volcanism [2,3]. These meteorites offer a reflection of a range of lithologies and can serve as critical sources of information about the compositional diversity of the lunar crust, particularly in areas outside of the sampled PKT regions.

In this study, we discuss the petrology of mineral and lithic clasts among lunar regolith breccia meteorites and their possible genetic relationships with the known lithologies of the Moon. The results of the bulk major and trace element analyses indicate that these samples originated from areas beyond the PKT. The variety of clasts and their compositional variations highlights the diversity in the lunar crust. The basaltic clasts present in these samples provides additional constraints on the magmatic history of the lunar regions sampled by these meteorite breccias.

References: [1] Joliff, B.L. et al. (2000) JGR, 105(E2), 4197-4216. [2] Korotev, R.L. et al. (2003) GCA, 67, 4895-4923. [3] Day, J.M.D. et al. (2006) GCA, 70(24), 5957-5989.

A Theoretical Investigation on Hydrogen Abstraction Reactions of Sulfur CompoundsHSXOH and CH_3SXOH where X=C or S by OH Radical

Kanika Guleria[1], Ranga Subramanian[2*]

[1] Department of Chemistry, Indian Institute of Technology, Patna, Bihar, India, 801103
[2] Department of Chemistry, Indian Institute of Technology, Patna, Bihar, India, 801103
*ranga@iitp.ac.in

The mechanistic, thermochemical, and kinetic study of oxidation reactions of HSC(O)H, HSS(O)H, CH_3SC(O)H, and CH_3SS(O)H molecules by OH radicals is performed using high-level theoretical calculations. CH_3SC(O)H is formed in the atmosphere by the oxidation reaction of dimethyl sulfide [1]. Similarly, HSC(O)H, HSS(O)H, and CH_3SS(O)H are formed in the atmosphere by oxidation reactions of various sulfur compounds [2], [3]. Two isomers, cis and trans, are observed for both HSC(O)H and HSS(O)H molecules. Trans-HSC(O)H has also been found in the interstellar medium (ISM) [4]. The potential energy profiles for the titled reactions are constructed at the CCSD(T)/aug-cc-pVTZ//M06-2X/aug-cc-pVTZ level.

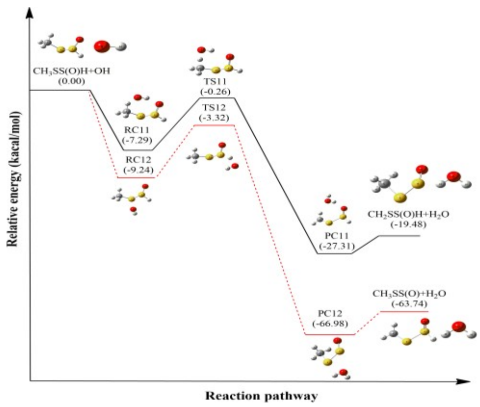

Figure 1: Potential energy diagram of the CH_3SS(O)H + OH reaction at CCSD(T)/aug-cc-pVTZ// M06-2X/aug-cc-pVTZ level of theory.

Reaction enthalpies and reaction Gibbs free energies are calculated employing M06-2X/aug-cc-pVTZ method. The temperature-dependent rate coefficients are calculated with the help of the dual-level direct dynamics method using canonical variational transition state theory and small-curvature tunneling in the temperature range of 210-350 K. CVT/SCT rate coefficients are then utilized for calculating overall rate coefficients and branching ratios. The atmospheric lifetimes of these four sulfur compounds are also calculated. The geochemical cycle of dimethyl sulfide may be extended by incorporating CH_3SC(O)H + OH reaction.

References:

[1] Hynes A. et al. (1986) *J. Phys. Chem., 90(17), 4148-4156.*
[2] Pillai S. and Bozzelli J. W. (2012) *J. Phys. Org. Chem. 25(6), 475-485.*
[3] Tang Y. Z. et al. (2008) *Theor. Chem. Acc., 121(3), 201-207.*
[4] García D. L. C. et al. (2022) *Astron. Astrophy., 658, A150.*

A Study of Venus Atmosphere from Radio Science Experiment OnboardAkatsuki

by

Tirtha Jyoti Kalita and Varun Sheel

Physical Research Laboratory, Ahmedabad, 380058, India

Abstract

The venus' clouds have been an area of interest for decades and were first studied by spectroscopy and polarisation in 1960's, later confirmed by successful Venera-12 measurements. Since then many techniques and instruments were developed for furtherdetailed studies of the clouds and atmosphere of Venus. The Radio Occultation(RO) experiment, estimates the amount of shift in frequency of the radio signal transmitted from a spacecraft through the atmosphere of a planet. Retrieval algorithms are then used to obtain profiles of the atmospheric parameters. We have analysed data obtained from the Radio Scienceexperiment onboard Venus Climate Orbiter(Akatsuki), received with a 32 m antenna at IndianDeep Space Network(IDSN), Bangalore, India that is recorded and digitised with desired sampling size. We predicted the theoretical doppler by using NASA's SPICE toolkit, capable of precisely measuring the ephemeris data for planetary bodies and spacecrafts.Then the difference between observed and predicted doppler, called the frequency residuals is calculated. The obtained frequency residuals, indicating bending of the radio ray path and consequent refractivity of the atmosphere is the input to the retrieval algorithm to get the ionospheric and atmospheric profiles. We report the doppler residuals and atmospheric parameters for 14th April, 2020. The loss in power of the transmitted signal traversing throughthe atmosphere will be studied for profiling the cloud constituents and more significantly, the sulphur species.

Volcanism in the Crisium Basin on the Moon: Insights from Remote Sensing Data

Ankita Yadav[1*], Neha Panwar[2], Neeraj Srivastava[2]

[1]Banasthali Vidyapith, Rajasthan- 304022
[2]Physical Research Laboratory, Ahmedabad- 380009

*ankita.sol123@gmail.com

The Crisium Basin (17.0 °N, 59.1 °E) is a ~1100 km wide Nectarian multi-ring basin on the eastern nearside of the Moon. The inner depression of the basin is filled with basalts ranging from Imbrian to Eratosthenian in age. Volcanism expanded from 3.45 to 2.52 Ga within the basin occurring in multiple eruptive phases, as inferred from the Luna 24 samples [1]. It has been observed that the TiO_2 wt.% varies from 6~10 wt.% in the east to <2 wt.% in the west within these basalts [2]. The basin consists of 4 rings delineated from the GRAIL data [3]. Several mare patches are present in the south-eastern part of the Crisium Basin along these rings. The study aims to delineate the compositional diversity within the basalts associated with the Crisium Basin using high-resolution hyperspectral data from Moon Mineralogy Mapper (M^3)- a payload on- board Chandrayaan-1 orbiter. The reflectance spectra of the basalts inside the inner depression and at the rings of the basin have been used to determine their mineralogy and observe the compositional variations between them. The derived information has been used to understand the various geological factors that govern volcanism within large impact basins on the Moon. The primary results show that these basalts are characterized as high- Ca pyroxene with the values of Band Center 1 varying from ~944 nm– 1008 nm and the Band Center 2 varying from ~ 1985 nm – 2233 nm.

References

[1] Fernandes, V.A., & Burgess, R. (2005) *Geochim. Cosmochim. Acta*., *69, 20, 4919–4934* *[2]* Lu, X. et al. (2021) *Remote Sensing, 13, 23, 4828* [3] Neumann et al. (2015) *Sci. Adv., 1, 9*

Switchbacks Observed by Parker Solar Probe

Dipali Vadher[1], Kamlesh Pathak[1]

[1]Sardar Vallabhbhai National Institute of Technology, surat-395007 (d21ph004@phy.svnit.ac.in)
*Corresponding Author E-mail: d21ph004@phy.svnit.ac.in

The Parker Solar Probe (PSP) mission launched in 2018 is the closest spacecraft to the Sun in history. One of the most striking observations made by Parker Solar Probe during its first solar encounter is the omnipresence of rapid polarity reversals in a magnetic field that is otherwise mostly radial. The S-shaped magnetic structure in the solar wind formed by the twisting of magnetic field lines is called a switchback, whose main characteristics are the reversal of the magnetic field and the significant increase in the solar wind radial velocity. I focus here on the radial component of magnetic field and solar wind velocity; their fluctuations appear to be correlated.

References:

[1] Fox, N. J, vol. 204, no. 1–4, pp. 7–48, 2016. doi:10.1007/s11214-015- 0211-6.

[2] Zank. et al(2020), The Astrophysical Journal, vol. 903, no. 1.

Paleorecord of Variation in Cosmic Ray Flux from Extraterrestrial Chromite Grains

[1*]Subhasmita Swain, [2]Ramakant Mahajan, [2]Dipak Kumar Panda, [1]Surya Snata Rout, [3]Birger Schmitz
[1]School of Earth & Planetary Sciences, NISER, HBNI, 752050-Odisha, India
[2]Planetary Science Division, Physical Research Laboratory, Navrangpura, 380009 Ahmedabad, India
[3]Astrogeobiology Laboratory, Lund University, Sweden
*subhasmita.swain@niser.ac.in

Introduction: Cosmic ray tracks are formed when high energy galactic cosmic rays of Fe group ions (Z = 20-30) collide with meteorites/micrometeorites in space. The density of tracks is directly proportional to the cosmic ray flux. The production of these tracks also varies with size of the meteorite, with depth, and with the exposure time [1]. To study the variation in cosmic ray flux in the past 500 Myrs we plan to study cosmic ray tracks in silicate inclusions within sediment dispersed extraterrestrial chrome-spinel (SEC) grains from fossil micrometeorites extracted from sedimentary rocks from various time windows [2]. Before using the precious SEC grains, in this study we are looking for differences in density of tracks within mineral grains and mineral inclusions in chromite grains from one solar gas-rich meteorite. Additionally, we are also studying mineral grains from three other gas-rich meteorites to refine our track finding methods, including mounting, polishing, and etching.

Samples & Methods: For the study we are taking four different gas rich meteorites: Kapoeta (Howardite), Weston (H4), Lohawat (Howardite), Ghubara (L4). From Kapoeta and Lohawat we selected pyroxene grains in the size range of approximately 100-150 μm followed by embedding and polishing. The polished samples were etched in a boiling solution of 6g NaOH and 4mL H_2O [3] for 20 minutes. We then observed the etched samples under an optical microscope for the presence of cosmic ray tracks.

Results & Discussions: We counted tracks that are greater than 5μm in size in Kapoeta and Lohawat. Keeping the etching time same for all, the density of tracks for Kapoeta is falling in the range of ~1-1.2 × 10^6 cm^{-2}, the previous works have shown a value of 3-5 × 10^6 cm^{-2} [4]. Lohawat has a density of ~ 2.6 × 10^5 to 3.8 × 10^4 cm^{-2}. Previous works have reported a number of 1.26-1.8 × 10^6 cm^{-2} in plagioclase grains [5].

Future work: We plan to etch more pyroxene grains from Kapoeta and Lohawat and olivine grains from Weston and Ghubara and also extract chromite grains from Ghubara through acid dissolution. Any chromite grains with silicate inclusions will then be etched to reveal tracks. Noble gas concentration within a batch of the chromite grains will also be measured to infer their exposure history.

References:[1] Price P.B. et al., (1967) JGR, 72(4), 1377-1388. [2] Terfelt, F. and Schmitz, B., (2021) PNAS, 118(24). [3] Lal et al., (1968) Earth Planet. Sci. Lett., 111-119. [4] Wilkening et al., (1971) Earth Planet. Sci. Lett., 10(3), 334-340. [5] Sisodia et al., (2001) Meteorit Planet Sci, 36(11), 1457-1466.

On the limits of meteoroid ion production rates on Mars

Jayesh Pabari*, Srirag Nambiar, Rashmi and Sonam Jitarwal

Physical Research Laboratory, Navrangpura, Ahmedabad-380009

* E-mail: jayesh@prl.res.in

Interplanetary dust particles enter a planetary atmosphere continuously [1]. These particles are ablated in the atmosphere, causing release of gas and metallic ions. At certain altitudes [2] from surface, a peak may be observed in the electron density profile [3] due to meteoroid ablation. It can further affect conductivity of the atmosphere. Any surviving particles can reach surface and add in the surface material. In this work, a meteoroid ablation model is presented for Mars and inputs parameters are discussed. Further, extreme conditions are considered for the dust flux as well as the temperature. Our results [4] provided limits of metallic ion production rate for Mars, which are compared with existing results.

References: [1] Vondrak, T. et al. (2008) *Atmos. Chem. Phys.*, 8, 7015-7031. [2] Crismani, M. M. J. et al., (2017) *Nat. Geosci.*, 10, 401-404. [3] Patzold, M. et al. (2005) *Science*, 310 (5749), 837-839. [4] Pabari, J. P. et al. (2023) *PSS, 226*, 105617.

Nature and Variability of the Electron Velocity Distribution Functions and the Nonequilibrium Boltzmann Entropy in the Solar Wind at the First Lagrangian Point(L1) During the Halo CME Event on 25 July 2004

Govind G. Nampoothiri[1, 2 *], R. Satheesh Thampi[1], Smitha V. Thampi[1,] Tarun K. Pant, Abhishek J.K.

[1]Space Physics Laboratory, Vikram Sarabhai Space Centre, Thiruvananthapuram 695022, India
[2]Department of Physics, Cochin University of Science and Technology, Cochin, Kerala 682022

*Corresponding Author E-mail: govindgn9@gmail.com

In this work, using the electrons velocity distribution functions (EVDFs) measurements at the Sun-Earth first Lagrangian point (L1) the phase space behavior of electrons during the passage of a halo Coronal Mass Ejection (CME) have been studied. This particular halo CME erupted on 25 July 2004 (Carrington rotation 2019) from the active region NOAA AR 10652 (N04W30) and the ICME reached at the L1 point approximately 31 hours after the eruption. Solar wind measurements from three Dimensional Plasma Instrument (3DP) on board WIND spacecraft and CME observations from Large Angle and Spectroscopic Coronagraph (LASCO) on board Solar and Heliospheric Observatory (SOHO) have been used for performing the present analysis. The electron velocity distributions of observed at the L1 point show peculiar features representing the passage of the ICME plasma and its magnetic cloud. The relative enhancements in the core and suprathermal electron population were quantified from the EVDF measurements. This study shows that, relative to the ambient solar wind condition, the suprathermal electron population enhanced more than the core electron population during the ICME passage. Following the CME sheath plasma, a non-thermal bi-directional electron streaming representing a closed magnetic field topology was observed. The Boltzmann entropy analysis of the event shows the CME magnetic cloud to be holding the largest non-equilibrium Boltzmann entropy among all the ICME sub-structural elements.

Aerosol Radiative Forcing using Radiative Transfer Model

Parth Patel[1], Kamlesh Pathak[2], Tejas Turakhia[2]

[1]Sardar Vallabhbhai National Institute of Technology, Surat-395007 (d21ph015@phy.svnit.ac.in)
[2]Sardar Vallabhbhai National Institute of Technology, Surat-395007 (knp@phy.svnit.ac.in)
[2]St. Xavier's College Ahmedabad, Ahmedabad-380009 (tejas.turakhia@sxca.edu.in)
*Corresponding Author E-mail: d21ph015@phy.svnit.ac.in

Abstract:

Aerosols are suspended particles in the air which has a significant impact on our climate and our health. Aerosols have an enormous effect on the Earth's radiation balance as they canabsorb and scatter incoming solar radiation. Radiative forcing happens when the amount of energy that enters the Earth's atmosphere differs from the amount of energy that leaves it. To calculate radiative forcing different Radiative Transfer Model is used. Here I have tried to calculate radiative flux using the SBDART model. Aerosol Optical Depth (AOD) values are used in the input file, which is a measure of the extinction of light due to aerosols. The radiativeflux is calculated with and without aerosols at the surface and Top of the Atmosphere (TOA) over Surat city (21.5 N, 72.5 E). The month of May for three consecutive years, 2020, 2021 and 2022, is chosen for study. We can observe the variation of flux year-wise at TOA and at the surface from the results.

References:

[1] A. Jayaraman, et al., (2006), Spatial variations in aerosol characteristics and regional radiative forcing over India: Measurements and modeling of 2004 road campaign experiment, *Atmospheric Environment*; Vol. 40, Issue 34, Pages 6504-6515, ISSN 1352-2310, https://doi.org/10.1016/j.atmosenv.2006.01.034

[2] John M. Wallace, Peter V. Hobbs, (2006), Atmospheric Science (Second Edition), *Academic Press*; Pages 113-152, ISBN 9780127329512, https://doi.org/10.1016/B978-0-12-732951-2.50009-0

[3] Ricchiazzi, P., Yang, S., Gautier, C., & Sowle, D. (1998). SBDART: A Research and Teaching Software Tool for Plane-Parallel Radiative Transfer in the Earth's Atmosphere, *Bulletin of the American Meteorological Society*; 79(10), 2101–2114. http://www.jstor.org/stable/26214876

Exposure Ages of Track-Rich Mineral Grains from Regolith Breccia: Implication for Space Weathering on Asteroid Surface

Swarna Prava Das[1*], Surya Snata Rout[1], Dipak Kumar Panda[2], Ramakant Mahajan[2], Guneshwar Thangjam[1] [1]School of Earth and Planetary Sciences, NISER, HBNI, Bhubaneswar-752050, India
[2]Planetary Science Division, Physical Research Laboratory, Navrangpura, Ahmedabad, India
***swarnaprava.das@niser.ac.in**

The process of space weathering (SW) is an active process on the surface of numerous airless solar system worlds due to the direct interaction of solar wind, cosmic rays, and micrometeorites with their surface [1,2]. It alters the physical, chemical, and optical properties of the surface with time [3]. SW on the surface of the Moon and on S-type asteroids (e.g. Itokawa) is fairly well understood due to the direct availability of samples. However, the rate and effect of SW are dependent on different factors: surface composition, location with respect to the Sun, and local environment (e.g. temperature). Due to the different combinations of all these parameters SW on various solar system bodies is poorly understood. Regolith breccia meteorites contain regolith components from the surface of their parent asteroid. This can be used to get direct insight into the interaction of solar wind particles and micrometeorite impact on the surface of asteroids. Solar energetic particles (SEP) can penetrate regolith materials by a few millimeters and in insulating materials, they leave a trail of ionization damage that accumulates over time and gives hints about the exposure age and evolution of regolith materials [4].

Recently, a TEM-based calibration for the SEP track production rate of $4.4 \pm 0.4\times10^4$ tracks $cm^{-2}yr^{-1}$ at 1 AU was calculated [5]. This can be potentially used to measure the exposure age of grains inside a regolith breccia meteorite. In this study, we plan to measure the exposure ages of individual pyroxene and olivine grains from three different meteorites. We are looking for grains that show signatures of direct exposure to the solar wind and solar energetic particles: i.e. with a strong gradient in track density from surface to center. We assume that the selected grains were not exposed to solar energetic particles while their parent body was traveling in space. Additionally, we are considering that the grains suffered a 2π irradiation on the surface of the regolith.

We are using grains extracted from different regolith breccia meteorites with signatures of high solar wind-implanted gases: Kapoeta (Howardite), Khor Temiki (Aubrite), Weston (H4), Fayetteville (H4) and Lohawat (Howardite). We mounted and polished individual grains using the method described previously by [6]. 100 grains of pyroxene with a size >50 µm were partially etched (5 minutes) in a boiling solution of NaOH (6 g NaOH: 4 g H_2O) in order to visualize tracks. We found 3 grains in Kapoeta and 2 grains in Weston with high track density. Detailed work is in progress in finding more grains with tracks followed by FIB-SEM and TEM studies.

Reference:

[1] Chapman, C. R., 2004 Earth Planet. Sci. 32, 539-567 [2] Hapke B., 2001 J. Geophys. Res. 106 (E5), 10,039-10,074. [3] Pieters, C. M et al., 1993 J. Geophys. Res. Planets 98, 20817-20824. [4] Rajan R. S 1974 Geochimica et Cosmochimica Acta. vol. 38. pp. 777 to 733. [5] Keller L.P et al ., 2021 Meteorit. Planet. Sci., 56, Nr 9, 1685–1707 [6] Lal D et al., 1968 Earth Planet. Sci. Lett. 5, 111

MG-SULFATE IN JEZERO CRATER, MARS

A. Rani[1,*], A. Basu Sarbadhikari[1], Y. Srivastava[1,2] and V.M. Nair[1,2]

[1] Physical Research Laboratory, Ahmedabad 380009, India

[2] Indian Institute of Technology Gandhinagar, Gujarat 382355, India

* E-mail: alka@prl.res.in

Jezero, a paleo-lacustrine lake, has been the subject of extensive photogeological and spectroscopic studies and was chosen as the landing site for the Mars 2020 mission. The crater, which consists of the Late Noachian/Early Hesperian watershed for the Jezero Crater open basin lake and associated delta deposits, lies at the compelling stratigraphic contact between the Noachian-aged Isidis basin and the Hesperian-aged Syrtis Major volcanic flows and the Noachian-aged Isidis Basin. It contains a variety of geological and mineralogical units of astrobiological interest, including two fan deposits, and km-scale deposits of carbonates, phyllosilicates, smectite serpentine, and potassium and ferric-iron sulfate [1-3]. Thus far, most spectral work has focused on constraining spectral signature to one spectrally dominant mineral, and associating geologic units to that one mineral. In reality, minerals usually occur in assemblages whose composition can provide important information on their genesis.

This present study includes sedimentary rocks in the Jezero Crater western delta with exceptionally well-preserved Mg- Sulfate exposed at the wall's cross-section. These detections, including previous secondary mineral exploration in this crater point to a multi-stage, multi-chemistry history of water in the Jezero crater and the surrounding region. This can provide new information for guiding the Mars-2020 Perseverance rover's landed exploration. Moreover, identifying rare phases, even in just a few pixels, enables the characterization of the mineral assemblages within a geologic unit, which are critical for identifying the thermodynamic conditions and fluid composition during interactions of rocks with liquid water.

References: [1] Ehlmann, B. L., (2009). JGR: Planets, 114(E2). [2] Dundar, M., et al., (2019); arXiv preprint arXiv:1909.02387. [3] Meslin, P.-Y., (2022); 53rd LPSC abstract (ID#2694).

Posidonius crater: A potential candidate to investigate the tectonic evolution on Moon.

K.B. Kimi[1,2], K.S. Sharini[3], Harish[4], S. Tuhi[5], Anil Chavan[1], S. Vijayan [1*]

[1]Planetary Sciences Division, Physical Research Laboratory, Ahmedabad, India, [2]Indian Institute of Technology, Gandhinagar, India, [3]College of Engineering, Guindy, Anna University, Chennai, India, [4]Space and Planetary Science Center and Department of Earth Sciences, Khalifa University, Abu Dhabi, UAE, [5]Auburn University, USA,

* *vijayansiva@gmail.com*

In the past, when extensional tectonics predominated during global expansion, magmatism—magma infilling, intrusion, and subsidence dominated [1]. This was followed by global cooling, which produced compressional tectonic features, including wrinkle ridges and lobate scarps [1]. Lunar impact craters containing the signatures from past and present geological activities provide us with an opportunity to understand the tectonic evolution of the Moon. The Posidonius crater, centred at 32ºN, 30ºE and located on the north-eastern rim of the Mare Serenitatis, is one such crater which archived the geological activities that occurred on the Moon since early history. In this study, we observed that the Posidonius crater floor has mare infilling [2] and fractured floor (FFC) [3]. It has compressional features─ wrinkle ridges and lobate scarps, extensional features─small-scale grabens and collapsed features such as pits. We observed that features such as wrinkle ridges, lobate scarps, and small-scale grabens are mainly distributed in the western part of the Posidonius craters and its region. They are of Copernican period, and orientations of wrinkle ridges and lobate scarps (N-NW) in our study area are similar to the orientations of the predicted faults due to a combination of recession stresses, diurnal tidal stresses at apogee, and global contraction [4]. Overall, we expect our study area has undergone intense modification since its formation to the present and has recorded one of the youngest activities of the Moon.

[1] Solomon, 1977, PEPI, 135-145. [2] Kimi et al., 2023, Icarus, vol. 390, 115298. [3] Jozwiak et al., 2012, Icarus, vol. 117. [4] Watters et al., 2015, vol. 43, 851-854

Compositional and morphological study of Zucchius crater

D. D. Patel[1], S. M. Patel[2*], P. M. Solanki[1] (Times New Roman, font size 12pt)

[1]M. G. Science Institute (Navrangpura, Ahmedabad, Gujarat, India, 380009)

[2]Khalifa University (Shakhbout Bin Sultan St, Hadbat Al Za'faranah, Zone 1, Abu Dhabi, U.A.E.)

*Corresponding Author E-mail: deepp213@gmail.com

Abstract: Zucchius (61.4°S, 50.3°W) is a prominent lunar impact crater located on the near side of the moon, near the southwestern limb with an average diameter of 64 kilometres [1]. Because of its location, the crater appears oblong-shaped due to foreshortening when viewed from the earth. It lies just to the south-southwest of the crater Segner, and northeast of the much larger walled plain Bailly. To the southeast is Bettinus, a formation only slightly largerthan Zucchius. To the northeast of Zucchius is the Schiller-Zucchius Basin, a Pre-Nectarian basin (peak ring basin). This basin has received the unofficial designation 'Schiller Annular Plain' among lunar observers. The crater rim is symmetrical and shows little significant wear from impacts. The inner wall is terraced, and there is a group of small central peaks that formsa curving arc around the middle of the floor. Due to its ray system. It is mapped as a part of the Copernican system [2]. Zucchius has a crater frequency identical to that of the Copernicus crater.

In this study, we use Chandrayaan-1's Moon Mineralogy Mapper (M^3) data for compositional analysis. The composition within the crater is dominated by Low (LCP) and High Calcium Pyroxenes (HCP). The central peak indicates the dominant composition of LCP while the walls of the crater are composed of HCP. The central peaks exhibit the noritic and gabbroic upper crustal composition while the walls exhibit the gabbroic composition of the lunar crust. A detailed morphological map of the crater features including the crater floor, central peak, wall terraces, impact melt ponds etc. was generated utilizing Narrow Angle Camera (NAC) images from the Lunar Reconnaissance Orbiter.

References: **[1]** Andersson, L. A., & Whitaker, E. A. (1982). NASA catalogue of lunar nomenclature (No. NAS 1.61: 1097), **[2]** Fortezzo, et al. (2020). Release of the Digital Unified Global Geologic Map of the Moon At 1:5,000,000- Scale. 51st LPSC, 2326-2020.

Subsurface study of the Tharsis graben system using SHARAD data

Rajiv R. Bharti[1, 4], Isaac B. Smith[2, 3], Shital H Shukla[4]

1. Physical Research Laboratory, Navrangpura, Ahmedabad, India 380009
2. York University, Toronto, Ontario, Canada, M3J 1P3
3. Planetary Science Institute, Lakewood, CO, USA 80401
4. Gujarat University, Ahmedabad, India 380009

*Corresponding Author E-mail: rajiv@prl.res.in

Abstract: Mars crust has an extensive grabens system that covers a region more than 8,000 km in diameter and nearly one-third of the planet's circumference. They are long-lived features, and many of them trend radially outward from the Tharsis volcanic shield. These thousands of grabens were discovered in the early 1970s and have been studied extensively with different hypotheses about their formation throughout the literature. These hypotheses include eithercaused by tectonic or magmatic processes or a combination of both processes, but no consensus has been reached so far. In this study, first time, we explore the subsurface of two narrow graben systems using SHARAD data to understand the formation process of the martian graben system. We found subsurface reflections at the rim of Mangala Fossa and at the floor of Labeatis Fossa. Even though they are separated by >5,000 km, all these reflections are associated with the Tharsis graben system. The loss tangent is in the range of 0.009 to 0.03, consistent with low to moderate density basalt. In this study, we found subsurface reflections are associated with the riftzone volcanism and inferred that the martian graben system formation involved tectonic and magmatic processes.

References:

[1] Banerdt, W.B., et al. (1992). Stress and tectonics on Mars. In: Kieffer, H.H., et al. (Eds.), Mars, Univ. Arizona Press, pp. 249–297.

[2] Campbell, B., Carter, L., Phillips, R., Plaut, J., Putzig, N., Safaeinili, A., Seu, R., Biccari, D., Egan, A., and Orosei, R. (2008). SHARAD radar sounding of the Vastitas BorealisFormation in Amazonis Planitia, J. Geophys. Res., 113, E12010, 10.1029/2008JE003177

[3] Carter, L. M., Campbell, B. A., Holt, J. W., Phillips, R. J., Putzig, N. E., Mattei, S., Seu, R., Okubo, C. H., and Egan, A. F. (2009). Dielectric properties of lava flows west of Ascraeus Mons, Mars. Geophys. Res. Lett., 36, L23204. 10.1029/2009GL041234.

[4] Morgan, G. A., Campbell, B. A., Carter, L. M., and Plaut, J. J. (2015), Evidence for the episodic erosion of the Medusae Fossae Formation preserved within the youngest volcanic province on Mars, Geophys. Res. Lett., 42, 7336– 7342, doi:10.1002/2015GL065017

[5] Seu, R., Biccari, D., Orosei, R., Lorenzoni, L. V., Phillips, R. J., Marinangeli, L., Picardi, G., Masdea, A., & Zampolini, E. (2004). SHARAD: The MRO 2005 Shallow radar. Planetary and Space Science, 52(1-3), 157– 166.

Geological Context of Elemental Maps from Chandrayaan-2 Large Area Soft X-ray Spectrometer (CLASS): New Results

Deepak Dhingra[1*], Shyama Narendranath[2] and Satyendra Kumar[1]

[1] Department of Earth Sciences, IIT Kanpur, Kanpur, UP 208016

[2] Space Astronomy Group, U R Rao Satellite Centre, ISRO, Bengaluru

*Corresponding Author E-mail: deepdpes@gmail.com, ddhingra@iitk.ac.in

We present the first results from the integration of Chandrayaan-2 derived elemental maps with their detailed geological context (obtained from several other missions). This integration is enabling the interpretation of the compositional variations at small spatial scale (few kilometers) which is otherwise not possible with x-ray derived elemental maps (with spatial resolution > 25 km/pixel). Our hybrid maps are essential to associate geographical trends in elemental composition with various geological features including units of impact craters and basins (viz. central uplift, crater wall, floor, basin rings), small spatial exposures of mare basalt and landforms of special interest including domes. The elemental maps are key inputs in understanding the geological evolution of a planetary body.

The elemental maps in this work have been derived from Chandrayaan-2 Large Area Soft X-ray Spectrometer (CLASS) which is a state-of-the-art payload currently in orbit around the Moon onboard ISRO's Chandrayaan-2 orbiter [1, 2]. CLASS is producing global elemental maps (viz. Na, O, Si, Al, Mg) of the Moon at a resolution of 12.5 km/pixel (best case scenario), the highest ever produced by any mission sent to the Moon [2,3]. CLASS elemental maps are based on the direct interaction between solar x-rays and the constituent elements of the lithologies on the lunar surface. This is in contrast to the derived elemental maps from reflectance data, which produces high resolution maps but with significant uncertainty or elemental maps available from gamma-ray spectroscopy which have poor spatial resolution [4, 5]. Besides, relatively limited number of elements can be mapped using the reflectance spectroscopy technique.

We will present hybrid elemental maps for the selected regions on the Moon and discuss the geological insights derived from these maps.

Acknowledgement: This research is funded by ISRO under the Chandrayaan-2 Announcement of Opportunity (AO) grant.

References:

[1] Vanitha, M., et al. (2020) Chandrayaan-2: The second Indian Mission to the Moon, *Lunar and Planetary Science Conference*, abstract# 1994. [2] Pillai, N. S., et al. (2021), *Icarus*, 363, 11436, https://doi.org/10.1016/j.icarus.2021.114436 [3] Narendranath S. et al. (2022) *ApJ Letters*, 937: L23, https://doi.org/10.3847/2041-8213/ac905a. [4] Lucey, P. G. et al., 2000), *J. Geophys. Res.*, 105, 20,297–20,306. [6] Lawrence, D. J., et al. (2002) *J. Geophys. Res.*, 107(E12), 5130, doi:10.1029/2001JE001530

Study of Noble Gas and Cosmic Ray Exposure ages in Selected Chondrules

Avadh Kumar[1*], R. R. Mahajan[1]

[1]Physical Research Laboratory, Ahmedabad-380009, India
*Corresponding Author E-mail: avadh@prl.res.in

Abstract: A chondrule is a round grain found in a chondrite. Chondrules form as molten or partially molten droplets in space before being accreted to their parent asteroids. Because chondrites represent one of the oldest solid materials within the Solar System and are believed to be the building blocks of the planetary system. Chondrules are believed to have formed by a rapid heating and melting of solid dust aggregates of approximately Solar composition under temperatures of about 1000 K. [1]

These temperatures are lower than those under which CAIs are thought to have formed. It follows that an understanding of the formation of chondrules is important to understand the initial development of the planetary system. Different kinds of the stony, non-metallic meteorites called chondrites contain different fractions of chondrules. In general, carbonaceous chondrites contain the smallest percentage (by volume) of chondrules, including the CI chondrites which, paradoxically, do not contain any chondrules despite their designation as chondrites, whereas ordinary and enstatite chondrites contain the most. Because ordinary chondrites represent 80% of the meteorites that fall to earth, and because ordinary chondrites contain 60-80% chondrules. Chondrules can range in diameter from just a few micrometers to over 1 cm (0.39 inch). [2,3]

They are made up of silicates, metal, and sulfide, and they appear to have formed as molten droplets at high temperatures in the early solar nebula. The chondrules are set in a fine-grained matrix that binds them together. Chondrites are divided into three main classes based on their bulk chemical compositions, oxygen isotopic compositions, and petrology. These are carbonaceous chondrites, ordinary chondrites, and enstatite chondrites. [4]

CRE ages is the duration in which meteorites travel through the space after ejection from asteroid parent body due to various impacts and collisions in the asteroidal body until the fall on the Earth as meteorites. In this work we measured the Noble gas and its isotopic abundances in Itawa Bhopji (L3-5) and Dergaon(H5). Further, Using the noble gases isotopes abundances we calculate the Cosmic Ray Exposure (CRE) ages of chondrules using latest production rate formula of cosmogenic ^{21}Ne of these chondrules. [5,6]

References:

[1] Grady M. et al. (2014) Atlas of Meteorites [2] Ozima M. and Podosek F. A. (2002) *Noble Gas Geochemistry,* 2nd Ed. [3] Eugster O. et al. (1988) GCA 52, 1649-1662 [4] Kumar A. et al. *52nd LPSC LPI Contrib. No*. 2548 [5] Kumar A. et al. (2020), Span study of CRE ages in Ordinary chondrites, IPSC0055 [6] Dalcher N. et al. (2013) Meteorit. Panet. Sci. 48, 1841-1862

Micro-spectroscopic characterization of alunite from the Puga hot springs, Ladakh (UT),India: Implications for future rover-based IR-spectroscopy of altered Venusian basalts

KVNG Vikram, Satadru Bhattacharya*, Aditya Dagar and Sriram Saran Bhiravarasu
Planetary Sciences Division, Space Applications Centre (ISRO), Ahmedabad – 380 015
*Correspondence to: Satadru Bhattacharya, satadru@sac.isro.gov.in

A state-of-the-art planetary spectroscopy laboratory (PSL) has recently been developed at Space Applications Centre (ISRO), Ahmedabad primarily for characterization of planetary analogues and meteorites in a wide spectral range from 400-25000 cm^{-1}. The integrated Vertex80V FT-IR spctrometer and HYPERION 3000 FT-IR imaging microscope from M/s. Bruker Optik GmbH, Germany is being used for analyzing the samples collected from the Puga Geothermal Field situated within the Indus-Tsangpo Suture Zone (ITSZ) in the eastern Ladakh, India from the perspective of astrobiological and mineralogical analogues to the terrestrialplanets, in particular, the Venus and the Mars. The Puga hot spring deposits represent unique association of hydrated sodium borates and a suite of hydrous sulfates including acid sulfates such as jarosite, alunite, and copiapite along with tamarugite, native sulfur and gypsum (*Sarkaret al., 2022*). We conducted spectral measurements at an elevated temperature (that is expected atthe Venusian surface) on the alunite sample (PUG-18-5-D_powder) collected from the Puga hot springs (please see *Sarkar et al., 2022* for details about the sample used in this study). Because ofthe elevated SO_2 fugacity as expected in the Venusian atmosphere due to recent volcanic activities as suggested by recent studies (e.g., Shaligin et al., 2015), the possibility of development of weathering rinds (Filiberto et al., 2020; Reid, 2021) comprising acid sulfates cannot be ignored.

The spectral measurements at the PSL have been carried out using LINKAM stage that is connected with the HYPERION3000 microscope and can vary temperature from ~-196°C to 600°C. Here, we present NIR spectra of alunite at 6 different temperatures, i.e., 50°C, 100°C, 200°C, 300°C, 400°C and 450°C in the spectral range of 1.0-2.5 µm. It is evident from the present study that as the alunite sample is raised from lower to a higher temperature, the spectral band center of the 2.2-µm doublet feature systematically shifts towards the longer wavelength and also the band strength of the longer wavelength minimum of the 2.2-µm doublet and the 2.3-µm (single and more or less symmetric) features diminishes as alunite loses its crystalline OH/H_2O at elevated temperatures that one expects at the surface of the Venus. Based on these preliminary observations, we would conduct experiments at simulated Venusian surface temperature for a suite of acid sulfates collected from the Puga Geothermal Field in the VNIR- Mid-IR region as a pre-investment study for future rover-based IR-spectroscopy of selected Venusian science targets. Additionally, we will analyze polarimetric radar data (C-/L-band) of this region to understand the diverse compositional variations within the hot spring deposits as a function of their dielectric properties.

References

Filiberto, J., Trang, D., Treiman, A. H., & Gilmore, M. S. 2020, SciA, 6, eaax7445

Reid, R. B. 2021, MSc Dissertation Thesis, The University of Tennessee, Knoxville

Sarkar, S., Moita, H., Bhattacharya, S., Dagar, A., Ray, D., Gupta, S. et al. 2022, JGR-Planets, doi: 10.1029/2022JE007299

Shalygin, E. V., Markiewicz, W. J., Basilevsky, A. T., Titov, D. V. N., Ignatiev, I., & Head, J. W. 2015, GRL, 42, 4762–4769, doi:10.1002/2015GL064088

Design of Multi-axis manipulator for laboratory experiments and simulated space environment chamber.

Jayvir Rajgor[1*], Janmejay[2], K. Durga Prasad[2], Megha Bhatt[2], K G DAVE[1]

[1]LD College of Engineering, Ahmedabad, India

[2]Physical Research Laboratory, Ahmedabad, India.

*Corresponding Author E-mail: rajgorjayvir2000@gmail.com, janmejay@prl.res.in

This research work aims to design a multi-axial manipulator which will be used inside a vacuum chamber with a simulated space environment. The manipulator will be used to control the movement of reflectance probe of a reflectance spectrometer.

Present systems use can perform only one sample at a time after that we will require to open the vacuum chamber and re-adjust the test samples and probe. It also leads to recreation of a vacuum which consume unnecessary time and energy. It shows that there is a need for development to overcome present limitations which can be solved with the help of multi axis manipulator which can take multiple spectra of analogue samples with more precision and flexibility.

Configuration design of Multi-axis manipulator has been completed. Design and structural analysis of components has been done by using SOLIDWORKS and ANSYS respectively. Design parameters such as space limitations inside the vacuum chamber, torque requirement, motion have been considered to minimize the stresses, deflection and vibration induced during motion. Also I am working on the circuit design and coding for axial and rotational movement ofmanipulator.

References:

[1] Cloutis, E. A., M. A. Craig, R. V. Kruzelecky, W. R. Jamroz, A. Scott, F. C. Hawthorne, and S. A. Mertzman. "Spectral reflectance properties of minerals exposed to simulated Mars surface conditions." Icarus 195, no. 1 (2008): 140-168.

[2] Batzer, T. H. ”Mechanical Motion in Vacuum” No. UCRL-7830. Lawrence Radiation Lab., Univ. of California, Livermore, 1964.

Development of electronics for Dielectric permittivity measurements for future Lunar missions

Chandan Kumar[1*], K Durga Prasad, Sanjeev Mishra, P Kalyan Reddy, Janmejay Kumar

[1]Physical Research Laboratory, Navrangpura, Ahmedabad
*Corresponding Author E-mail: chandankr@prl.res.in

Evidence for water/ice on the moon provided by various missions requires further studies by in-situ measurements. Although the observations so far indicate lunar water/ice, in-situ investigations are necessary to understand its nature, distribution and process of formation/accumulation and its quantification for future in-situ resource utilisation. Given this, an experiment is needed for in-situ detection and quantification of water ice mixed with lunar surface and sub-surface soil using a rover/lander platform. The experiment consists of a multipurpose probe that will be deployed into ~20-30 cm of the lunar surface to scout and quantify the presence of water ice. Using its probe, it will carry out in-situ probing of electrical properties with thermal properties to detect and quantify the water-ice mixed in the lunar regolith.

The permittivity of materials is their ability to oppose the applied external electric field. When applied with an external electric field, a material tends to nullify the build-up of the electric field inside it. Application of an external electric field leads to creating and moving these dipoles even in a non-polarized material. Some materials with very good polarizability have high dipole moments, making them nullify greater electric field intensity. At lower frequencies, apart from the molecular vibrations, other physical phenomena contribute to the overall dielectric permittivity. One such phenomenon is the dielectric relaxation of water ice. At low frequencies, water ice exhibits a sharp change in its dielectric constant which is unique to it and distinguishes it from other typical constituents of the medium, such as clay, basalt etc. This property is used to detect the presence of wastewater ice samples.

Thus, we are developing electronics that will generate the frequency-varying electric field and detect ultra-low voltages with AC signals with varying frequencies and phase differences. These signal conditioning electronics will be aided by FPGA-based processing electronics, which will carry out onboard processing of these received signals and interface with the rover/Lander. The design and development of the electronics of the proposed experiment will be presented further at the conference.

Anorthosite bonded with Avocados yielding 3D structure - A Suitable soil simulant for construction over Moon without Water and added an Anti-Cancerous agent for Cancerwith validation via ROS Anti-Oxidant analysis- An Astro-Biological approach

Yamini Malhotra
Research Scholar, Department of Earth Sciences, Annamalai University, Tamil Nadu, India
yaminipriya2008@gmail.com

ABSTRACT- In order to reduce the cost estimation of lunar missions with respect to lunar habitats via introducing Anorthosite as building material, the author demonstrated the lunar equivalent Salem's Anorthosite as a Regolith simulant with Avocados as binders, a perfect concrete to be in use over Moon, a possible hassle-free technique for shielding habitats and building lanes prior to arrival of the Astronauts with no extra instrumentation that involved a total of 31 days to get the material dried and ready to mount. The authors too tested the medicinal importance of anorthosite via MTT (3-4, 5 dimethylthiazol-2yl-2, 5-diphenyl tetrazolium bromide) Assay for breast cancer with ROS (Reactive Oxygen Species) Antioxidant analysis along with FTIR (Fourier Transform InfraRed Spectroscopy), as an added benefit to astronauts in anti-gravity that is having radiation effects via Biotechnology for *in-vitro* trials on Cell line studies. On an all, anorthosite is having power to treat cancer in space when applied as an anti-cancer drug and added, a suitable building material for construction over Moon.

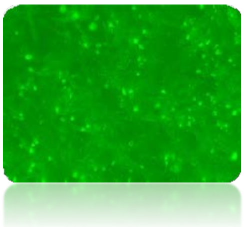

Drug treatment imaging with concentration as 500ug/ml in compliance with DMSO (Dimethyl Sulfoxide) so captured from Elisa Plate Reader reflecting cell death in highlighted bright green.

KEYWORDS- Anorthosite, Lunar Simulant, Avocados, 3D Sintering, Cancer Drug Agent, Natural Compound, Innovation

References

1. Mosmann, Tim. "Rapid colorimetric assay for cellular growth and survival: application to proliferation and cytotoxicity assays." *Journal of immunological methods* 65, no. 1-2 (1983): 55-63.
2. Marshall, N. J., C. J. Goodwin, and S. J. Holt. "A critical assessment of the use of microculture tetrazolium assays to measure cell growth and function." *Growth regulation* 5, no. 2 (1995): 69-84.
3. Budholiya, S., Krishnamoorthy, V., Bhat, A., Venugobal, T., Subramanian, K. L., Narayan, S. L., Babu, S. P. M., Sivaprahasam, V., Bhardwaj, A., Meka, J. K., and Sivaraman, B.: 3D printing the Sittampundi anorthosite - Indian lunar soil simulant, European Planetary Science Congress 2021, online, 13–24 Sep 2021, EPSC2021-535, https://doi.org/10.5194/epsc2021-535, 2021.
4. Yamini, SR Singara Subramanian., Lunar Geology- An Overview., Journal of Emerging Technologies and Innovative Research, pages. 861-868.

Electrostatic solitary waves over the lunar magnetic anomaly region

R. Rubia[1*], M. B. Dhanya[1], S. V. Singh[2], G. S. Lakhina[2], V. K. Yadav[1], R. S. Thampi[1]

[1]Space Physics Laboratory (SPL), Vikram Sarabhai Space Center (VSSC), Indian Space Research Organization (ISRO) , Thiruvananthapuram - 695022

[2]Indian Institute of Geomagnetism, Navi Mumbai - 410218

*Corresponding Author E-mail: rubi.r92@gmail.com

In the absence of a global magnetic field and a significant atmosphere, the solar wind interaction with the moon results in absorption of the solar wind particles in the dayside and a cavity in the night side referred as lunar wake [1]. The interplanetary magnetic field (IMF) penetrates the lunar surface undisturbed [1]. However, there are numerous observational evidences of existence of local crustal magnetic field referred as lunar magnetic anomaly (LMA) on the lunar surface [2, 3]. These LMA's deflect solar wind particles striking the lunar surface [4]. The deflected solar wind particles along with backscattered photoelectrons and particles counter stream relative to the incident solar wind, eventuating in varied elementary plasma processes like electrostatic waves and instabilities that affects the lunar plasma environment [5].

Electrostatic solitary waves (ESWs) is a prevalent phenomenon in the space plasma environment. The ESWs are often associated with electron and/or ion beams [6]. The ESWs account for the electrostatic turbulence and broadband electrostatic noise (BEN) which is an ubiquitous phenomenon in the space plasma environment. From KAGUYA observations, Hashimoto et al. [7] reported the existence of ESWs generated due to counter streaming electrons with respect to the solar wind electrons over the magnetic anomaly. Chu et al. [5] reported the occurrence of electrostatic waves over the lunar crustal magnetic anomalies on the basis of ARTEMIS observation. The characteristics and existence domain of ESWsoccurring above the lunar magnetic anomaly region is studied using KdV equation. The plasma over the LMA region is modelled using a four-component magnetized plasma comprising of protons, Helium ions, superthermal electrons and electron beam. For parameters relevant to the LMA, the model supports the existence of slow and fast ion- acoustic solitons and electron-acoustic solitons. The electric field, potential, width obtained from the model is compared with the observations.

References:

[1] Tao J. B., Ergun R. E., Newman D. L., … (2012) JGR, 117, A03106.
[2] Tsunakawa H., Takahashi F., Shimizu H. , … (2015) JGR: Planets, 120, 1160–1185.
[3] Mitchell, D. L., Halekas, J. S., Lin, R. P., … (2008) Icarus, 194, 401–409.
[4] Dhanya M. B., Bhardwaj A., Alok A., … (2018) GRL, 45, 8826-8833.
[5] Chu F., Halekas J. S., Cao X., ... (2021), JGR: Space Phys., 126.
[6] Lakhina G. S., Singh S. V., Rubia R., and Sreeraj, T. (2018), Phys. of Plasma, 25.
[7] Hashimoto K., Hashitani M., Kasahara Y., … (2010), GRL, 37, 1–6.

Formation of Organic Species in the Gas Phase Cometary Coma

Sana Ahmed[1] and Kinsuk Acharyya[1]

[1]Planetary Sciences Division, Physical Research Laboratory, Ahmedabad 380009.

*Corresponding Author E-mail: ahmed.sana92@gmail.com

Abstract: Comets are the relics of the protoplanetary disk that formed the Solar System and are made up of volatile ices, which have been largely unprocessed since their incorporation in the cometary interiors. Comets are likely to have delivered volatile organics and prebiotic material to the planet by impact processes [1,2]. Organics are the seeds for creating molecules of biological interest, and investigations of their formation in comets can give clues towards understanding the prebiotic chemistry. Many volatile species have been detected in comets from remote and in situ measurements. At present, the total number of volatile species identified in comets, including tentative detections, stands at 72, out of which 37 are complex organic molecules [3]. It has not yet been proven that all of the molecules observed in the coma of comets originate from the ices inside the cometary nucleus. Thus, it is pertinent to study the coma chemistry, with emphasis on the gas-phase formation pathways and how successful they are in producing organics in a cometary coma.

We selected a sample of four comets for our study: C/1996 B2 (Hyakutake), C/2012 F6 (Lemmon), C/2013 R1 (Lovejoy) and C/2014 Q2 (Lovejoy). All of these are bright comets, with high production rates near perihelion, which facilitated the remote detection of many organic molecules, while sensitive upper limits were obtained for some other organics. The coma of these comets is modelled by using a combined chemical-hydrodynamical multi-fluid model that is based on the fluid conservation equations of number density, mass, momentum, and energy [4]. The model also uses a large chemical network to define an active gas phase coma chemistry that includes photochemical reactions, bimolecular ion-neutral and neutral-neutral reactions, recombination reactions and electron impact reactions. The multi-fluid approach is to divide the neutral species, ions and electrons into three separate fluids, and energy exchange between the fluids is included. Our model results show that by incorporating gas phase formation pathways, the production rates for several complex organic molecules can be increased, which can account at least partially towards the total coma abundance of these species. We also found that factors such as initial volatile abundance, relative abundances of the reactants and temperature of the reacting species significantly affect the formation rates of molecular species in different regions of the coma.

References:

[1] Chyba C. F., et al. (1990) *Science, 249 (4967)*, 366.
[2] Ehrenfreund P., et al. (2002) *Reports on Progress in Physics, 65 (10)*, 1427.
[3] Rubin M., et al. (2019) *ACS Earth and Space Chemistry, 3(9)*, 1792.
[4] Ahmed S. and Acharyya K. (2021) *ApJ, 923(1)*, 91.

Spectroscopic Calibration of AOTF for Space Applications

Shrikant Muduli[1*], Bhavesh Jaiswal[2], Swapnil Singh[2], Anuj Nandi[2], Sumanta Sarkhel[1]

[1] Indian Institute of Technology Roorkee, Uttarakhand, India
[2] Space Astronomy Group, U. R.Rao Satellite Centre, Bengaluru, Karnataka, India

*Corresponding Author E-mail: shrikant_m@ph.iitr.ac.in

Acousto-Optic Tunable Filter (AOTF) is an electro-optical device that functions as an electronically tunable filter to select the wavelength of light from the broadband input. The main advantage of this technique is the absence of any moving part (unlike a filter wheel), and no order overlap (unlike a grating spectrograph), as the principle of AOTF is based on 1st-order Bragg diffraction. Further, the AOTF avoids the need for a multi-pixel array detector for spectroscopy as it acts as a narrow-band tunable filter; hence a single-pixel detector can be effectively used for such applications by scanning RF frequency corresponding to the wavelength. AOTF is used in various applications like spectrophotometry, spectral analysis, and hyperspectral imaging [1-3]. The successful demonstration of AOTF technology in space-based missions was SPICAM on Mars Express [4,5] and SPICAV on Venus Express [6].

This work is aimed at the spectroscopic calibration of AOTF in the Near-Infrared (NIR) wavelength range of 1.0-1.7 µm. The AOTF used in this work is based on Tellurium-dioxide (TeO2) crystal that functions as a dispersing medium and is driven by an external Radio Frequency (RF) signal. The spectroscopic characterisation of dual-beam AOTF is based on the wavelength-tuning frequency relation and spectral bandwidth as a function of wavelength through the AOTF transfer function. For calibration, we scan the intensity profile of a halogen lamp as a function of RF frequency for a monochromatic input to AOTF. The plot of diffracted light intensity vs RF is called the Transfer Function of AOTF. Theoretically, the AOTF transfer function may be modelled as a sinc^2 function. However, data processing demonstrated that a sinc^2 function does not correctly reproduce the AOTF function. So the bandpass function is modelled as the sum of several sinc^2 functions [7]. This study has demonstrated that at least 5 sinc^2 functions must be introduced to better quantify the relative importance of the side lobes. After determining the transfer function, it is convolved with the observed O_2 absorption lines of Earth to demonstrate the response of the AOTF to the atmospheric oxygen spectra.

The AOTF function determined in this work can be used for the analysis of the atmospheric spectra of any planet. This spectroscopic calibration is being done for future interplanetary missions of ISRO to study the atmosphere of planets such as Venus and Mars.

References: [1] Bucher, E.G., Carnahan, J.W. (1999) Appl. Spectrosc. 53, 603–611. [2] Rajwa, B., et al. (2005) Proc. SPIE 5694, 16–23. [3] Glenar, D.A., et al. (1994) Appl. Opt. 33(31), 7412–7424. [4] Bertaux, J.L., et al. (2004) Eur. Space Agency Spec. Publ ESA-SP 1240, 95–120. [5] Korablev, O.,et al. (2006) J. Geophys. Res. 111, E09S03. [6] Bertaux, J.L., et al. (2007) Planet. Space Sci. 55, 1673–1700. [7] Mahieux, A., Wilquet, V., Drummond, R., Belyaev, D., Federova, A., & Vandaele, A. C. (2009). *Optics Express*, *17*(3), 2005-2014.

Study of the Hydrogen and Oxygen escape from Mars

Siddhi Shah[1*] and S. A. Haider[1]

[1] Physical Research Laboratory, India

*Corresponding Author E-mail: (siddhi@prl.res.in)

The atmospheric loss on Mars are responsible due to thermal escape of hydrogen atoms and photochemical escape of oxygen atoms [1, 2]. These are the most important escape processes in Martian atmosphere. Direct measurement of the escaping neutral hydrogen and oxygen atoms is not available due to the low density and energy of escaping neutrals [3]. However, when they ionized and picked up by the solar wind, these escaping atoms can be detected. The Supra Thermal and Thermal Ion Composition (STATIC) instrument on board Mars Atmosphere and Volatile EvolutioN (MAVEN) has measured the pickup ion H^+ and O^+ flux [4]. STATIC instrument detects pickup ions H^+ and O^+ with energies up to 30 keV. These pickup ion measurements of STATIC on board MAVEN constrain neutral escape rates of hydrogen and oxygen. We have study the escape flux and escape rate of oxygen and hydrogenduring the presence and absence of dust storm. Our estimated escape rate is larger by a factor of 5-10 than that produced before or after the dust storm.

References:

[1] Hunten D. M. and McElroy M. B. (1970) *JGR 75(31)*, 5989–6001.
[2] Nagy, A. F., & Cravens, T. E. (1988) *GRL 5(5)*, 433–435.
[3] Bougher et al. (2015) Science, *350(6261).*
[4] Rahmat et al. (2017) JGR, *122*, 3689–3706

Study of IOM of Diyodar Meteorite

Neha[1*], S. Natrajan[2], K.K. Marhas [2]
[1]Banasthali Vidyapith, Rajasthan 304022, India
[2]Physical Research Laboratory, Ahmedabad 380009, India
*Corresponding Author E-mail: nehathakran333gmail.com

On August 17th, 2022, the Diyodar meteorite fell in the Banaskantha district of Gujarat, India, witnessed by the villagers of Rantila and Ravel. The Physical Research Laboratory (PRL) collected this sample of the meteorite and identified it as an Aubrite. In this study, I would compare the Insoluble Organic Matter (IOM) extracted from Diyodar with IOM from other aubrites (Norton County, Pesyanoe, Bishopville, Mt. Egerton, and Cumberland Falls). Organic matter consists of soluble and insoluble fractions. The Insoluble Organic Matter (IOM) is a macromolecular structure composed of small aromatic moieties held together by short highly branched aliphatic chains and ether linkages. This research aims to analyze the chemical composition of organic matter in meteorites, providing insight into our solar system's formation and evolution, the potential for life on other planets, and the origin of life on Earth. The study could result in the discovery of new organic compounds. Additionally, it could suggest the presence of organic matter in undifferentiated meteorites, whether they originate from carbon-rich asteroids or survive the differentiation process after a planetary body's formation.

The extraction of organic matter from meteorites, particularly aubrites (differentiated meteorites), is a crucial step in obtaining a pure sample for accurate analysis and characterization. The extraction process involves several steps, including sample preparation, solvent extraction, purification, and analysis. In sample preparation, the meteorite is crushed into a fine powder and treated to remove surface contaminants. Solvent extraction follows, where the crushed sample is mixed with a solvent such as methanol with dichloromethane to dissolve the organic matter, separating the soluble and insoluble fractions. The insoluble organic matter (IOM) is then extracted using a mixture of cesium fluoride salt and dioxane-carbon sulfide and washed with 1M HCl to remove impurities before being dried. The purified organic matter is then analyzed using techniques FTIR and Raman Spectroscopy on the extracted organics to study the functional group, and chemistry to compare and depict their evolution and origin.

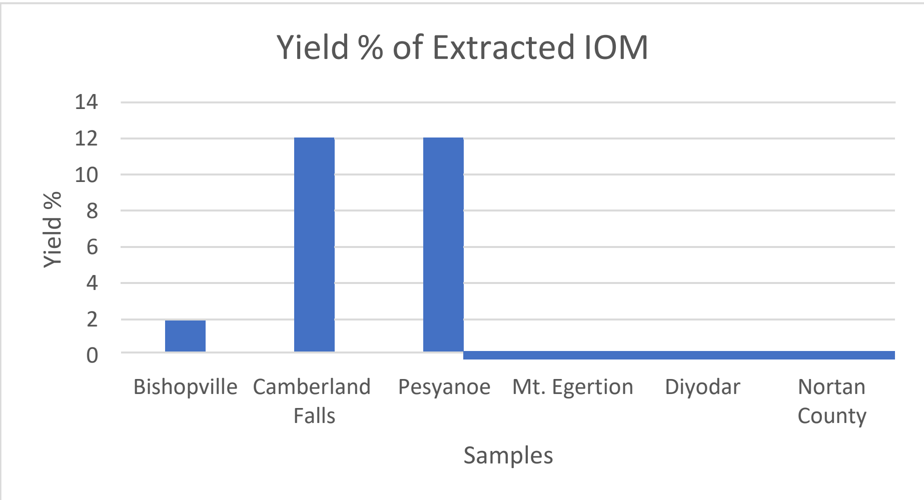

References:

[1] G. D. CODY, C. M. O’D. ALEXANDER and F. TERA (2002) Geochimica et Cosmochimica Acta, 60, 1851–1865.
[2] C.M.O'D. Alexander, G.D. Cody, B.T. De Gregorio, L.R. Nittler, R.M. Stroud, (2017), Chemie der Erde, 77,227–256.
[3] George D. Cody, and Conel M. O’D. Alexander, (2015) Geochimica et Cosmochimica Acta, 69, 1085–1097

A petrographic and electron microscopic evaluation of Carbonaceous Chondrite: LON94101

Debarun Mukherjee[1]* and Dwijesh Ray[2]

[1]Department of Geology, Presidency University, 86/1 College Street, Kolkata 700073, India.
[2] Physical Research Laboratory, Ahmedabad 380009, India
*Corresponding Author E-mail: mukherjeedebarun29@gmail.com

Abstract: Meteorites, the extraterrestrial material from space, holds the clu**e** on the origin and evolution of early solar system. There are three main types of meteorites, Stony, Iron and Stony iron. The Stony meteorites are of two categories: Chondrites (85% of falls) and Achondrites [1]. Chondrites are composed of millimeter to submillimeter sized spherules of Fe Mg silicates called chondrules, that were formed by refractory melting of protoplanetary material. Presence of typical igneous textures of Chondrules hints at melting and crystallization as precursor events for chondrule formation. Chondrules are also usually thought to have been relatively unaffected post formation in the parent body [1]. Amongst the Chondrites, Carbonaceous Chondrites (CC) are known for its primitive and pristine nature and its composition similar to the solar photosphere. The CM chondrite is the most abundant group (~25%) of CC class and provide important constraint on the hydrology of parent body in its early geologic history. The CM chondrites also offer potential analog to the asteroid returned samples during Ryugu and OSIRIS-REx missions. Various sub classes of CC exist to account for the abundance of various phases. We here work with and report one such type, named CC LON 94101, which is a CM2 (Carbonaceous Mighei type) chondrite [4] as understood from low parent body aqueous alteration. The specimen is matrix dominated (> 85% by volume); Chondrules make up less than 5% of the total volume and isolated grains of olivine and calcite make up the rest. The dominant mineralogy of the chondrite includes Olivine and Pyroxene, both occurring within chondrules as well as isolated grains in the matrix. Calcite is the dominant carbonate present in the sample. Typical chondrule types include POP, PO, PP and C chondrules [5] indicating varying degrees of melting and crystallization, that occurred within the parent body during planetesimal accretion. Major deformation structures seen include Planar Deformation Features (PDFs, which are usually representative of shock deformation effects) forming planar fabrics within isolated olivine grains. Backscattered Electron images using Scanning Electron Microscopy reveals the presence of Al-Diopside as we find phases containing Al-Ca-Mg-Si by SEM-EDS. The petrography and electron microscopy of LON 94101 is consistent with typically altered CM chondrite. The presence of shock-induced microscopic feature further suggests for a possibility of impact-induced alteration in parent body.

References:

[1] Sears D.W.G. *Chondrites Ordinary Encyclopedia of Planetary Sciences 105-110*.
[2] Guita C. 2012 *Memorie della Societa Astronomica Italiana Supplement, 20, 74*.
[3] Gilmour I. *Meteorites Comets and planets. Treatise in Geochemistry 2003*. [4] Weisberg, M. K. ; McCoy, T. J. ; Krot, A. N. 2006 *Systematics and Evaluation of Meteorite Classification-Meteorites and the Early Solar System II, University of Arizona Press, Tucson, 943 p.19-52* [5] Wasson, J.T., Krot, A.N., Lee, M.S. and Rubin, A.E., 1995. *Compound chondrules. Geochimica et Cosmochimica Acta, 59(9), pp.1847-1869.*

Spectral Mixing and Statistical Analysis: An algorithm for estimating rock composition through remote sensing with reference to Lunar Basaltic Crust

Kuntal Saha[1*], Srinjit Datta[1]

[1]Department of Geology, Presidency University, Kolkata, India.

*Corresponding author E-mail: sahakuntal616@gmail.com

The lunar crust's mineralogical composition is a matter of great scientific interest, and a range of cutting-edge techniques have been utilized to decipher its nature. Specifically, the basaltic and andesitic nature of the lunar crust has been identified through the use of visible near-infrared (400-2500nm) spectroscopy and from return samples of various moon missions. However, in order to delve deeper into the composition of this crust with a larger spectral resolution, we have utilized hyperspectral instruments, such as the Chandrayaan-1 Moon mineralogy mapper (M3), Diviner, and Chandrayaan-2 Integrated Infrared Spectrometer (IIRS). Even these sophisticated instruments do not enable us to resolve to the mineral-scale identification (intrinsic to the restricted to the sensor resolution), as we do with earth samples under thin section petrography, we are limited to graduate our observation with limited spectral and radiometric resolutions and therefore come to a broad classification while naming the rock type. For example, we only get basalts on lunar crust, while we get a variety of mafic rocks on earth (kimberlites to basalt) within similar time frame. We believe that this is due to our shortcomings in the understanding of subtle spectral variations that are associated with the spectra obtained by the sensors and payloads. In order to prove this, we have undertaken a pilot study, wehre we do a rigorous analysis of the geometry of the spectral curves. The process involves the acquisition of spectra of constituent minerals of basalt from existing and established spectral library and we have mixed those mineral spectras in appropriate proportions (as we find in the basalts) to form a simulated basalt spectra (SBS). Subsequently, we correlate this SBS with the natural basalt spectra (NBS, from well-established libraries) using auto-correlational statistical techniques. We find a statistical discrepancy between the derived spectra and a true basalt spectra to a 95% confidence limits, implying deviations from basalt. This study brings out our shortcomings in the estimation (errors) of rocks that we generally do with spectral signatures and thereby has provides further scope to critically estimate the true nature of the lunar crust than. is usually done. We propose that such statistical analysis be applied to other planetary bodies, including Earth, to gain insights into their true nature by remote sensing methods. We understand that such errors are intrinsic to the sensor specifications, but if critically assessed these subtle differences may reveal different rock types hitherto not reported from lunar and other planetary bodies' crust.

Reference: [1] Clark, R. N., & Rencz, A. N. (1999). Spectroscopy of rocks and minerals, and principles of spectroscopy. *Manual of remote sensing*, *3*(11), 3-58. [2] Green, R. O., Pieters, C., Mouroulis, P., Eastwood, M., Boardman, J., Glavich, T., ... & Wilson, D. (2011). The Moon Mineralogy Mapper (M3) imaging spectrometer for lunar science: Instrument description, calibration, on-orbit measurements, science data calibration, and on-orbit validation. *Journal of Geophysical Research: Planets*, *116*(E10). [3] Chowdhury, A. R., Banerjee, A., Joshi, S. R., Dutta, M., Kumar, A., Bhattacharya, S., ... & Parasar, A. (2020). Imaging infrared spectrometer onboard Chandrayaan-2 orbiter. *Curr. Sci*, *118*(3), 368-375.

Modeling spectral unmixing for planetary surfaces: Mapping anorthite and olivine-rich regions

Maitreya Mohan Sahoo[1*], Shashikant Singh[1], Kalimuthu Rajendran[1],

Alok Porwal[1*], Debosmita Paul[1], and Shibu K. Mathew[2]

[1]Centre of Studies in Resources Engineering, Indian Institute of Technology Bombay, Mumbai 400076
[2]Udaipur Solar Observatory, Physical Research Laboratory, Udaipur 313001
*maitreyaiitb@gmail.com; *aporwal@iitb.ac.in

Abstract: Spectroscopic investigations of planetary surfaces allow us to infer their compositional information. Most of the planetary surfaces are made of regolith comprising intimate mixtures of soils of variable grain sizes formed by disintegration of rocks either by space weathering (e.g., Earth's moon) or physical weathering (e.g., Mars). Reflectance spectra of intimately mixed soils are typically nonlinear combination of the endmember spectra, involving complex multiple scattering of photons in the material [1]. Modeling spectral reflectance of these mixtures have been simplified with bidirectional measurements [2] that consider physical and geometrical properties of endmembers. Inversion of these physics-based models for spectral unmixing estimates the endmembers' fractional abundances and subsequent mineral mapping.

In this work, we report our experiment-based analysis of hyperspectral images of material approximating lunar soil at different grain sizes for different pixel sizes. The effects of varying fractional abundances of endmembers, grain size and instantaneous field of view (IFOV) on spectral shift in absorption bands, band depth, width and other features are modelled. This study can help in developing spectral unmixing models for planetary regoliths.

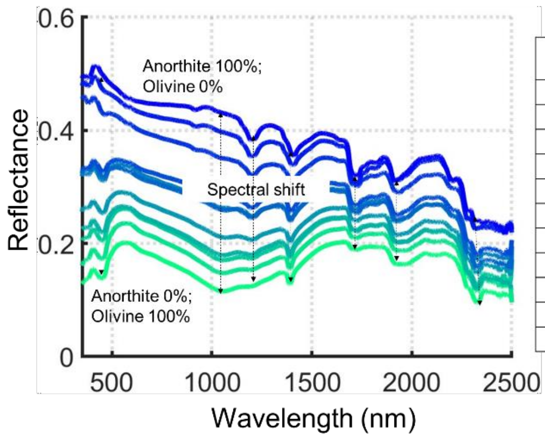

Percentage composition

Anorthite (%)	Olivine (%)
100	0
90	10
80	20
70	30
60	40
50	50
40	60
30	70
20	80
10	90
0	100

Figure 1: Reflectance spectra and trends observed for simulated physical mixtures of anorthite and olivine by varying their percentage composition

References:

[1] Mustard, J. F. and Pieters C. M. (1987). Quantitative abundance estimates from bidirectional reflectance measurements. *Proceedings of the Seventeenth Lunar and Planetary Science Conference, Part 2, Journal of Geophysical Research, 92(B4),* E617-E626.

[2] Hapke, B. (1981). Bidirectional Reflectance Spectroscopy- 1. Theory. *Journal of Geophysical Research, 86(B4*), 3039-3054.

Statistical analysis of HILDCAA events and response to total electron content duringgeomagnetic storm

Ayushi Nema[1*], Kamlesh Pathak[2], Abhirup Datta[2]

[1]Department of Physics, Sardar Vallabhbhai National Institute of Technology, Surat, Surat-395007, Gujarat, India (ayushinema24@gmail.com)
[2]Department of Physics, Sardar Vallabhbhai National Institute of Technology, Surat, Surat-395007, Gujarat, India (knp@phy.svnit.ac.in)
[2]Department of Astronomy, Astrophysics and Space Engineering, Indian institute of Technology Indore,Indore-453552, Madhya Pradesh, India (abhirup.datta@iiti.ac.in)
*Corresponding Author E-mail: (ayushinema24@gmail.com)

Abstract

When solar flares enter earth's magnetosphere, they cause geomagnetic storms of various intensities. Their intensities are generally verified by indices like disturbance storm time index (DST), auroral electrojet index (AE) etc. A special kind of storm called as HILDCAAs (High Intensity Long Duration Continuous AE Activity) classified by a DST>-50nT and AE>1000nT have been presented in this paper. The relative occurrence of HILDCAA events with mean sunspot numbers for a period of 1975 to 2018 were studied for 43 years. Additionally, the solar wind pressure and proton density fluctuation has been observed over the whole period. The ionospheric response has been noted for a HILDCAA event occurred from 17/08/2017 to 21/08/2017 over Indian region. This study would give a brief idea about HILDCAA-ionospheric relation by TEC estimation at IGS stations located in India and how the magnetosphere changes itself to entertain electrons and other charged particles during the time.

References:

[1] de Siqueira Negreti, P. M., de Paula, E. R., and Candido (2017), C. M. N., "Total electron content responses to HILDCAAs and geomagnetic storms over South America," *Ann. Geophys*., 35, 1309–1326, doi: 10.5194/angeo-35-1309-2017, 2017

[2] Adhikari B., Mishra R., Chapagain N., Baral R., Das P., Klausner V., Sharma M.(2020) "Variation of Solar Wind Parameters and Total Electron Content from Indian, Australian, Brazilian and South African Sectors during the Intense Geomagnetic Storms," doi: 10.1002/essoar.10503097.1

Spectral unmixing of hyperspectral images: Implications for estimating mineralabundances from Hyperspectral data

Soorya Suresh[1*], P.V. Arun[1*], Alok Porwal[2], and Guneshwar Thangjam[3]

[1]IIIT Sri City, Thirupathi, Andhra Pradesh, India

[2]IIT Bombay, Powai, Maharashtra, India

[3]NISER, Bhubaneswar, Odisha

*Corresponding Author Email: soorya.s@iiits.in, arun.pv@iiits.in

The Chandrayaan-2 mission provides hyperspectral images that help to understand themineral composition of the lunar surface .However, the noisy nature of the data, lack of trainingdata, and high data dimensionality limit the applicability of the existing state-of-the-art approaches for effectively unmixing the hyperspectral data. Although deep learning-based methods have yielded state-of-the-art results for terrestrial hyperspectral datasets, choosing the appropriate method for the lunar hyperspectral dataset is challenging because of prolific surfacesoil and regolith generated by space weathering, resulting in intense, intimate, microscopic mixing of disintegrated minerals.

Recent research on spectral unmixing of terrestrial geological material have shown the efficacy of deep-learning-based approaches in estimation of subpixel-level fractional abundances of endmember minerals. In general, deep learning-based approaches can be categorized into three types: generative network-based, autoencoder-based, and CNN-based approaches. This study will attempt to evaluate the existing state-of-the-art approaches with regard to not only accuracy and computational expenses but also explainability, generalizability, and the requirement of training samples. Additionally, the sensitivity to the noisy nature of the data will also be investigated.

The approaches that use CNN generally adopt the learned latent space to soft classify the spectra, and the soft classification score is approximated as the fractional abundance. These approaches have the capability to model the noisy nature of the data. However, the requirement of a large number of training samples, computational expenses, and lack of interpretability affect the practical implementation of these approaches for hyperspectral data. The autoencoder-based approaches generally implement the unmixing in a learned latent space by applying sparse regularization such as spectral angular distance and the root mean square error metric to evaluate the quality of estimated endmembers and assess the accuracy of estimated abundances. By using the multitask autoencoder for unmixing, it achieves fairly good results for abundance estimation. Although this method has very low variance, high consistency, and is robust to noise, it only considers the spectral information and ignores the spatial context. The Generative Adversarial Network uses the reconstruction error and the abundance root mean square error as the performance metrics for quantitative results in the case of synthetic data. This approach yields comparable performance to the existing state-of-the-art abundance estimation approaches. However, the approach lacks strong generalization capability, requires a large amount of training data, and fails to effectively model the end members.

In this regard, the use of the reconstruction error as a measure of the non-linearity of mixtures is embedded in the graph-based space to implement an interpretable unmixing. The graph-based approach improves the generalizability , efficiency and accuracy of the proposed approach and reduces the requirement for training samples.In addition, the normal convolution is not efficient for noisy data which affect the unmixing of the hyperspectral data, hence interpolation of convolution is explored. The efficiency of a graph depends on the graphical representation of the data, hence different graph formulation is explored and a novel approach optimal for unmixing. The approach has been applied to Cuprite bench-mark data for unmixing of surface geological material. The results indicate that it may be extrapolated to IIRS data.

References

[1] Rasti, B., Koirala, B. and Scheunders, P. (2022) "HAPKECNN: Blind nonlinear unmixingfor intimate mixtures using hapke model and convolutional neural network," *IEEE Transactions on Geoscience and Remote Sensing*, 60, pp. 1–15. Available at: https://doi.org/10.1109/tgrs.2022.3202490.

[2] Palsson, B., Ulfarsson, M.O. and Sveinsson, J.R. (2021) "Convolutional Autoencoder for spectral–spatial hyperspectral unmixing," *IEEE Transactions on Geoscience and Remote Sensing*, 59(1), pp. 535–549. Available at: https://doi.org/10.1109/tgrs.2020.2992743.

[3] Zhang, J. *et al.* (2022) "Nonlinear unmixing via deep autoencoder networks for generalized bilinear model," *Remote Sensing*, 14(20), p. 5167. Available at: https://doi.org/10.3390/rs14205167.

[4] Borsoi, R.A., Imbiriba, T. and Bermudez, J.C. (2020) "Deep generative endmember modeling: An application to unsupervised spectral unmixing," *IEEE Transactions on Computational Imaging*, 6, pp. 374–384. Available at: https://doi.org/10.1109/tci.2019.2948726.

[5] Audebert, N., Le Saux, B. and Lefevre, S. (2018) "Generative adversarial networks for realistic synthesis of hyperspectral samples," *IGARSS 2018 - 2018 IEEE International Geoscience and Remote Sensing Symposium* [Preprint]. Available at: https://doi.org/10.1109/igarss.2018.8518321.

[6] Tang, M., Qu, Y. and Qi, H. (2020) "Hyperspectral nonlinear unmixing via Generative Adversarial Network," *IGARSS 2020 - 2020 IEEE International Geoscience and Remote Sensing Symposium* [Preprint]. Available at: https://doi.org/10.1109/igarss39084.2020.9324087

[7] Hong, D. *et al.* (2022) "Endmember-guided unmixing network (EGU-net): A general deep learning framework for self-supervised hyperspectral unmixing," *IEEE Transactions on Neural Networks and Learning Systems*, 33(11), pp. 6518–6531. Available at: https://doi.org/10.1109/tnnls.2021.3082289.

[8] Ozkan, S., Kaya, B. and Akar, G.B. (2019) "EndNet: Sparse AutoEncoder Network for endmember extraction and hyperspectral unmixing," *IEEE Transactions on Geoscience and Remote Sensing*, 57(1), pp. 482–496. Available at: https://doi.org/10.1109/tgrs.2018.2856929.

[9] Gao, L. *et al.* (2022) "Cycu-net: Cycle-consistency UNMIXING network by learning cascaded autoencoders," *IEEE Transactions on Geoscience and Remote Sensing*, 60, pp. 1–14. Available at: https://doi.org/10.1109/tgrs.2021.3064958.

[10] Rasti, B. *et al.* (2022) "Undip: Hyperspectral unmixing using Deep image prior," *IEEE Transactions on Geoscience and Remote Sensing*, 60, pp. 1–15. Available at: https://doi.org/10.1109/tgrs.2021.3067802.

[11] Tong, L. *et al.* (2014) "Dual graph regularized NMF for hyperspectral unmixing," *2014 International Conference on Digital Image Computing: Techniques and Applications (DICTA)* [Preprint]. Available at: https://doi.org/10.1109/dicta.2014.7008103.

Spectrochemical Characterization of Evaporites from Sambhar Lake, Rajasthan, Northern India: Implication For Hypersaline Lake As PotentialTerrestrial Martian Analogue

Preeti Kumari., Kavish Madhan, and V.J. Rajesh
Department of Earth and Space Sciences, Indian Institute of Space and Science Technology, Valiamala P.O., Thiruvananthapuram, 695547, India

Presenting author: Preeti Kumari (preetikumari.22@res.iist.ac.in)

Abstract

Sambhar Lake, is one of the largest Hypersaline lakes in the world, covering around 7560 km^2 of the area in Sambhar town, Rajasthan, northern India. Sambhar lake extends over the rain-shadowed region of Sandmata Complex, which is overlaid by the arkose-pelite-greywacke suite of Ajmer formation of the south Delhi fold belt. This disposition of the lake makes it perfect for the formation of various evaporite deposits such as chloride (halite and sylvite), sulfates (polyhalite, anhydrite, and kieserite), and carbonates (dolomite and calcite). The evaporite minerals such as halite, kieserite, and other similar sulfates have also been reported from the Martian surface. The mineralogical similarities of Sambhar Lake with that of Mars make them a potential analogue material as well as a site that can provide significant insight into the physiochemical conditions and formation mechanism on Mars. The evaporites were formed in a hypersaline environment that serves as a habitat for some of the halophile extremophiles. These extremophilic biomolecules are entrapped by certain evaporites during their crystallization, which aids geologists and geo-microbiologists in understanding their environmental conditions. Therefore, a detailed investigation of the evaporites of Sambhar Lake from an astrobiological perspective is also important to understand the possible past signature of life forms on mars. The molecular structure and chemical composition of these minerals can be precisely determined through spectrochemical studies, which in turn help us comprehend the physio-chemical conditions that led to the development and evolution of a certain mineral and the presence of biosignatures if any. In the present study, we characterize the mineral associations of Sambhar Lake using various spectrochemical techniques such as Vis-NIR reflectance spectroscopy, Fourier Transform Infrared Spectroscopy, and Laser Raman analysis. The spectral signatures of the various samples confirm the presence of different minerals such as halite, sylvite, and kieserite, which are a few of the characteristic evaporite reported from Mars. The laboratory-obtained spectral data were compared with the library spectra and their contour parts using Compact Reconnaissance Imaging Spectrometer for Mars from Mars Reconnaissance Orbiter. Similar features are noted from the Olympia Undae, Mars. Some of the evaporite samples collected from the study area, including salt-pan wasteland are showing the presence of biomolecules in and around the crystal lattice. In addition to the spectral similarities, large-scale geomorphological resemblance (mud cracks, dunes, etc) have also been observed on the Martian surface.

Keywords: Sambhar Lake, gypsum, halite, terrestrial analogue studies, spectral characterization.

References

[1] Cabrol, Nathalie A., and Edmond A. Grin, eds. From Habitability to Life on Mars. Elsevier, 2018.
[2] Mukherjee, Pralay, and Prabal Rakshit. "Late Quaternary climatic vicissitudes as deciphered from the study of lacustrine sediments of Sambhar Lake, Rajasthan, India." Indian Journal of Geosciences 66.4 (2012): 213-224.

UV reflectance of Venus: Spatial variability

Sandhya K Nair, Tarun Kumar Pant, Madhusoodanan MS

Space Physics Laboratory, VSSC, Trivandrum
Amity University, New Delhi
Email: sandymad@gmail.com

Venus is surrounded by a dense atmosphere composed of mostly Carbon dioxide, Nitrogen and Water vapor. It has been observed that the spectrum of solar radiation reflected by Venus has broad absorption feature between 0.2 μm and 0.5 μm and 0.2 and 0.32 μm is well explained by the presence of SO_2 at the cloud tops. The spectrum above 0.32 μm implies the presence of unknown absorber that has not been identified so far. Venus reflected spectrum includes: (a) SO2 concentration and its variation over time and space (b) the nature and originof the UV absorber, together with its temporal variability The objective of the present study isto examine the spatial variability of UV features in the cloud top using *Akatsuki* UV imager. We have observed large contrasts in the UV images captured and detailed features are quite different from each other. The radiance of a 365 nm image is about ten times larger than that of a 283 nm image. The 365 nm image shows more contrast and bright area in the equatorial region near the centre of the image. These differences in UV images suggest that the spatial distributions of SO_2 and unknown UV absorbers are governed by, at least partly, different chemical and/or dynamical processes. The observed features are also compared with reflectance observed by earth.

- Lee YJ, Imamura T, Schröder SE, Marcq E, Long-term variations of the UV contrast on Venus observed by the Venus Monitoring Camera on board Venus express, *https://doi.org/10.1016/j.icarus.2015.02.015*, *Icarus* 253:1-15, **2015**.

Potential landing sites in lunar South Pole: An integrated study using radar and spectral properties

Nikhil Keshav[1*], Guneshwar Thangjam[1], Sriram Saran Bhiravarasu[2]

[1]National Institute of Science Education and Research, Bhubaneswar, Odisha 752050

[2]Space Applications Centre, ISRO, Ahmedabad 380015

*Corresponding Author E-mail: (nikhil.keshav@niser.ac.in)

The Lunar Polar Regions have been of high interest for a long time. The potential water-ice and volatile deposits in the permanently shadowed regions (PSRs), poorly understood physical and chemical processes with wealth of information to understand the geologic processes makes it one of the prime study areas. All the 13 candidate landing sites for the Artemis III lunar landing mission are also located within six degrees of latitude of the lunar South Pole [1]. The proximity of volatile-rich PSRs and the low grazing angle of the sun in these regions can lead to very different surface chemical composition and morphological characteristics compared to other non-polar regions such as the Apollo sites. Several previous radar studies have attempted to explain the anomalous nature of some PSRs using ground- and orbital-based radar instruments [e.g., 2, 3]. In this study, we have selected two sites around Haworth and Faustini craters in the lunar South Polar Region, based on a previous study that showed high potential for the presence of surface and subsurface ice within these craters [4]. The polarization properties of these regions derived from DFSAR on board Chandrayaan-2 orbiter are compared with average annual temperature derived using DIVINER along with the altitude and albedo derived from LOLA observations. We observed that the distribution of radar circular polarization ratio (CPR) from these regions does not provide a reliable signature for the presence of pure water ice.

The chemical composition of these regions can be studied using the 0.8-5µm spectra observed from the Imaging Infrared Spectrometer (IIRS) on board the Chandrayaan-2 orbiter. Since these regions receive sunlight only at low grazing angles and are topographically diverse, proper thermal and photometric corrections are required for a robust spectral analysis. The thermal correction models applied by [5] over some IIRS data yielded interesting results. A comparative study between different thermal correction and photometric models is also being done to find the best suited model for IIRS observations. The high CPR values caused by the water ice deposits or high surface roughness within the PSRs might show different spectral behaviour compared to the surrounding regions. This would give us a better understanding of the volatile deposition and the regolith mixing process.

References:

[1] Lloyd, V. et al. (2022) *NASA Press release 22-089*. [2] Fassett, C. I., er al. (2018) *JGR, 123, 3133*. [3] Spudis, P. D., et al. (2013) *JGR 118, 2016.* [4] Brown, H.M. et al. (2022) *Icarus 377*. [5] Verma, P.A. et al (2022) *Icarus 383.*

Thermal Correction of Lunar Hyperspectral Data from Chandrayan-1

Sourav Mahato[1]*, Guneshwar Thangjam[2]*, Sunil Behera, Nikhil Keshav National Institute of Science Education and Research, 752050 [1]*Corresponding Author E-mail: sourav.mahato@nise.ac.in

[2]*Corresponding Author E-mail: thangjam@niser.ac.in

Observed radiance in hyperspectral imagery represents both surface reflectivity and thermal emissivity. In order to properly analyze the spectral reflectance that indicates surface chemical composition as well as physical properties, it is necessary to decouple the thermal component. The thermally corrected data of Chandrayaan 1's M^3 by the empirical or semi-empirical approach of Clark et al. show the presence of water particularly in higher latitudes and lunar polar areas[1-2]. A recent thermal correction method developed by Wohler et al. 2017 shows the presence of OH/H2O and their spatial and temporal variations even at lower latitudes [3]. Therefore, the development of the thermal correction approach by Wohler et. al. 2017 is attempted so that it can be applied to other interesting areas to investigate the nature of hydration and/or the presence of water. The Von Karman crater on the lunar farside is chosen as the study area (It is the landing site of Chang'e 4 rover which is part of Chinese Lunar Exploration Program). Wohler et al. 2017 approach consists of three major steps. The first step, which is a rough estimation of surface temperatures and thermal corrections using the estimated temperatures, has been implemented[3-5]. The results obtained after the first step show strong absorption due to OH/H2O. The second step uses the Hapke Single Scattering model [6] which is primarily used for photometric corrections accounting microscopic roughness parameters and equations by Shkuratov et al.[7] for estimating refined value of surface temperatures. In this model Hapke method is used to refine the estimated values of parameters responsible for the thermal radiation. Till now, the partial modeling of Hapke scattering has been performed which shows a highly scattered nature of light, likely due to rough and heavily cratered terrain in the lunar farside. In the third step, correction due to macroscopic surface roughness effect on temperature of the lunar surface has to be determined through constructing random surface. Further analysis is in progress to complete the thermal and photometric corrections.

References:

[1] C. M. Pieters et al. (2009), science, 326(5952), 568–572. [2] R. N. Clark et al. (2011), Journal of Geophysical Research:Planets, 116(E6). [3] C. Wohler et al. (2017), Science advances, 3(9), e1701286. [4] Grumpe et al. (2015), Planetary and Space Science, 111, 1-33. [5] Wohler et al. (2012), Springer, In Innovations for Shape Analysis: Models and Algorithms, pp. 467-492. [6] B. Hapke (2012), Cambridge university press. [7] Shkuratov et al. (2011), Planetary and Space Science, 59(13): 1326-71.

Laser Ablation of Meteorite and Biomolecules in Liquid Environment (LAMB-LE): Simulating impact conditions in laboratory

Surendra V Singh[1, *], Gaurav Rai[2], Kavil Mehta[3], Swetapuspa Soumyashree[1], Prashant Kumar[1], J K Meka[1], T Vijay[2], S Vijayan[1], Anil Bhardwaj[1], N J Mason[4], B Sivaraman[1, *]

[1]Physical Research Laboratory, Ahmedabad, India
[2]Indian Institute of Technology Gandhinagar, India
[3]Pandit Deendayal Energy University, Gandhinagar, India
[4]University of Kent, Canterbury, UK

*Corresponding Author E-mail: surendra@prl.res.in, bhala@prl.res.in

Natural impact-shock processes are very complicated in terms of their physical and chemical characteristics. Since it is impossible to conduct a comprehensive investigation of the full-scale effect of the impact process, laboratory investigations are focused only on a limited aspect of the impact process at a time. Most common impact experiments are performed using accelerating devices capable of firing projectiles at a velocity of a few km s^{-1}. A wide variety of accelerating devices are available in the laboratory, such as single-stage and two-stage light-gas guns, Van de Graaf accelerators, etc. [1]. The high-temperature heating effect of the impact process can be simulated in the laboratory to investigate the chemical modification induced by impact. Such methods simulate characteristic temperatures (thousands of kelvins) to understand impact-induced melting, vaporization and chemical reactions at high temperatures. Our recent experiments using shock tube have shown that they can be a valuable tool for understanding impact-induced shock and related processes [2, 3]. Shock tubes offer interesting characteristics such as a sharp increase in temperature within a very short time scale and subsequent cooling at a rate of millions of degrees per second. Such transient events are expected to occur in catastrophic impact events. Among various sources used to simulate such rapid heating, powerful pulsed lasers are also proven to be valuable source. We present new experimental technique LAMB-LE to simulate impact conditions in the laboratory using high-intensity pulsed laser, which is based on the LALE technique [4]. It is a straightforward technique, providing high pressure and temperature condition during target ablation. This will be a useful technique to simulate meteorite impact in the water, oceanic and splash pool/lake impacts, also environments where water is present, even momentarily. Such fundamental investigations are essential for understating impact delivery, sample extraction, and mixing in simulated relevant conditions. In this presentation the details of LAMB-LE setup and preliminary results will be discussed.

References:

[1] Gerasimov, M., et al. (1998) Earth, Moon, and Planets, 80(1): p. 209-259. [2] Singh, S.V., et al. (2022) Molecules, 25: p. 5634. [3] Roy, A., et al. (2022) Monthly Notices of the Royal Astronomical Society, 517(4): p. 4845-4855. [4] de Azevedo, W.M., et al. (2016), IntechOpen.

Persistent Late Amazonian fluvial activity on Mars

Harish[1*], S Vijayan[2] and M. R. El-maarry[1]

[1]Space and Planetary Science Center and Department of Earth Sciences, Khalifa University, UAE
[2]Planetary Science Division, Physical Research Laboratory, Ahmedabad 380009, India

*Corresponding Author E-mail: harish@ku.ac.ae

Inverted landforms are positive relief features whose formation is initiated by the deposition of sediments by fluvial activity and later exhumed by aeolian activity [1-3]. Fluvial activity is extensively reported on Mars from Noachian to the Hesperian period [4]; however, few studies [5,6] suggest prolongation to the early Amazonian epoch. However, episodes of fluvial activities during the younger Amazonian epochs and the environmental conditions during those epochs are still uncertain. This study focused on a better understanding of formation conditions and epochs of inverted landforms on Mars. For the preliminarily topographical, morphological and chronological analysis, we used HRSC-MOLA blended DEM [7] and MRO-CTX mosaic [8]. High-resolution HiRISE DEM generated using MarsSI [9] with HiRISE [10] and CaSSIS color [11] images were used for the detailed analysis of the stratigraphy and morphology.

In this study, we focused on an unnamed crater located to the northwest of the Orcus Patera. The southern wall is carved by fluvial channels associated with inverted channels and clearly shows the transition from negative-relief fluvial channels to positive-relief inverted channels. The thickness of the inverted channels within the crater varies from ~5 m to ~12 m. We also observed the association of inverted channels with fan-shaped deposits on the crater floor and we interpreted them as potential inverted fans. Additionally, these fans show a superposition relationship from right to left (younger to older in age based on the principle of superposition). We have identified at least three clear superposition relationships, which plausibly suggest either three or more episodes of water-flowing activity in this crater on Mars or multiple deposits would have occurred at the same time. Furthermore, to limit the period of fluvial activity within this crater, we determined the modeled absolute age of the crater using the crater-size frequency distribution of the primary craters on the ejecta of the studied crater. This study reveals that the inverted landforms formed post to 1.9 Ga and thus acclaims recent fluvial activity on Mars within the last 2 billion years. Overall, this crater on Mars hosts evidence of recent and recurring fluvial activity.

References: [1] Jacobsen and Burr (2017), Geosphere, 13, 2154–2168. [2] Davis et al., (2016), Geology, G38247.1. [3] Zaki et al., (2018), Icarus, 309, 105-124. [4] Carr and Head (2012), EPSL, 294, 185-203. [5] Vijayan and Sinha (2017), JGR Planets, 122, 917-949. [6] Harish et al., (2021), 361, 114397. [7] Fergason et al., (2018), USGS. [8] Dickson et al., (2018), 49th LPSC, 2480. [9] McEwen et al., (2007), JGR Planets, 112, E05S02. [10] Malin et al., (2007), JGR Planets, 112, E05S04. [11] Thomas et al., (2017), SSR, 212, 1897-1944.

Maskelynite in terrestrial and extra-terrestrial materials

Shivani Baliyan[1*], Dwijesh Ray[1]

[1]Physical Research Laboratory, Ahmedabad
*shivanib@prl.res.in

Shock-deformation features in extraterrestrial basalts maybe recorded as brecciation, impact melt, deformation of mineral crystal lattices, planar-deformation features, development of shock veins, production of high-pressure polymorphs of common minerals, formation of diaplectic glass or fused glass and the mineral maskelynite (e.g., [1]). A lot of terrestrial rocks and meteorites includes the plagioclase as abundant rock-forming mineral in which shock characteristics can be examined to assess peak shock pressures and temperatures.

Maskelynite is first discovered by [2] as a new phase in Shergotites, as an optically isotropic and amorphous material transformed from plagioclase feldspar caused due to hypervelocity impact [3, 4, 5]. Maskelynite is formed by shock metamorphism under high pressure and thus has been recognized as a significant indicator of the degree of shock induced during the impact [2, 6]. However, the formation has been debatable as: a) feldspar undergone solid-state transformation to produce diaplectic glass. b) melting and quenching of meteoritic plagioclase under high pressure. The shock pressure for the formation of maskelynite depends on the composition and structural state, and other properties of feldspar (e.g., composition, grain size, porosity, etc.) of target objects. Specific feldspar composition directly relates to the pressures, viz. more calcic feldspars transform at a slightly lower pressure as compared to the more sodic-end-members due to the differences in their Si-O and Al-O bonding parameters [5]. Solid-state and melting related formation mechanisms are distinct processes and have different implications for the geochemical behavior of the rock during impact deformation. In order to comprehend the process by which naturally occurring shock-induced amorphous glass formed, the study examines the textural and chemical relationships of maskelynite in shocked meteorites in comparison to shocked terrestrial samples.

[1] Bischoff A. and Stöffler D. (1992) *Euro. J. Min., 4,* 707-755. [2] Tschermak G. (1872) *Nature, 62, 122-146.* [3] Fritz, J., Greshake A., and Stöfflerr D. (2005) Antarct. Metorite Res., 18, 96– 116. [4] Jaret et al., (2015) United States N. [5] Rubin, A.E. (2015) Icarus 257, 221-229. [6] Stöffler & Hornemann (1972) Meteoritics, 7, 371–394.

STUDY OF STATISTICAL PROPERTIES OF 3D MAGNETOHYDRODYNAMIC TURBULENCE

Pratik Patel[1*], and Sharad K Yadav[1]

[1]Department of Physics, Sardar Vallabhbhai National Institute of Technology (SVNIT), Surat 395007, Gujarat, India

[*]Corresponding Author E-Mail: d21ph012@phy.svnit.ac.in

Abstract

The statistical properties of magnetohydrodynamic (MHD) turbulence have been extensively studied due to their wide range of applications in astrophysical and space plasma physics. All of these studies report the same universal scaling exponent, $k^{-5/3}$ [1] in the inertial region for both kinetic and magnetic energy spectra. In this work, we present various statistical parameters as well as the energy spectra of MHD turbulence for different initial energy spectra. We performed direct numerical simulations for fully developed homogeneous, isotropic, and incompressible MHD turbulence using the pseudospectral method in three dimensions, without a mean magnetic field. We have shown the evolution of energy dissipation rates and energy with time and the variation of kinetic energy and magnetic energy spectra with wavenumbers. And we observe almost the same behavior as reported in the literature [2-3]. We have also shown the results for the different length scales and the vorticity and current density fields.

References:

[1] Frisch U. and Kolmogorov A.N. (1995), *Cambridge University Press*

[2] Sahoo G. et al. (2011) *New J. Phys., 13(1), 0130-036*

[3] Yadav S.K. et al. (2022) *Phys. Fluids, 14(9), 095-135*

Thermal and photometric correction of Chandrayaan-I M3 data to understand physical and chemical nature of OH/H_2O

Sunil Behera* Guneshwar Thangjam, Sourav Mahato
National Institute of Science Education and Research, NISER, HBNI, Jatni, 752050, Odisha
*Corresponding Author E-mail: sunilbehera696@gmail.com

Data collected by lunar orbiter using remote sensing technique have detected spectral characteristics that indicate the existence of OH/H_2O on the lunar surface. Since spectral radiance of moon is highly influenced by both surface reflectivity and thermal emissivity, it is important to consider and decouple surface emissivity component in order to retrieve the true surface reflectivity. It is worth mentioning that initial studies (Pieters et al. 2009; Clark et al. 2009; Sunshine et al. 2009) reported detection of OH/H_2O at higher lunar latitudes using empirical thermal correction approach of Clark et. al. 1979[1][2], however recent studies with improved thermal correction models (Bandfield et al. 2018, Whoeler et al. 2017, Li and Milliken 2017) claimed widespread presence on lunar surface. The recent works used different thermal correction methods, but it is worth mentioning that Milliken & Li 2017, and Woehler et al. 2017[4] adopted semi-empirical thermal correction approaches, while Bandfield et al. incorporated a new physics based thermal and roughness model[5][6]. Here, we used Bandfield et al. 2018 approach of thermal correction and data correction. Our study aims to study the physical and chemical nature of OH/H2O on lunar surface.

The Bulliadus and Copernicus caters are chosen as study area. The crater with central peak is geologically diverse which can provide insights into the underlying geology of the moon and providing the access to materials that are not visible on the surface. The first step, that includes the initial surface temperature, albedo, rms slope value and other parameters were estimated using Chandrayaan-I M3 OP2C1 data and LOLA DEM for thermal and roughness model. Additional investigation is currently underway to finalize the rectification and analysis.

Reference: [1] Pieters, C. M. et al. (2009), *Science, 326, 568–572.* [2] Clark, R. N. et al. (1979), *Icarus, 40, 94.* [3] Milliken, R. and, Li, S. et al, (2017), *Nature Geosci, 10, 561–565.* [4] Woehler C, et al, 2017 *Sci Adv 3,9* [5] Bandfield, J. L. et al. (2018) *Nature Geosci, 11, 173-177.* [6] Bandfield, J. L.et al (2015), *Icarus 248, 357–372.*

Planetary Exploration using X-ray Instruments

M. Shanmugam, *Physical Research Laboratory, Ahmedabad – 380009, India*
Email: shansm@prl.res.in

The technique of remote X-ray Fluorescence spectroscopy has been employed since early days of space exploration to determine elemental composition of lunar surface. When solar X-rays having sufficiently high energy interact with the atoms on surface, characteristic X-ray lines are produced which can provide quantitative information about elemental abundance. The experiment involves measuring spectra of fluorescent X-rays from lunar surface from a low energy X-ray detector onboard an orbiting satellite. However, it is well known that the solar X-rays are extremely variable in both intensity as well as their spectral shape; and that the flux of fluorescent X-ray lines from the lunar surface critically depend on the flux and spectral shape of incident solar X-rays. Therefore, it is absolutely necessary to have simultaneous measurements from both these components are essential for interpreting the X-ray Fluorescence data in terms of the abundances of the major elements. Thus, typically a remote X-ray Fluorescence Spectroscopy experiment contains two components – (1) a large area X-ray detector, to measure the fluorescent X-ray spectra from the lunar surface; and (2) a small X-ray detector, to measure the X-ray spectra incident directly from the Sun. Both these components can be independent payloads with separate interface with the spacecraft, but the data from both the payloads is essential to quantitatively interpret the remote X-ray fluorescence spectroscopy data. Chandrayaan-2 had both the components – lunar X-ray observations and solar X-ray observations. The X-ray spectrometer for measuring fluorescence spectra from lunar surface (Chandra Large Area Soft x-ray Spectrometer – CLASS) is being designed and developed by the Space Astronomy Group, ISAC. The X-ray spectrometer for solar X-ray observations – Solar X-ray Monitor (XSM) is being designed and developed at the Physical Research Laboratory, Ahmedabad. On the other hand, for the in-situ elemental composition measurements, PRL has developed an instrument named Alpha Particle X-ray Spectrometer (APXS) for Chandrayaan-3 rover. The design and performance details of these X-ray instruments will be discussed in the conference.

Thermophysical Behaviour of Chandrayaan-3 and other selected Landing Sites on the Moon

K. Durga Prasad, G. Ambily and P. Kalyan Reddy

Physical Research Laboratory, Ahmedabad

Insights from recent studies have shown that the thermophysical behaviour of the lunar surface show distinct variations owing to several aspects. While the surface temperatures of Moon are dictated only by the incident solar heat flux, the subsurface temperatures change as a function of several parameters viz. latitude, regolith cover, density/porosity, morphology, composition and so on. An important aspect of such studies which is often ignored is the lateral heat transport. However, lateral heat transport has been shown to affect the near surface thermophysical behaviour, particularly at local and regional scales. This has several implications not only for understanding the lunar thermophysics but also to drive future lunar exploration.

We have developed and validated a comprehensive three-dimensional finite element thermophysical model of the Moon capable of addressing all the above-mentioned aspects. A unique feature of the model is to use the actual topography of any location on the Moon to compute its thermophysical behaviour at varied scales. Using this model, simulations were carried out to estimate the thermophysical behaviour of the proposed landing site of upcoming Chandrayaan-3 mission. Some other selected landing sites on the Moon were also considered for a comparative study. Topographic data from LOLA (Lunar Orbiter Laser Altimeter) instrument onboard LRO has been used in conjunction with the model and the surface and subsurface temperatures were derived. Results showed a distinct thermophysical behaviour at these sites. Also, a significant effect due to local topography on the surface and subsurface temperatures was also observed for all the sites. Details of the study, comparative results and their implications on in-situ exploration will be discussed.

Mars Ionospheric Disturbances induced by strong Solar Flares from January 2021– January 2023

Sayanee Haldar[1]

[1]National Institute of Technology Rourkela (NIT Rourkela, Sector 1, Rourkela, Odisha768009)
Email ID: sayanee.nitrkl@gmail.com

Abstract

The Chapman theory predicts that the peak electron density and altitude are both affected by the angle at which the sun is viewed from the horizon. Although the quantitative dependence of peak electron densities on solar irradiance is not as strong as theoretically predicted, they are still sensitive to the Sun's rotation and solar flares. In regions of a strong and vertical magnetic field, peak electron densities are increased, perhaps as a result of a two-stream plasma instability that raises electron temperatures. The photoionization of neutral species by solar extreme ultraviolet (EUV) and x-ray photons is the primary source of ions and electrons in a planet's ionosphere. Observed plasma density increases more than expected based solely on increased ionization, and the electron temperature decreases below expected depth; both effects can be explained by an expanded neutral atmosphere, which efficiently dissipates any flare-induced heat, but this requires a detailed study of solar flares that impacted Mars over the past two years while the Mars Atmosphere and Volatile EvolutioN (MAVEN) orbiter was characterizing the Mars upper atmosphere.

Keywords: Mars Ionosphere, plasma density, solar flares.

Selected References:

[1] Mendillo, M., Withers, P., Hinson, D., Rishbeth, H. and Reinisch, B., 2006. Effects of solar flares on the ionosphere of Mars. *Science*, *311*(5764), pp.1135-1138.

[2] Ramstad, R., Barabash, S., Futaana, Y., Nilsson, H. and Holmström, M., 2017. Global Mars-solar wind coupling and ion escape. *Journal of Geophysical Research: Space Physics*, *122*(8), pp.8051-8062.

[3] Thiemann, E.M.B., Andersson, L., Lillis, R., Withers, P., Xu, S., Elrod, M., Jain, S., Pilinski, M.D., Pawlowski, D., Chamberlin, P.C. and Eparvier, F.G., 2018. The Mars topside ionosphere response to the X8. 2 solar flare of 10 September 2017. *Geophysical Research Letters*, *45*(16), pp.8005-8013.

[4] Withers, P., 2009. A review of observed variability in the dayside ionosphere of Mars. *Advances in Space Research*, *44*(3), pp.277-307.